

Nanocomposite Gas Separation Membrane

**Dissertation to attain the academic degree
Doctor of Natural Sciences (Chemistry),
University of Hamburg**

Jun Qiu

Adviser: Prof. Dr. -Ing. W.-M. Kulicke

14. April 2009

**1. Gutachter: Prof. Dr. -Ing. W.-M. Kulicke
2. Gutachter: Prof. Dr. W. Kaminsky**

Tag der Disputation: 17. Juli 2009

For my mother Kouying

my wife Bing

Die vorliegende Arbeit wurde in der Zeit von August 2003 bis Oktober 2006 am Lehrstuhl für Technische und Makromolekulare Chemie der Universität Hamburg unter der Leitung von Prof. Dr. W.-M. Kulicke angefertigt. Die praktischen Arbeiten wurden am Institut für Polymerforschung des Forschungszentrums GKSS Geesthacht GmbH, unter der Leitung von **Prof. Dr. K.-V. Peinemann** durchgeführt.

Ohne die Unterstützung vieler Menschen ist eine solche Arbeit undurchführbar.

Meine besonderer Dank an:

- Prof. Dr. K-V. Peinemann als meinem Doktorvater für die interessante Themenstellung, die Bereitstellung der Arbeitsmittel, seine wissenschaftliche Begeisterungsfähigkeit,
- Prof. Dr. W.-M. Kulicke als meinem Doktorvater an der Universität Hamburg für die freundliche Übernahme meiner Arbeit.
- Dr. J.-M. Zheng für viele hilfe und –lehrreiche Diskussionen und die kritische Durchsicht der Arbeit.
- Frau G. Johannsen für fachliche Unterstützung und viel Hilfestellung und freundliche Arbeitsatmosphäre.
- Prof. Dr. V. Abetz für die Zugangsmöglichkeit und Unterstützung für die Arbeit.
- Dr. S. Shishatskiy für die Einweisung in die Membranherstellung.
- Frau M. Eggers, Herrn M. Schossig, Frau M. Aderhold, Frau C. Abetz and Herrn K.Scholles für ungezählte DSC, NMR, IR, REM, AFM, Gas Permeabilitäts-Messungen und die engagierten analytischen Diskussionen.
- Die Mitarbeiter des Instituts für Polymerforschung für die fachliche Unterstützung und wertvolle Diskussion, die vielen Hilfestellungen und die freundliche Arbeitsatmosphäre.
- Meine Mutter und meine Frau für Ihre Unterstützung und Verständnis.

Aim of the study

The goal of this study is to develop novel nanocomposite membranes for gas separation. These nanocomposite membranes are constructed by incorporation of novel nanometer size organic fillers into high free volume polymer (i.e., poly(trimethylsilyl-propyne (PTMSP)) and low free volume polymer (i.e., ethylcellulose (EC)). These new nanometer size organic fillers are silylated-saccharides. The guidelines of design of silylated-saccharides are based on the bulky structure of the alkyl-silyl group (especially trimethylsilyl group) which can introduce excess free volume into the filled matrix, and the high flexibility of the siloxane linkages which can cause elevated mobility in the filled matrix. Two types of silylated-saccharides have variable size, free volume, and mobility, which will cause considerable changes on free volume and mobility in the filled polymer system. They are: (1). various molecular weight trimethylsilyl-saccharides (i.e., trimethylsilyl-glucose (TMSG) ($M_w = 180$), trimethylsilyl-dextran-1 (TMSD1) ($M_w = 900-1200$), and trimethylsilyl-dextran-500 (TMSD500) ($M_w = 350-550$ kD)); (2). various silylated glucose (i.e., trimethylsilyl-glucose (TMSG), triethylsilyl-glucose (TESG), triisopropylsilyl-glucose (TIPSG), and diphenylmethylsilyl-glucose (DPMSG)).

Gas transport properties in high free volume polymer PTMSP and low free volume polymer EC containing these silylated-saccharides have been intensively examined using the time-lag method. This study is an attempt to gain more fundamental understanding of gas molecule transport properties (i.e., gas diffusivity and solubility) in these nanocomposite systems in terms of fractional free volume (FFV) and chain mobility. The comprehensive studies of gas diffusivity and solubility in these nanocomposites as well as temperature dependent transport properties have been intensively discussed in terms of the pre-exponential factor and the activation energy in the Arrhenius equation, which are closely related to gas molecule size and polymer properties such as local chain mobility and free volume.

In addition to understand the transport mechanism, this study is also intended to develop a new application-oriented composite membrane (e.g., EC filled with trimethylsilyl-saccharose (TMSSA)) with improved separation performance in oxygen/nitrogen, compared to the commercially applied EC membrane.

Structures of the thesis

Chapter 1

1. Introduction

Chapter 2

2. Experiment

Chapter 3

In this chapter, a novel composite membrane made of the high free volume polymer poly(trimethylsilyl-propyne) (PTMSP) and the small organic filler trimethylsilyl-glucose (TMSG) with the size of approximately one nanometer is reported. The permeabilities, diffusivities, and solubilities of six gases (He, H₂, CO₂, O₂, N₂, and CH₄) are systemically decreased with increasing TMSG loading in PTMSP, which are determined by the time-lag method. It is found that the gas transport in pure PTMSP and PTMSP/TMSG composites follows different mechanisms. Additionally, the PTMSP/TMSG composite membranes offer a readily accessible mean to physically modify the fractional free volume in PTMSP, and to achieve the desired gas permeability and permselectivity compared to the pure polyacetylene polymers.

Chapter 4

This chapter reports a novel mixed matrix membrane containing the filler (TMSG) in ethylcellulose (EC). The permeabilities, diffusivities, and solubilities of six gases (He, H₂, CO₂, O₂, N₂, and CH₄) are determined in these EC/TMSG composites with a series of TMSG loading using the time-lag method. Systemically increase of TMSG contents in EC result in a distinct increase of permeabilities for all tested gases. These transport properties, together with glass transition temperature (T_g) measured by differential scanning calorimetry (DSC) analysis, suggest that the dominant reason for the permeability enhancement and permselectivity alteration is the increase in chain mobility by introducing of the TMSG filler. Interestingly, the increased $P(O_2)$ is accompanied with the unchanged $P(O_2)/P(N_2)$ selectivity up to a certain TMSG loading in EC.

Chapter 5

This chapter aims to systematically investigate the gas transport behavior in two glassy polymers. One is the rigid, high fractional free volume (FFV) poly(1-trimethylsilyl-1-propyne) (PTMSP) and the other is the relatively flexible, considerably lower FFV ethylcellulose (EC). Both polymer systems are filled with a

series of various molecular weight (Mw) trimethylsilyl-saccharides (TMSS) (i.e., trimethylsilyl-glucose (TMSG) (Mw= 180), trimethylsilyl-dextran-1 (TMSD1) (Mw= 900-1200) and trimethylsilyl-dextran-500 (TMSD500) (Mw= 350-550 kD)).

The decreases in gas permeability, diffusivity and solubility of six gases (He, H₂, CO₂, O₂, N₂, and CH₄) are directly related to the decrease of FFV in PTMSP caused by the incorporation of the various Mw fillers at equivalent loading amounts. In addition, the extent of reduction of gas permeability, diffusivity, and solubility in these composites is closely related to the Mw of TMSS fillers at an equivalent loading of various TMSS in the PTMSP matrix. In contrast, a systematic increase of gas permeability and diffusivity was obtained for the EC/TMSS system with increasing loading of TMSS fillers. The gas diffusivity increase for the EC/TMSS system correlated well with the Mw of the TMSS fillers. However, no consistent change of solubility was observed in EC/TMSS.

Chapter 6

In this chapter, the six gases (He, H₂, CO₂, O₂, N₂, and CH₄) permeability, diffusivity, and solubility in ethylcellulose (EC) filled with a series of various silyl-agents glucose (i.e., trimethylsilyl-glucose (TMSG), triethylsilyl-glucose (TESG), triisopropylsilyl-glucose (TIPSG), and diphenylmethylsilyl-glucose (DPMSG)) were determined at 30 °C with the time-lag method. In addition, the transport properties in EC filled with a representative plasticizer dioctylphthalate (DIPH) and one glucoside based derivate pentacetate-glucose (PAG) are included for comparison. The increased alkyl chain length attached on the silane leads to more flexibility (i.e., increased diffusivity), but less excess FFV (i.e., decreased diffusivity). The overall gas transport properties are the consequences of the combination of both factors. In the oxygen/nitrogen separation, the EC/TMSG exhibits the improved separation performance relative to the unfilled EC. This readily physical introduction of trimethylsilyl (TMS) group via organic filler creates a similar effect to the chemical modification of polymer with TMS group.

Chapter 7

This chapter systemically investigates the effect of the addition of low molecular filler trimethylsilyl-saccharose (TMSSA) on the temperature dependent gas transport properties in ethylcellulose (EC) composites membranes. The activation energies of permeation and diffusion (E_P and E_D), and heat of solution (ΔH_S) are obtained

following the Arrhenius - van't Hoff rule by fitting permeability (P), diffusivity (D), and solubility (S) data, which are measured at 20, 30, 40, and 50 °C with a pressure increase time-lag method. The present work also studies the compensation relationship between the activation energies (E_P and E_D) as well as heat of solution (ΔH_S) and natural logarithm of the pre-exponents factors ($\ln P_0$, $\ln D_0$, as well as $\ln S_0$) in EC/TMSSA composite membranes, comparing to these in a number of rubbery and glassy homopolymers. It shows that the composite membranes exhibited different behaviors in regard to the compensation relationship due to special local environment around the permeating molecule. It is concluded that the study of the compensation effect provided a useful insight into the polymer structure.

Table of Contents

1. Introduction	
1.1 Brief history of gas separation membrane	11
1.2 Gas transport through the polymer membrane – theory and background	
1.2.1 The solution-diffusion mechanism	13
1.2.1.1 The permeation term	13
1.2.1.2 The diffusion term	14
1.2.1.3 The sorption term	15
1.2.1.4 The permselectivity and permeability/selectivity trade-off relationship	17
1.3 The structure and transport properties relationship	17
1.3.1 Fractional free volume (FFV) in polymer	18
1.3.2 The most permeable glassy polymer with high FFV	19
1.3.3 The most permeable rubbery polymer with high flexibility	20
1.3.4 The introduction of bulky trimethylsilylated group into polymer matrix	21
1.3.5 Composite membranes	22
1.3.5.1 Mixed matrix membranes with inorganic fillers	22
1.3.5.2 Mixed Matrix membranes with organic fillers	24
1.3.5.3 Design of novel organic fillers for composite membrane	24
1.4 References	25
2. Experiment	29
2.1 Synthesis of silylated-saccharides	
2.1.1 Chemicals	29
2.1.2 Synthesis and characterization of trimethylsilyl-glucose	29
2.1.3 Synthesis and characterization of trimethylsilyl-saccharides	30
2.1.4 Synthesis and characterization of trimethylsilyl-1,3-dimethyl-1,1,3,3-tetraphenylsilyl-glucose (DPMSG), triethylsilyl-glucose (TESG), and triisopropylsilyl-glucose (TIPSG)	31
2.2 Film preparation	
2.2.1 General procedures of nanocomposite films preparation	32
2.3 Composite film characterizations	33
2.3.1 Glass transition temperature	33
2.3.2 Optical inspection of composite film	33
2.3.3 Scanning electron microscopy	33
2.3.4 Gas transport properties with time-lag	34
2.4 References	35
3. Gas transport properties in a novel PTMSP composite membrane with the nanosized organic filler TMSG	37
3.1 Abstract	37

3.2 Introduction	37
3.3 Results and discussion	38
3.3.1 Gas permeability and permselectivity in PTMSP/TMSG	38
3.3.2 Gas diffusivity in PTMSP/TMSG	44
3.3.3 Gas solubility in PTMSP/TMSG	47
3.3.4 Activation energies of gas permeation in PTMSP/TMSG	50
3.4 Conclusions	53
3.5 References	54
4. Gas transport properties in a novel EC composite membrane with the nanosized organic filler TMSG	56
4.1 Abstract	56
4.2 Introduction	56
4.3 Results and discussion	58
4.3.1 Density of EC/TMSG	58
4.3.2 Glass transition temperature of EC/TMSG	59
4.3.3 Gas permeability and permselectivity of EC/TMSG	60
4.3.4 Gas diffusivity and solubility in EC/TMSG	65
4.3.5 Activation energies of gas permeability in EC/TMSG	70
4.4 Conclusions	71
4.5 References	72
5. Gas transport properties in PTMSP and EC composite membranes with organic filler trimethylsilylsaccharides with different molecular weight	74
5.1 Abstract	74
5.2 Introduction	75
5.3 Results and discussion	75
5.3.1 Phase behavior of PTMSP/TMSS and EC/TMSS	76
5.3.2 Glass transition temperature of EC/TMSS	78
5.3.3 The transport properties of PTMSP/TMSS	78
5.3.3.1 Gas permeability in PTMSP/TMSS	78
5.3.3.2 Gas diffusivity and solubility in PTMSP/TMSS	82
5.3.4 The transport properties of EC/TMSS	86
5.3.4.1 Gas permeability in EC/TMSS	86
5.3.4.2 Gas diffusivity in EC/TMSS	87
5.3.4.3 Gas solubility in EC/TMSS	89
5.3.5 Permselectivity of PTMSP/TMSS and EC/TMSS	91
5.3.5.1 He/CH ₄ permselectivity in PTMSP/TMSS and EC/TMSS	91
5.3.5.2 O ₂ /N ₂ permselectivity in PTMSP/TMSS and EC/TMSS	92
5.4 Conclusions	93

5.5 References	94
6. Gas transport properties in EC composite membranes with various nanosized silylated- glucoses	96
6.1 Abstract	96
6.2 Introduction	96
6.3 Results and discussion	97
6.3.1 Permeability and permselectivity of EC/silylated-glucose	97
6.3.2 Diffusivity and solubility of EC/silylated-glucose	106
6.4 Conclusion	112
6.5 References	113
7. Temperature dependence of gas transport in EC composite membranes with trimethylsilyl-saccharose filler	115
7.1 Abstract	115
7.2 Introduction	115
7.3 Results and discussion	117
7.3.1 Effect of TMSSA loading on activation energies and heat of solution	117
7.3.2 Compensation effect	121
7.4 Conclusions	135
7.5 References	136
8. Summary	140
8. Zusammenfassung	141
8.1 References	142
9. Appendix	143
9.1 Outline of tables	143
9.2 Outline of figures	145
9.3 Dispose of Chemicals	150
9.4 Statement	151

Chapter 1

1. Introduction

1.1 Brief history of gas separation membrane

Since T. Graham has systemically studied the gas penetration through natural rubber in 1850, ^{1, 2} the idea to separate gases using polymer membranes was known. ³ However, industrial application based on gas separation membrane was around one hundred years later. ⁴ Thanks to the invention of Leob and Sourirajan, ⁵ the integrally anisotropic membrane structure laid down a technical breakthrough for formation of a thin, dense, defect-free, and selective layer supported by a more open, porous, and asymmetric layer. ⁶ Afterwards, this asymmetric structure leads to a flourishing development of reverse osmosis membrane on large industrial scale. ⁷ At the beginning of 1980, Permea (now a division of Air Products) launched a first commercially used membrane for H₂/N₂ separation based on polysulfone hollow fibre membrane (named “Prism”).

In the past 25 years, sales of membrane based gas separation unit have grown to a \$150 million/year business. ⁸ The gas separation membrane unit business is estimated to grow at a rate of 8% per annual. ⁸ Table 1 shows commercial applications and some of major suppliers of membrane gas separation units. ⁸ The gas separation membrane becomes more and more important in terms of environmental issue compared to traditional processes (e.g., cryogenic, pressure swing absorption etc.). The advantages of membranes are low capital investment, ease of operation, and low energy consumption at low gas volumes, good weight and space efficiency. ⁸ Currently, the new application fields with membrane is to purify hydrocarbons in petrochemical processing applications ⁴ and also to capture global warming gas CO₂. The milestone steps of gas separation membrane are displayed in Figure 1.1, which is summarized by Richard Baker. ⁴

Figure 1.1 Milestones in the development of membrane gas separations. ⁴

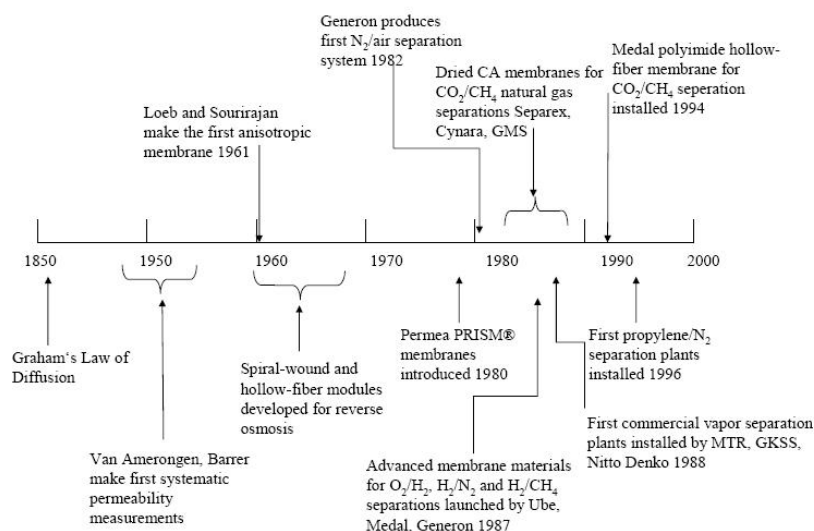


Table 1.1 Commercial applications and major suppliers of membrane gas separation units ⁸

Gas separation	Application	Supplier
O ₂ /N ₂	Nitrogen generation Oxygen enrichment	Permea (Air Products) Generon (IGS), IMS (Praxair) Medal (Air Liquide) Parker Gas Separation, Ube
H ₂ /hydrocarbons	Refinery hydrogen recovery	Air Products, Air Liquide Praxair, Ube
H ₂ /CO ₂	Syngas ratio adjustment	As above
H ₂ / N ₂	Ammonia Purge gas	As above
CO ₂ /CH ₄	Acid gas treatment enhanced oil recovery landfill gas upgrading	Cynara (NATCO), Kvaerner Air Products Ube, UOP (Separex)
H ₂ S/hydrocarbon	Sour gas treating	As above
H ₂ O/hydrocarbon	Natural gas dehydration	Kvaerner, Air Products
H ₂ O/air	Air dehydration	Air Products, Parker Balxston Ultratroc, Praxair
Hydrocarbons/air	Pollution control hydrocarbon recovery	Borsig, MTR, GMT NKK
Hydrocarbons from process streams	Organic solvent recovery monomer recovery	Borsig, MTR, GMT SIHI

Meantime, in academic research, numerous polymers based membrane materials have been evaluated, and some of them exhibited encouraging performance. However, in real life, just less than 10 polymers are used. Because the properties of the selectivity and permeability membrane aren't the only requirements for a successful application, in addition, the stability and difficulty to make thin films are other major hurdles. ^{4,9}

1.2 Gas transport through the polymer membrane - theory and background

1.2.1 The solution-diffusion mechanism

1.2.1.1 The permeation term

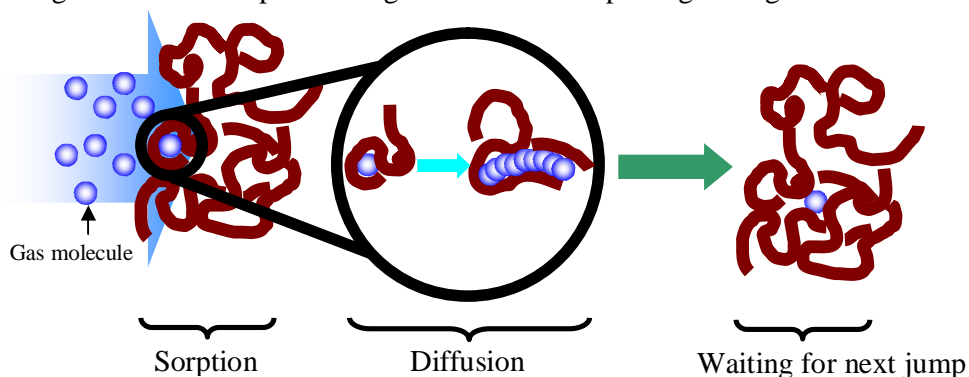
Permeation of a gas molecule through a dense polymer film is usually described by a solution-diffusion mechanism.¹⁰⁻¹³ High permeability polymers increase the productivity, and thereby decrease the required membrane area to treat a given amount of gas, and reduce the capital cost of membrane units, make membrane technology more competitive to other processes.⁴ The permeability is the product of diffusivity and solubility, which is expressed by Equation 1.1,

$$P = D \times S \quad (\text{eq. 1.1})$$

where P (cm^3 (STP) $\text{cm}/(\text{cm}^2 \text{s cmHg})$) is the permeation coefficient. D (cm^2/s) is the diffusion coefficient, which is a kinetic term. S (cm^3 (STP)/($\text{cm}^3 \text{ cmHg}$)) is the sorption coefficient, which is a thermodynamic term.

Nonporous, dense polymer membranes generate penetrant-scale transient gaps by the thermally agitated motion of chain segments in the polymer networks, which allow gas molecules to penetrate from one side of the membrane to the other side by the concentration gradient difference.^{10, 11, 13} The gas molecule through the membrane consists of three continuous steps, (1) gas molecule absorbs on one side of the membrane; (2) gas molecule diffuses through the membrane; (3) gas molecule desorbs from the other side of the membrane. The transport process has been schematically described in Figure 1.2.

Fig. 1.2 Schematic picture of gas molecule transporting through membrane



The temperature dependence of permeability can be described by the Arrhenius expression within a defined temperature range, where the polymer has no significant thermal transitions. Arrhenius expression is depicted by Equation 1.2,

$$P = P_0 \exp\left(-\frac{E_p}{RT}\right) \quad (\text{eq. 1.2})$$

where E_p (kJ/mol) is the activation energy of permeation, the pre-exponential factor P_0 has the same unit as the permeability, R is the gas constant (8.314 J/(mol K)) and T is the absolute temperature (K).

In 1954, Brubaker and Kammermeyer¹⁴ observed that E_p and $\ln P_0$ also exhibited a good linear relationship when studied gases permeate in several plastic membranes made of a couple of rubbery and glassy polymers. Later, van Krevelen¹⁵ suggested the following empirical correlation (Equation 1.3) through fitting available experimental data,

$$\ln P_0 = \alpha_p + \beta_p E_p \quad (\text{eq. 1.3})$$

where α_p and β_p are fitting parameters. According to van Krevelen, β_p is a universal constant. Regarding to α_p , two different values were proposed for rubbery and glassy polymers, respectively, and the larger one is for rubbers. Both α_p and β_p are independent of permeating species. Besides these works, Equation 1.3 has also been re-evaluated by Yampolskii et al.¹⁶ for gas permeating in different glassy polymers. In chapter 3, 4, and 7, the relationship between E_p and $\ln P_0$ will be further discussed.

1.2.1.2 The diffusion term

Theoretically, the diffusion coefficient reflects the effective gas molecule size and polymer's fractional free volume (FFV) as well as polymer chain mobility.^{10, 11, 13, 17, 18} Cohen and Turnbull¹⁹ firstly formulated the mathematical relationship between the gas diffusion coefficient and the penetrate size combined with the polymer FFV. The eq. 1.4 expresses this correlation,

$$D = A \exp\left(-\frac{\gamma}{V_f} v^*\right) \quad (\text{eq. 1.4})$$

where A is a pre-exponential factor slightly dependent on temperature, γ is an overlap parameter, v^* is the size of permeate, V_f is the fractional free volume. The eq. 1.4 obviously suggests that the decreased FFV will result in the diffusivity decrease.

Teplyakov and Meares²⁰ formulated a correlation between molecular effective diameter and its diffusion coefficients for more than 50 polymeric materials. Equation 1.5 expresses the mathematical relationship,

$$\ln D = k_1 + k_2 d_{eff}^2 \quad (\text{eq. 1.5})$$

where k_1 and k_2 are fitting parameters which are polymer type dependent, d_{eff} is the effective molecular diameter. From this equation, it can be read out that the diffusion selectivity for any chosen gas-pair in a polymer is determined by the parameter k_2 .

Within a narrow temperature range, the temperature dependence of diffusivity can be also subjected to the Arrhenius expressions (Equation 1.6),

$$D = D_0 \exp\left(-\frac{E_D}{RT}\right) \quad (\text{eq. 1.6})$$

where E_D is the activation energy of diffusion; and D_0 is the pre-exponential factor.

As early as in 1942, Barrer²¹ noted a simple linear relation between E_D and $\ln D_0$ for diffusion of different gases in different rubbers, which was interpreted by the zone theory for diffusion.^{21, 22} Afterwards, such a behavior is observed and extensively discussed in a numbers of studies.^{23, 24} At present, a well-accepted equation (eq. 1.7) to relate E_D and D_0 is:

$$\ln D_0 = \alpha_D + \beta_D E_D \quad (\text{eq. 1.7})$$

where α_D and β_D are fitting parameters. This correlation could be quite good when applied to the diffusion of penetrants in a number of rubbery polymers. However, Equation 1.7 is rather limitative when relating the data reported for glassy polymers. Good correlations could only be observed for certain gas molecules diffusing in a group of glassy polymer. What is more, it is interesting to find that the $\ln D_0$ vs. E_D relationship could “feel” the properties of glassy polymers, like flexibility and volumetric property.¹⁶ The further discussion will be continued in chapter 7.

1.2.1.3 The sorption term

The sorption of non-polar gas depends on the penetrant condensability, interactions between the polymer and penetrant, and the polymer fractional free volume. Theoretically, rubbery polymers are in thermodynamic equilibrium, the gas solubility can be explained with Henry’s law, which is derivate from gas solubility in a liquid solution.^{10, 11, 13} In contrast, glassy polymers are in the thermodynamic non-equilibrium state, sorption of gas molecules in glassy polymers can be described by the dual-mode sorption model, which has been put forward by Koros and Paul.²⁵ In this model, gas molecules dissolve themselves in the equilibrium state of the glassy polymer (Henry’s mode) and absorb in the non-equilibrium excess fractional free volume (i.e., microvoids) of the glassy polymer (Langmuir’s mode). The dual-mode sorption can be expressed mathematically as equation 1.8,

$$C = k_D p + \frac{C'_H b p}{1 + b p} \quad (\text{eq. 1.8})$$

where C is the total concentration of the penetrant in the polymer, k_D is the Henry's law constant, C'_H is the hole saturation constant or Langmuir sorption capacity, b is the Langmuir affinity parameter, and p is the pressure.

The correlation between gas solubility and gas condensability has been attempted. Representatively, Teplyakov et al.²⁰ has also put forward a linear correlation between the gas solubility coefficients and the Lennard-Jones temperature (ε/k), which is expressed as Equation 1.9

$$\ln S = k_3 + k_4(\varepsilon/k) \quad (\text{eq. 1.9})$$

where k_3 and k_4 are fitting parameters which are polymer type dependent.

The temperature dependence of solubility can be also described by the Arrhenius expressions (Equation 1.10),

$$S = S_0 \exp\left(-\frac{\Delta H_s}{RT}\right) \quad (\text{eq. 1.10})$$

where ΔH_s is the activation energy of sorption; and S_0 is the pre-exponential factor.

However, few studies are known concerning that the relationship between $\ln S_0$ and ΔH_s , corresponds to gas solubility/sorption in polymer films. Pasternak et al.²⁶ were the first to note a correlation between $\ln S_0$ and ΔH_s when they studied gases/vapors solubility (or sorption) in a copolymer of hexafluoropropylene and tetrafluoroethylene. This correlation is suggested as eq. 1.11,

$$\ln S_0 = \alpha_s + \beta_s \Delta H_s \quad (\text{eq. 1.11})$$

where α_s and β_s are fitting parameters. Recently, Lin and Freeman²⁷ also used equation 1.11 to fit their data obtained for gas/vapor solubility in cross-linked amorphous poly(ethylene glycol) diacrylate. Bondar et al.²⁸ used equation 1.11 to derive their equation which describes the dependence of the logarithm of solute solubility on the square of solute critical temperature in polymeric membranes. Besides, Yampolskii et al.¹⁶ found that enthalpy and entropy of combination (ΔH_m and ΔS_m) exhibited good linear relationship for gas/vapor sorption in several rubbery and glassy polymers as Equation 1.12. In chapter 7, this relationship will be discussed in more details.

$$\Delta S_m = \alpha_m + \beta_m \Delta H_m \quad (\text{eq. 1.12})$$

1.2.1.4 The permselectivity and permeability/selectivity trade-off relationship

Higher permselectivity polymer results in higher purity product gas. Since the permeation coefficient is the product of the diffusion coefficient and solubility coefficient, the permselectivity for two gases can be expressed (Equation 1.13) as the production of diffusion selectivity and solution selectivity,

$$\alpha_{A/B} = \frac{D_A}{D_B} \times \frac{S_A}{S_B} \quad (1.13)$$

where $\alpha_{A/B}$ is the permselectivity.

Polymers with both high permeability and selectivity are desirable. However, a strong inverse relationship between permeability and selectivity of polymer membrane materials exists.² Polymers that are more permeable are generally less selective, and vice versa. This is also called Robeson's trade-off curve,²⁹ which surveyed comprehensive literatures and plotted lines that combined permeability and selectivity of known polymer membrane materials for the selective gas pairs (e.g., O₂/N₂ and H₂/N₂ etc.). The Robeson's trade-off curve (i.e., upper-bond) was empirically described by the following Equation 1.14.

$$\alpha_{a/b} = \frac{\beta_{a/b}}{P_a^{\lambda_{a/b}}} \quad (\text{eq. 1.14})$$

Where, $\alpha_{a/b}$ is the selectivity of fast permeable (gas a)/(gas b), P_a is the permeability of gas a, $\beta_{a/b}$ are empirically values. In addition, Freeman derivates this upper-bond relationship theoretically.¹⁸ Most glassy polymers are noticeably closer to the upper bond than the rubbery polymers. Since 1991, enormous new membrane materials has been synthesized and evaluated for gas separation performance, the Robeson's upper bond has been further moved. Although, the improved separation performance with new membrane materials has been observed, the movement of the upper bound has obviously slowed down significantly since 1991. Moreover, in the real industrial application, these newly synthesized membrane materials are still not in practice.

1.3 The structure and transport properties relationship

Gas transport properties are closely related to two major polymer physical properties (i.e., FFV and chain mobility) as above discussed theoretically. In practice, Stern et al. firstly found out good relationship between gas permeability and side chain change on

siloxane rubber polymers.³⁰ This systemic change is also observed in main chain changes.³⁰ For example, the decreased gas permeability is accompanied with the reduced main chain flexibility in replacement of oxygen atom in PDMS by carbon atom (polydimethylsilylmethylene).³⁰ Koros and Paul et al., intensively studied the substitution of hydrogen atom in polycarbonate and polysulfone with larger groups, which lead to variations of chain mobility and polymer packing, further resulting in corresponding gas transport changes.^{31, 32}

1.3.1 Fractional free volume in polymer

It is generally believed that the overall gas transport process in a polymer depends on two major factors: polymer segmental mobility (free volume) and excess free volume in the non-equilibrium glassy state (microvoid, frozen hole, etc.).^{2, 10, 11, 13, 15} Fractional free volume refers to all space, which is not occupied by the constituent atoms of polymer in polymer matrix and the fraction of the total volume is accessible to the penetrant.³³ The FFV can be approximately estimated by the Bondi method,³⁴ which can be calculated by the Equation 1.15 as following:

$$FFV = \frac{V - V_0}{V} = \frac{V - 1.3V_w}{V} \quad (\text{eq. 1.15})$$

where V_0 , the specific occupied volume, is taken as $1.3 V_w$. V_w is the specific van der Waals volume, and V is the polymer specific volume. Van der Waals volume was calculated via the group contribution method of Bondi.³⁴

It is well known, that a surplus in FFV (i.e., excess FFV) in glassy polymers exists due to restricted polymer segmental mobility in glassy state when glassy polymers compare to rubbery polymer in an equilibrium state. The glassy polymer is in a metastable and unrelaxed state, consisting of excess free volume, which is frozen into the polymer matrix.^{13, 15} In Figure 1.3, the relationship between polymer specific volume and temperature in rubber and glass state is depicted.

Figure 1.3 schematically presents the relationship between polymer specific volume and temperature in rubber and glass state.¹⁵ V_0 is the volume occupied by polymer chains, V_f refers to polymer specific volume, V_g is the polymer specific volume including unrelaxed free volume.

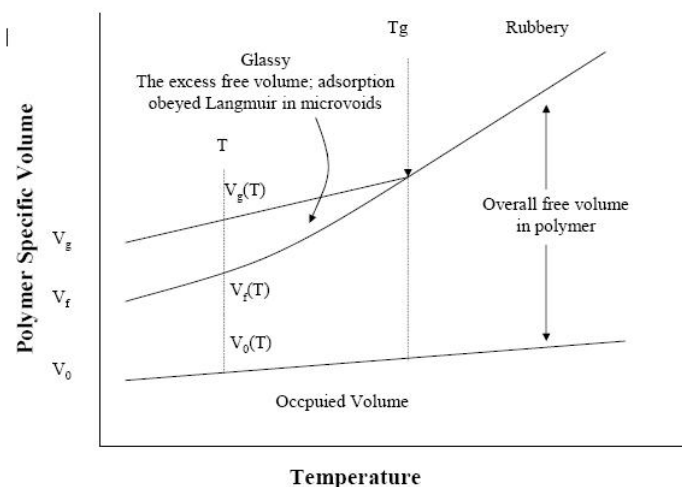


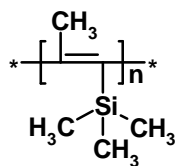
Fig. Schematic representation of the relationship between the polymer specific volume and temperature in amorphous polymers

It is of the greatest interest to understand the correlations between the free volume properties and the gas transport properties. Lee³⁵ has firstly correlated the FFV to the gas permeability on the basis of a specific free volume diffusion theory. Furthermore, Park and Paul¹⁷ have made a progress in more accurately predicting the relationship between FFV and permeability.

1.3.2 The most permeable glassy polymer with high FFV

Poly(1-(trimethylsilyl)-1-propyne) (PTMSP) has the highest gas permeability among all known polymers, and has been synthesized and described first by Masuda et al.³⁶ For example, the oxygen permeability in PTMSP is nearly four orders of magnitude higher than that of low FFV, conventional glassy polymers such as polysulfone.³⁷ These unusual transport properties are predominantly attributed to the extremely high FFV (0.29),³⁸⁻⁴⁰ which constructs an interconnected network making up to about 20-25% of total volume in the PTMSP polymer. Hence, PTMSP may be regarded as a polymer with an intrinsic microporosity.^{41, 42} Srinivasan et al.³⁹ and Pinnau et al.⁴⁰ supposed that gas permeation takes place in this microporous network. As we can see from the chemical structure of PTMSP shown in Figure 1.4, the high FFV primarily results from the rigid -C=C- backbone containing the bulky trimethylsilyl pending group, which prevents the polymer chains from effectively packing.^{38, 43}

Figure 1.4 The chemical structure of poly(1-(trimethylsilyl)-1-propyne)

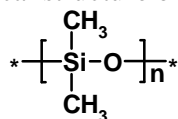


The distinctive gas transport properties and unusual FFV in PTMSP have raised a large interest in synthesizing numerous derivatives of polyacetylenes by modifying the bi-substitutes attached to the double bond.³⁷ Noticeably, the polyacetylene family exhibits a wide range of difference in permeability. Some polyacetylenes even display three orders of magnitude lower permeability compared to that of PTMSP. For example, oxygen permeability is just 3.8 Barrer (1 Barrer = 10^{-10} cm³(STP)·cm/(cm²·s·cmHg)) in poly[1-phenyl-2-[4-(triphenylsilyl)phenyl]acetylene] (pPh3SiDPA) reported by Teraguchi et al.⁴⁴ The extremely large differences in gas permeability for the polyacetylene family result from varied polymer chain packing, which leads to the corresponding various size of FFV, inter-chain spacing and connection behavior of the free volume.³⁷ Until now, more than 50 polyacetylenes with various pending groups have been synthesized, PTMSP with nonpolar bulky side groups -Si(CH₃)₃ still has unprecedented fast permeability over its analogues.³⁷

1.3.3 The most permeable rubbery polymer with high flexibility

Polydimethylsiloxane (PDMS), the most permeable polymer before the invention of PTMSP, is used commercially for organic vapors and non-condensable gases separation. In contrast to conventional glassy polymers, PDMS is permeable to many organic vapors (e.g., butane) faster than to smaller gases (e.g., methane), and PDMS separates gases based on the solubility selectivity. Stern et al.,³⁰ has systemically investigated the transport behavior correlated to the backbone and side chain changes in silicone polymers. Compared to PDMS, the decreased diffusivity and solubility have been observed to various extents in the substituted silicone polymers with various bulky functional groups in the side and backbone chains. The highly permeable PDMS is attributed to the high flexibility of the siloxane (Si-O) linkages, and its large free volume with bulky pending group -CH₃, which gives PDMS very low cohesive energy density (228.2 J/cm³) and high FFV, respectively. The PDMS structure is shown in Figure 1.5.

Figure 1.5 The chemical structure of polydimethylsiloxane



1.3.4 The introduction of bulky trimethylsilyl group into other polymer matrices

Previous structure/properties studies have provided some empirical rules for designing polymeric membrane materials. The highest permeable polymer PTMSP originates from the lowest critical surface tensions trimethylsilyl group and methyl group in each segment, resulting in a large excess free volume in the unrelaxed (Langmuir) domains of this glassy polymer that is indicated by unusually high gas solubility.³⁸ This phenomenon from polyacetylenes stimulates a huge interest in the introduction of TMS group into various polymer backbones. Several works revealed that the silyl groups often favored high gas permeability with minimal sacrifice in selectivity. For instance, it was found that, the substitution of trimethylsilyl (TMS) group of one proton of polyethylene significantly increased the oxygen permeability of 44 Barrer compared to the unmodified one of 2.2 Barrer, and even the oxygen/nitrogen selectivity increased from 2.9 to 4.0.⁴⁵ Table 1.2 summarizes the oxygen permeability and oxygen/nitrogen selectivity in TMS-substituted polymers and their precursor polymers. The presence of bulky silyl groups on the polymer chain is of special interest to gas separation because of their potential to inhibit chain mobility and to give more open chain packing. This restricted main chain motions and increased interchains distances will result in increased size selectivity and increased gas solubility, respectively. This optimized combination of chain mobility and chain packing can lead to improved separation performances in gas permeability and permselectivity.

Table 1.2 Summary of the oxygen permeability and oxygen/nitrogen selectivity in TMS-substituted polymers and their precursor polymers.

Polymer	Structure	FFV	P(O ₂)	P(O ₂)/P(N ₂)	Ref.
Polyethylene		-	2.9	2.9	45
Poly(vinyltrimethylsilane)		-	44	4.0	45
Polystyrene		-	2.9	5.5	46
Poly(p-trimethylsilylstyrene)		-	56	3.5	46
Polynorbornene		0.15	6.9	4.6	47
Poly(trimethylsilylnorbornene)		0.275	780	2.6	47
Poly(1,4-dimethylphenylene oxide)		-	10.6	4.1	48
Poly(1,4-dimethylphenylene oxide) with 100% TMS-substitution		-	46.5	3.9	48
Ethylcellulose		0.185	18	3.6	49
TMS-ethylcellulose		0.180	45	3.2	49
Cellulose acetate		-	0.27	6.14	50
TMS-cellulose acetate		-	7.4	4.11	50

1.3.5 Composite membranes

1.3.5.1 Mixed matrix membranes with inorganic fillers

As an alternative to new polymer synthesis, mixed matrix membranes (MMMs) are to combine the readily processable polymer with high selectivity inorganic molecular

sieve to overcome the trade-off limitation of polymer membranes.⁹ The MMMs for gas separation have been not only the subject of growing interest in the past 10 years,⁵¹ but also recommended to be a promising alternative for the next generation membrane. Generally, in MMMs the incorporated inorganic filler consists of well-defined porous structure such as zeolites, or carbon molecular sieves (CMS). For example, Kulprathipanja et al.⁵² observed that the incorporation of silicalite into cellulose acetate improved O₂/N₂ selectivity from 3.0 to 3.6. Jia and Peinemann⁵³ firstly reported the silicalite/PDMS mixed matrix membrane for a slightly improved selectivity in O₂/N₂ and CO₂/CH₄ compared to those of the unfilled PDMS. Moreover, the carbon molecular sieves (CMS) incorporated into cellulose acetate and polysulfones by Duval et al.,⁵⁴ and polyimides are reported by Vu et al.⁵⁴ This composite from Vu et al. even breaks through the empirical Robeson's upper bound for CO₂/CH₄ and O₂/N₂.²⁹ This polymer/inorganic hybridization seems to provide a readily means to obtain the optimal transport properties relative to the unfilled polymer.

Recently, one novel mixed matrix membrane with incorporated nonporous, nano-sized inorganic particle like silica has been added to the super glassy polyacetylene polymer matrix, resulting in the improved permselectivity for hydrocarbons over incondensable gases. This is attributed to increased fractional free volume by disrupting the polymer chain packing.^{55, 56, 57, 58, 59} This behavior is completely opposite to that of the traditional nonporous filler system, wherein this nonporous filler does not undertake the molecular sieve function in comparison of that of the conventional porous filler. Actually, by filling special particle, this way of the FFV modification owing to alternation of polymer chain packing offers another spectrum to fabricate a novel mixed matrix membrane with optimal performances. Recently, Gomes et al.⁶⁰ also observed the increased butane/methane selectivity in PTMSP/Silica nanocomposite membranes could be increased by the incorporation of silica by a sol-gel process. Yave et al.⁶¹ reported that a poly(1-trimethylgermyl-1-propyne) filled with TiO₂ nanoparticle system, which although does not show an improvement of gas transport performance, has obviously increased stability with loading of the filler after long time storage study.

However, the natural incompatibility between polymer host and inorganic filler leads to the inhomogeneous distribution of the filler and the unselective interface defect far

above molecular scale, which hinders the formation of the attractive composite materials for the practical application.^{62, 63}

1.3.5.2 Mixed matrix membranes with organic fillers

Compared to inorganic fillers, organic fillers exhibit remarkable better compatibility with polymer matrix system. In general, the addition of low molecular weight, organic molecules (i.e., diluents) into glassy polymer matrix results in increased polymer segments flexibility, and consequently increases the diffusion coefficient primarily by lowering the activation energy of diffusion. For example, Stannett suggests the additives decreases the polymer interchains cohesive force, resulting in an increase in segmental mobility.⁶⁴ However, the increased polymer chains mobility leads to a decreased excess FFV, which is caused by the unrelaxed free volume during polymer process. The loss in excess FFV will reduce the gas Langmuir absorption. Therefore, either increased or decreased permeability changes could be observed by filled polymer with additives, which is dependent on the extent of diffusivity and solubility changes. Simultaneously, the increased permeability is accompanied with decreased gas selectivity, and vice versa.

The physical incorporation of the low molecule weight, organic additives into membrane provides a simple way for modifying the gas separation properties of membrane materials. Maeda and Paul,⁶⁵⁻⁶⁸ Ruiz-Treviño and Paul,^{69, 70} Larocca and Pessan⁷¹ have systematically studied the gas transport properties in three practical membranes, i.e. polysulfone (PSF), poly(phenylene oxide) (PPO), and polyetherimide (PEI) with incorporation of various organic additives. Normally, it has been found that the addition of these fillers into glassy polymers reduces the gas permeability and enhances the selectivity, which can be interpreted by the retarded local chain mobility, reduced fractional free volume and the loss of excess free volume. However, no improvement in the separation performance has been reported.⁶⁸

1.3.5.3 Design of novel organic fillers for composite membrane

It is clear that the enhanced permselectivity phenomenon can only be exhibited if proper material selection and good interfacial interaction between the inorganic elements and polymeric matrix are fulfilled. However, the ability to form a defect-free ultra-thin top layer between inorganic fillers and polymer matrix seems to be an existing unprecedented hurdle, because of the intrinsic incompatibility between two phases. In order to obtain high permeation rates, the selective layer of gas separation membranes in practice must be extremely thin. For example, a typical and

commercially used membrane should have effective thicknesses of less than 0.5 μm and often less than 0.1 μm , which seem to be impracticable for traditional mixed matrix membranes with inorganic fillers.

As an alternative to circumvent the incompatibility, the organic fillers should be taken into account. However, in order to improve the separation performance of composites, the careful design of organic filler properties such as FFV and mobility might result in a commercially successful membrane.

1.4 Reference

1. Graham, T. *Philosophical Magazine* **1866**, 32, **401**.
2. Ghosal, K.; Freeman, B. D. *Polymer for advanced technologies* **1993**, 5, **673**.
3. Boeddeker, K. W. *J. Membr. Sci.* **1995**, 100, **1**.
4. Baker, R. W. *Ind. Eng. Chem. Res.* **2002**, 41, **1393**.
5. Loeb, S.; Sourirajan, S. *Adv. Chem. Ser.* **1962**, 38, **117**.
6. Petersen, R. J. *Journal of Membrane Science* **1993**, 83, **81**.
7. Kesting, R. E. *Synthetic Polymeric Membranes*, Wiley-Interscience, 2nd Ed., 1985.
8. Nunes, S.-P.; Peinemann, K.-V. Gas separation with membrane. In *Membrane technology in the chemical industry*; Nunes, S.-P.; Peinemann, K.-V., Eds.; Wiley-VCH: Weinheim, 2001; pp 39-67.
9. Peinemann, K. V. *Maku* **2006**, 31, **86**.
10. Petropoulos, J. H. *J. Membr. Sci.* **1990**, 53, **229**.
11. Petropoulos, J. H. *Membr. Proc., Indo-EC Workshop* **1991**, 253.
12. Wijmans, J. G.; Baker, R. W. *J. Membr. Sci.* **1995**, 107, **1**.
13. Petropoulos, J. H. *Polymeric Gas Separation Membranes*, CRC Press, chapter 2. D. R. Paul, Yu. P. Yampolskii (Eds.), 1994.
14. Brubaker, D. W.; Kammermeyer, K. *Ind. Eng. Chem.* **1954**, 46, **733**.
15. Van Krevelen, D. W. *Properties of Polymers* 3rd completely revised edition, Elsevier, 1990.
16. Yampolskii, Y.; Shishatskii, S.; Alentiev, A.; Loza, K. *J. Membr. Sci.* **1998**, 148, **59**.
17. Park, J. Y.; Paul, D. R. *J. Membr. Sci.* **1997**, 125, **23**.
18. Freeman, B. D. *Macromolecules* **1999**, 32, **375**.
19. Cohen, M. H.; Turnbull D. *J. Chem. Phys.* **1959**, 31, **1164**.

20. Teplyakov, V.; Meares, P. *Gas Sep. & Purif.*, **1990**, 4, **66**.
21. Barrer, R. M. *Trans. Faraday Soc.* **1942**, 38, **322**.
22. Barrer, R. M. *J. Phys. Chem.* **1957**, 61, **178**.
23. Van Amerongen, G. J. *J. Appl. Phys.* **1946**, 17, **972**.
24. Meares, P. *J. Am. Chem. Soc.* **1954**, 76, **3415**.
25. Koros, W. J.; Paul, D. R. *J. Polym. Sci.*, **1978**, 16, **1947**.
26. Pasternak, R. A.; Burns, G. L.; Heller, J. *Macromolecules* **1971**, 4, **470**.
27. Lin, H.; Freeman, B. D. *Macromolecules* **2005**, 38, **8394**.
28. Bondar, V. I.; Freeman, B. D.; Yampolskii, Y. P. *Macromolecules* **1999**, 32, **6163**.
29. Robeson, L. M. *J. Membr. Sci.* **1991**, 62, **165**.
30. Stern, S. A.; Shah, V. M.; Hardy, B. J. *Journal of Polymer Science Part B: Polymer Physics* **1987**, 25, **1263**.
31. Muruganandam, N.; Koros, W. J.; Paul, D. R. *Journal of Polymer Science, Part B: Polymer Physics* **1987**, 25, **1999**.
32. McHattie, J. S.; Koros, W. J.; Paul, D. R. *Polymer* **1991**, 32, **840**.
33. Adam, G.; Gobbs, J. H. *J. Chem. Phys.* **1965**, 43, **139**.
34. Bondi, A. *Journal of Polymer Science Part A* **1964**, 2, **3159**.
35. Lee, W. M. *Poly. Eng. Sci.* **1980**, 20, **65**.
36. Masuda, T.; Isobe, E.; Higashimura, T.; Takada, K. *Journal of the American Chemical Society* **1983**, 105, **7473**.
37. Nagai, K.; Masuda, T.; Nakagawa, T.; Freeman, B. D.; Pinnau, I. *Progress in Polymer Science* **2001**, 26, **721**.
38. Ichiraku, Y.; Stern, S. A.; Nakagawa, T. *J. Membr. Sci.* **1987**, 34, **5**.
39. Srinivasan, R.; Auvil, S. R.; Burban, P. M. *J. Membr. Sci.* **1994**, 86, **67**.
40. Pinnau, I.; Toy, L. G. *J. Membr. Sci.* **1996**, 116, **199**.
41. Wang, X. Y.; Lee, K. M.; Lu, Y.; Stone, M. T.; Sanchez, I. C.; Freeman, B. D. *Polymer* **2004**, 45, **3907**.
42. Shantarovich, V. P.; Kevdina, I. B.; Yampolskii, Yu. P.; Alentiev, A. Yu. *Macromolecules* **2000**, 33, **7453**.
43. Fried, J. R.; Goyal, D. K. *Journal of Polymer Science Part B: Polymer Physics* **2000**, 36, **519**.
44. Teraguchi, M.; Masuda, T. *Macromolecules* **2002**, 35, **1149**.

45. Plate, N. A.; Durgarjan, S. G.; Khotimskii, V. S.; Teplyakov, V. V.; Yampolskii, Yu. P. *J. Membr. Sci.* **1990**, *52*, **289**.
46. Khotimskii, V. S. *J. Appl. Polym. Sci.* **2000**, *78*, **1612**.
47. Finkelshtein, E. S.; Makovetskii, K. L.; Gringolts, M. L.; Rogan, Yu. V.; Golenko, T. G.; Starannikova, L. E.; Yampolskii, Yu. P.; Shantarovich, V. P.; Suzuki, T. *Macromolecules* **2006**, *39*, **7022**.
48. Zhang, J.; Hou, X. H. *J. Membr. Sci.* **1994**, *97*, **275**.
49. Khan, F. Z.; Sakahguchi, T.; Shiotsuki, M.; Nishio, Y.; Masuda, T. *Macromolecules* **2006**, *39*, **6025**.
50. Morita, R.; Khan, F. Z.; Sakaguchi, T.; Shiotsuki, M.; Nishio, Y.; Masuda, T. *J. Membr. Sci.* **2007**, *305*, **136**.
51. Kulprathipanja, S. *Annals of the New York Academy of Science* **2003**, *984*, **361**.
52. Kulprathipanja, S.; Neuzil, R.W.; Li, N. N. *U.S. Patent 4740219* **1988**.
53. Jia, M. D.; Peinemann, K. V.; Behling, R. D. *J. Membr. Sci.* **1991**, *57*, **289**.
54. Koros, W. J.; Vu, De. Q.; Mahajan, R.; Miller, S. J. *U.S. Patent 6562110* **2001**.
55. Merkel, T. C.; Freeman, B. D.; Spontak, R. J.; He, Z.; Pinnau, I.; Meakin, P.; Hill, A. J. *Science* **2002**, *296*, **519**.
56. Merkel, T. C.; Freeman, B. D.; He, Z.; Morisato, A.; Pinnau, I. *Proc. Am. Chem. Soc. Div. Polym. Mater.: Sci. Eng.* **2001**, *85*, **301**.
57. Merkel, T. C.; Freeman, B. D.; He, Z.; Pinnau, I.; Meakin, P.; Hill, A. J. *Chem. Mater.* **2003**, *15*, **109**.
58. Merkel, T. C.; He, Z.; Pinnau, I.; Freeman, B. D.; Meakin, P.; Hill, A. J. *Macromolecules* **2003**, *36*, **6844**.
59. Pinnau, I.; Morisato, A. *Desalination* **2002**, *146*, **11**.
60. Gomes, D.; Nunes, S. P.; Peinemann, K. V. *J. Membr. Sci.* **2005**, *246*, **13**.
61. Yave, W.; Peinemann, K. V.; Shishatskiy, S.; Khotimskiy, V.; Chirkova, M.; Matson, S.; Litcinova, E.; Lecerf, N. *Macromolecules* **2007**, *40*, **8991**.
62. Mahajan, R.; Zimmerman, C. M.; Koros, W. J. *In Polymer Membranes for Gas and Vapor Separation: Chemistry and Materials Science*; Freeman, B. D.; Pinnau, I., Eds.; American Chemical Society: Washington, DC, **1999**, 277-286.
63. Mahajan, R.; Koros, W. J. *Ind. Eng. Chem. Res.* **2000**, *39*, **2692**.
64. Crank, J.; Park, G. S. *Diffusion in Polymers*, London, Academic U.K., **1986**.
65. Maeda, Y.; Paul, D. R. *J. Polym. Sci., Part B: Polym. Phys.* **1987**, *25*, **957**.

- 66.** Maeda, Y.; Paul, D. R. *J. Polym. Sci., Part B: Polym. Phys.* **1987**, 25, **981**.
- 67.** Maeda, Y.; Paul, D. R. *J. Polym. Sci., Part B: Polym. Phys.* **1987**, 25, **1005**.
- 68.** Maeda, Y.; Paul, D. R. *J. Membr. Sci.* **1987**, 30, **1**.
- 69.** Ruiz-Trevino, F. A.; Paul, D. R. *J. Appl. Polym. Sci.* **1997**, 66, **1925**.
- 70.** Ruiz-Trevino, F. A.; Paul, D. R. *J. Appl. Polym. Sci.* **1998**, 68, **403**.
- 71.** Larocca, N. M.; Pessan, L. A. *J. Membr. Sci.* **2003**, 218, **69**

Chapter 2

2. Experiment

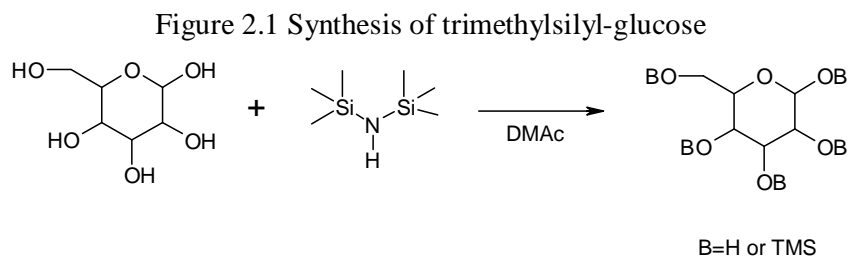
2.1 Synthesis of silylated-saccharides

2.1.1 Chemicals

Glucose was purchased from Aldrich, and dried in vacuum at 100 °C over night before use. 1,1,1,3,3,3-Hexamethyldisilazane (HMDS) (98%), chlorotriethylsilane (99%), chlorotri-*iso*-propylsilane (97%), 1, 3-dimethyl-1, 1, 3, 3-tetraphenyldisilazane (97%), and triethylamine (99%) were purchased from Acros chemicals, and were used without further purification. The solvent N,N-dimethylacetamide (DMAc) (99.5%), cyclohexane (99%) from Merck were degassed with nitrogen for 15 mins before use. Except silylated-saccharides, other two commercial available additives dioctylphthalate (DIPH) (99%) and pentaacetate glucose (PAG) (98%) were also used in this study. DIPH and PAG are purchased from Acros chemicals, which were used without further treatment.

2.1.2 Synthesis and characterization of trimethylsilyl-glucose

The synthesis of TMSG using the silyl-agent HMDS and glucose has been performed in DMAc at 80 °C under nitrogen atmosphere for 12 hours. The method is similar to that reported by Mormann et al. ¹ and Nouvel et al. ² Figure 2.1 shows the synthesis formula.

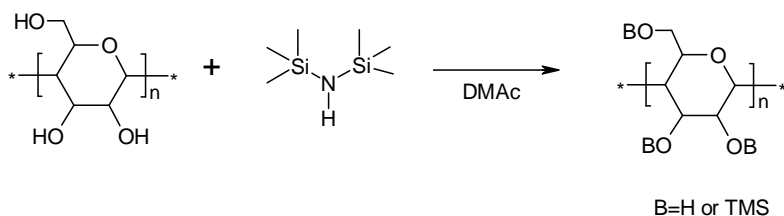


3 g Glucose was mixed with 120 ml DMAc in a 250ml round flask and stirred at 80 °C under nitrogen gas protection. The 50 ml HMDS has been dropwise added through a drop-funnel over 3 hours, and then the mixture was continuously stirred for 9 hours in order to increase the silylation degree. The mixture was allowed to slowly cool down to room temperature. Afterwards, the mixture was poured into a separation funnel and 400 ml ice water was added. Then 150 ml hexane was added to extract the product. The extracted product in hexane was dried with anhydrous sodium sulfate and subjected to a rotation-evaporator for removing the solvent. The crude product was dried under vacuum at room temperature for 24 hours. The transparent liquid

product was characterized by $^1\text{H-NMR}$ and thermogravimetry analysis (TGA). The overall silylation degree was 83% with a good reproducibility, which was estimated from $^1\text{H-NMR}$ spectra according to Nouvel et al. ² The thermal stability of TMSG is up to 110 °C measured by TGA. The density of TMSG is 0.96-0.98 g/cm³. The TMSG is soluble in a broad range of solvents from highly polar solvents such as methanol to highly unpolar solvents such as cyclohexane.

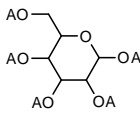
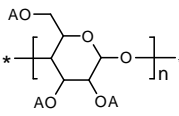
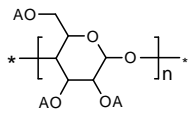
2.1.3 Synthesis and characterization of trimethylsilyl-dextran

Figure 2.2 Synthesis of trimethylsilyl-saccharides



Dextran (Mw= 900-1200) (Dextran1), and Dextran (Mw= 350-550 kD) (Dextran500) were obtained from Aldrich, and HMDS and all solvents were purchased from Merck. The saccharides were dried in a vacuum at 100 °C overnight before use. 3 g of saccharide was mixed with 120 ml DMAc in a 250 ml round flask and stirred at 80 °C under nitrogen gas protection. The 50 ml HMDS were added dropwise through a drop funnel over 3 h, and then the mixture was continuously stirred for 9 h in order to maximize the silylation degree. The mixture was allowed to slowly cool to room temperature. Afterward, the mixture was poured into a separation funnel, and 400 ml of ice water was added. Then 150 ml of hexane was added to extract the product. The extracted product in hexane was dried with anhydrous sodium sulfate and subjected to a rotation-evaporator for removing the solvent. The crude product was dried under vacuum at room temperature for 24 h. The product was characterized by $^1\text{H-NMR}$ and TGA. The overall silylation degree was 83 % for TMSG, 80 % for TMSD1, and 78 % for TMSD500 with a good reproducibility, which was estimated from $^1\text{H NMR}$ spectra according to Nouvel et al. ² The thermal stability determined by TGA, the glass transition temperature determined by DSC and the density of TMSS are presented in Table 2.1.

Table 2.1 Physical properties of trimethylsilylsaccharides (TMSS) fillers

name	trimethylsilyl -glucose	trimethylsilyl – dextran1	trimethylsilyl - dextran500
acronym	TMSG	TMSD1	TMSD500
structure ^a			
molecular weight ^b	180	900-1200	350-550k
silylation degree %	83	80	78
Tg (°C)	-	69.5	128.4-136.5
onset of weight loss (°C) ^c	110	240	-
density (g/cm ³) ^d	0.98 ± 0.15	0.97 ± 0.2	0.96 ± 0.2

a. A = -H or -Si(CH₃)₃

b. Molecular weight is based on the saccharides without silyl group.

c. Onset of weight loss is determined by TGA.

d. The density of polymers is determined from their weight and volume at room temperature.

2.1.4 The synthesis of 1, 3-dimethyl-1, 1, 3, 3-tetraphenylsilyl-glucose (DPMSG), triethylsilyl-glucose (TESG), and triisopropylsilyl-glucose (TIPSG)

1.5 g Glucose was mixed with 100 ml DMAc in a 250 ml round flask and stirred at 80 °C under nitrogen gas protection. The 10g 1, 3-dimethyl-1, 1, 3, 3-tetraphenyldisilazane dissolved in 20 ml DMAc has been dropwise added through a drop-funnel over 1 hour, and then the mixture was continuously stirred for 11 hours in order to maximize the silylation degree. The mixture was allowed to slowly cool down to room temperature. Afterwards, the mixture was poured into a separation funnel and 400 ml ice water was added. Then 150 ml hexane was added to extract the product. The extracted product in hexane was dried with anhydrous sodium sulfate and subjected to a rotation-evaporator for removing the solvent. The crude product was dried under vacuum at room temperature for 24 hours. The light yellow viscous liquid product was characterized by ¹H-NMR. The overall silylation degree was ~ 78 %, which was estimated from ¹H-NMR spectra. DPMSG is soluble in polar solvents like methanol as well as in unpolar solvents like cyclohexane.

The synthesis of TESG and TIPSG is similar to that of TMSG. Except that the suitable amount of triethylamine (with respect to chlorotriethylsilane and chlorotriisopropylsilane in molar ratio, respectively) was added into the mixture before

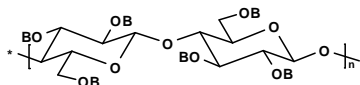
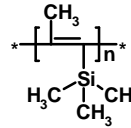
adding the corresponding silane agents. The silylation degree was determined by proton $^1\text{H-NMR}$ was 88%, 75% for TESG and TIPSG, respectively.

2.2 Film preparation

2.2.1 General procedures of nanocomposite films preparation

PTMSP and EC were purchased from Gelest and Aldrich, respectively. The physical properties for both polymers are presented in Table 2.2 (i.e., molecular weight, density, fractional free volume by Bondi method, and glass transition temperature by DSC). Before film preparation, PTMSP was purified via reprecipitation with methanol. EC was used directly without any treatment. For PTMSP/TMSS composite system, 1 % (w/v) PTMSP polymer solution in dry cyclohexane was prepared in a glass bottle at room temperature. Various amounts of TMSS were added to the PTMSP polymer solution. The transparent homogeneous solution was filtered and poured into an aluminum ring, which was supported by a dust-free, dry, and flat glass plate. Subsequently, the solvent was allowed to evaporate slowly for 1–2 days at room temperature by covering a glass dish. After solvent evaporation the film was further dried under an oil-free vacuum over night to completely remove residual solvent. The film was removed from the glass plate by immersion in water and dried under an oil-free vacuum overnight again. For EC/TMSS composites system, 2 % (w/v) EC polymer solution in dry chloroform was prepared in a glass bottle at room temperature. Various amounts of TMSS were added to the EC polymer solution. The membrane formation process is the same as described above for the PTMSP/TMSS system. Film thickness varied from 50 to 120 μm , which was measured by a digital micrometer with a precision of $\pm 2 \mu\text{m}$. Finally, the films were cut into a round disk with diameter of 4.6 cm for a time-lag test cell. The freshly prepared PTMSP/TMSS films were directly analyzed by time-lag in order to reduce the influence of PTMSP aging as much as possible. EC/TMSS films are storable at labor bench.

Table 2.2 Physical properties of ethylcellulose and poly(1-trimethylsilyl-1-propyne)

polymer	Ethylcellulose	poly(1-trimethylsilyl-1-propyne)
acronym	EC	PTMSP
Structure		
Molecular weight	-	480 kDa ²⁰
T _g (°C)	125 – 130	> 250 ²⁶
Density (g/cm ³) ^a	1.12±0.02	0.78±0.02
Fractional free volume	0.15	0.30
Ethoxy content	46 %	-

a. The density of polymers is determined from their weight and volume at room temperature.

2.3 Composite film characterizations

2.3.1 Glass transition temperature

Thermal analysis for EC/TMSS composites was carried out using a differential scanning calorimeter (DSC) (Netzsch Thermal Analysis DSC204, Germany). The glass transition temperatures for PTMSP/TMSS system are absent, because the polymer PTMSP doesn't exhibit a clear T_g . Before the analysis, the samples were dried in a vacuum oven at 80 °C overnight. DSC scans were performed in a nitrogen atmosphere at a heating rate of 10 °C /min from –50 to 110 °C for the first scan, and then cooling to –50 °C at the same rate. The second scan was heated from –50 to 150 °C for determination of glass transition temperature.

2.3.2 Optical inspection of composite film

All EC/Trimethylsilyl-glucose (TMSG), EC/Trimethylsilyl-saccharose (TMSSA), EC/Triethylsilyl-glucose (TESG), EC/Triisopropylsilyl-glucose (TIPSG), and EC/Diphenylmethylsilyl-glucose (DPMSG) and EC/Trimethylsilyl-dextran1 (TMSD1), PTMSP/TMSG and PTMSP/TMSD1 composite films are transparent and featureless via optical observation, indicating an excellent miscibility of EC/TMSG, EC/TMSSA, EC/TESG, EC/TIPSG, EC/DPMSG, EC/TMSD1, PTMSP/TMSG, and PTMSP/TMSD1 composites. In contrast, the EC/Trimethylsilyl-dextran500 (TMSD500) and PTMSP/TMSD500 composite films are opaque, suggesting the phase separation. The evaluation of the miscibility of composite material via the optical observation has been discussed elsewhere.³

2.3.3 Scanning electron microscopy

Scanning electron microscopy was performed to investigate the morphology of

EC/TMSS and PTMSP/TMSS composites with a LEO 1550 VP Gemini from ZEISS instrument. The specimens were frozen under liquid nitrogen, which was described elsewhere.⁴ then fractured, mounted, and coated with 2 nm Au/Pd by a magnetron sputtering process (Emitec K575). SEM cross-section micrographs were obtained at 1 and 3 kV accelerating voltage for EC and PTMSP composites, respectively. The low accelerating voltage was chosen for saccharides, which are electron beam sensitive.

2.3.4 Gas transport properties with time-lag

Gas permeation data were measured at 30 °C with six pure gases (helium, hydrogen, carbon dioxide, oxygen, nitrogen, and methane) by a pressure increase time-lag apparatus, which has been described elsewhere.⁵ The feed pressure used was between 200 and 400 mbar for the larger gases (carbon dioxide, oxygen, nitrogen, and methane) and around 100 mbar for smaller gases (helium and hydrogen). The permeate pressure was maintained at less than 10^{-7} bar with an oil-free vacuum pump. The gas permeability P was calculated under steady state (constant permeance) by the Equation 2.1:

$$P = \frac{V_p l}{ART\Delta t} \ln \left(\frac{p_f - p_{p_1}}{p_f - p_{p_2}} \right) \quad (\text{eq. 2.1})$$

where V_p is the constant permeate volume (m^3), l is the film thickness (m), R is the gas constant ($8.314 \text{ Pa m}^3 \text{ mol}^{-1} \text{ K}^{-1}$), A is the film area (m^2), T is the temperature (K), Δt is the time (s) for permeate pressure increase from p_{p_1} to p_{p_2} , p_f is feed pressure (Pa), and the unit of P is $\text{mol m}^{-1} \text{ s}^{-1} \text{ Pa}^{-1}$. To obtain the permeability in barrer ($1 \text{ barrer} = 10^{-10} \text{ cm}^3 (\text{STP}) \text{ cm}/(\text{cm}^2 \text{ s cmHg})$), the value has to be multiplied by 2.99×10^{15} .

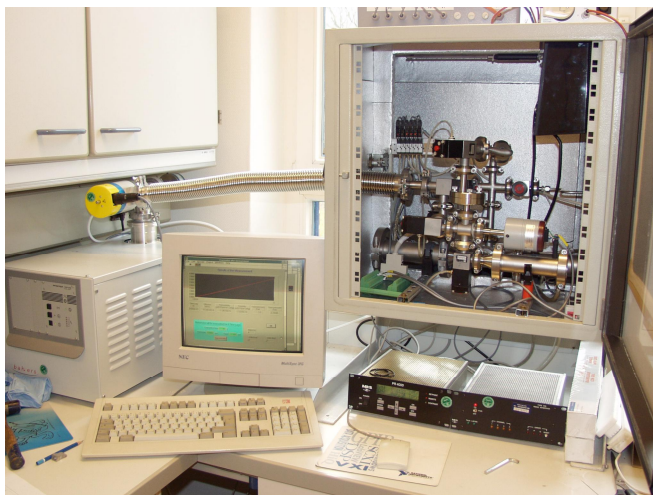
The solution-diffusion transport model is applied for gas transport process through dense polymer film. It means, that the permeability coefficient P can be defined as eq. 1.1 in Chapter 1. The diffusion coefficient D can be directly obtained by the time-lag method under the assumption of a constant diffusion coefficient. As the gas transport through the film reaches a steady state, the diffusion coefficient D can be calculated by eq 2.2

$$D = \frac{l^2}{6\theta} \quad (\text{eq. 2.2})$$

where θ is the time-lag (s). The solution coefficient can then be derived from eq 1.1. The vacuum time-lag equipment (Figure 2.3) is constructed in GKSS research centre, Geesthacht. It provides a method to assess the permeability and diffusion coefficients

of a gas through a polymer film for a given set of operating conditions (temperature and pressure). The permeate gas is allowed to accumulate in a pre-evacuated permeate side with a defined volume over time. The mathematical analysis is based on equation 2.2 for acquiring the diffusion coefficient.

Figure 2.3 Time-lag equipment



The permselectivity of a polymer film for component A relative to component B is the ratio of their permeation coefficients. Since the permeation coefficient is the product of the diffusion coefficient and solubility coefficient, the permselectivity for two gases has been described in eq. 1.14 in chapter 1.

The systematic error in the permeability measurements is mainly from the determination of the membrane thickness with an error of $\pm 5\%$. In addition, the systematic error of the diffusivity measurements originates mainly from the time resolution of the time-lag (time resolution: 0.05 s). In this study, the diffusivity systematic error is not beyond $\pm 6\%$. In addition, the time-lag has been verified to have high precision by Petropoulos et al.⁶

2.4 References

1. Mormann, W.; Demeter, J. *Macromolecules* **1999**, *32*, **1706**.
2. Nouvel, C.; Ydens, I.; Degée, P.; Dubois, P.; Dellacherie, E.; Six, J. L. *Polymer* **2002**, *43*, **1735**.
3. Roberto, A. K. Transmission and reflection of light in multiphase media. In *Polymer Blends: Formulation and Performance*; Paul, D.R. and Bucknall, C.B., Eds.; John Wiley & Sons; 2000; pp 301-304.
4. Schossig-Tiedemann, M. *Beitr. Elektronenmikroskop. Direktabb. Oberfl.* **1994**, *27*, **209**.

5. Shishatskii, S.; Yampolskii, Yu. P.; Peinemann, K. -V. *J. Membr. Sci.* **1996**, *112*, **275**.
6. Petropoulos, J. H.; Myrat, C. *J. Membr. Sci.* **1977**, *2*, **3**.

Chapter 3

Gas transport properties in a poly(trimethylsilyl-propyne) composite Membrane with nanosized organic filler trimethylsilyl-glucose

3.1 Abstract

A novel composite membrane made from the high free volume polymer poly(trimethylsilyl-propyne) and the small organic filler trimethylsilyl-glucose (TMSG) is reported. The permeabilities, diffusivities and solubilities of six gases (He, H₂, CO₂, O₂, N₂, and CH₄) were determined in these PTMSP/TMSG composites with a series of TMSG loading using the time-lag method. Increasing TMSG content in PTMSP resulted in substantial reduction of all gas permeabilities. The observed decrease in permeability was much larger than predicted by the Maxwell model for the incorporation of impermeable fillers. In addition, the permeability loss varied significantly from gas to gas, leading to increased selectivities for some gas pairs. For example, nitrogen permeability (9.6 Barrer) in PTMSP containing 56.8 vol.% TMSG decreased by more than 600-fold compared to that of unfilled PTMSP (5490 Barrer). Simultaneously, the O₂/N₂ selectivity increased from 1.5 up to 3.4. The varying permeability behavior in PTMSP/TMSG composites is in good agreement with the diffusivity change. In addition, a parallel reduction in solubility for all tested gases was observed. In these composites, the natural logarithms of the diffusivities and solubilities are well linearly related to the square of penetrant diameter and their condensability, respectively. It was observed that the activation energy of permeation increased with TMSG content. From the analysis of temperature dependence of the gas permeability, it is concluded that the gas transport in pure PTMSP and PTMSP/TMSG composites follows different mechanisms. Additionally, the PTMSP/TMSG composite membranes offer a readily accessible mean to physically modify the FFV in PTMSP polymer, and to achieve the desired gas permeability and permselectivity compared to the pure polyacetylene polymers.

3.2 Introduction

High free volume polymer PTMSP is the most gas permeable polymer, which is comprehensively discussed in the introduction part. Many efforts were also made to modify the FFV in PTMSP through physical means (e.g. particle-filling). For example, an increased FFV in PTMSP composite system by incorporating nonporous fumed silica (FS), thereby resulting in an increased gas permeability, was reported by Merkel

et al. ¹ and Gomes et al. ². On the other hand, a decreased FFV in fullerene filled PTMSP matrix causing a decreased permeability was described by Higuchi et al. ³ Li and Freeman also observed a drastically decreased permeability in PTMSP containing 1.5 nm POSS particles ⁴. In practice, Langsam et al. ⁵ has also reported a decreased permeability accompanied with an increased selectivity in PTMSP with a large number of additives such as silicon oils, non-ionic surfactants, hydrocarbon oils, flame retardant additives and so on. But, the systemic investigation for PTMSP with organic fillers is still missing. In addition, the commonly used fillers are inorganic particles, which have a notorious problem in compatibility with the polymer matrix, therefore, frequently producing defects. ⁶ In this study, a novel PTMSP composite membrane with the compatible organic filler trimethylsilyl-glucose is reported. The effect of TMSG addition on the FFV modification and the corresponding gas transport properties in PTMSP are discussed.

3.3 Results and discussions

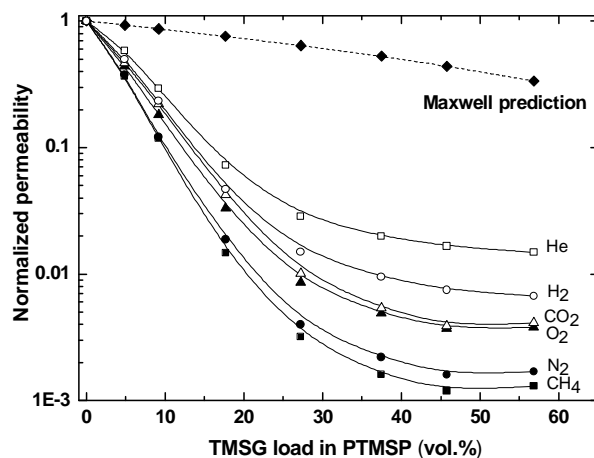
3.3.1 Permeability and permselectivity in PTMSP/TMSG

In Table 3.1 the effect of TMSG filler in PTMSP on the permeability coefficients of six light gases (He, H₂, CO₂, O₂, N₂, and CH₄) is illustrated. The incorporation of TMSG in PTMSP leads to a drastic decrease in gas permeability. For instance, in PTMSP loaded with 5 vol.% TMSG all gas permeability coefficients decreased by nearly 50 % compared to pure PTMSP. As PTMSP is loaded with 56.8 vol.% TMSG, the nitrogen permeability even reduces by more than 600-fold. Based on the data in Table 3.1, the normalized gas permeability (*calculated as the ratio of the permeability in the various amount TMSG filled PTMSP to the unfilled PTMSP*) as a function of the loading content of TMSG is plotted in Figure 3.1, where the prediction of the classical Maxwell model can be used to describe the decrease of permeability of a homogeneous polymer phase containing an impermeable filler. ⁷ Figure 3.1 demonstrates, that a significantly negative deviation of the gas permeability is observed relative to the Maxwell model. It means, the gas permeability reduction in PTMSP/TMSG composites can not be explained by the simple tortuous effect.

Table 3.1 Gas permeability of the PTMSP/TMSG composite membranes at 30 °C

Loading of TMSG in PTMSP (vol.%)	Permeability $\times 10^{10}$ (cm ³ (STP) cm/ (cm ² s cmHg))					
	He	H ₂	CO ₂	O ₂	N ₂	CH ₄
0.0	5690	15850	31333	8120	5490	14833
4.9	3223	7910	14600	3580	2070	5430
9.2	1680	3713	6923	1480	668	1760
17.7	413	743	1320	270	104	218
27.2	162	238	316	70	22	48
37.4	113	151	168	40	12	24
45.8	94	119	123	30	9	18
56.8	85	106	129	31	9	19

Figure 3.1: Normalized gas permeability coefficients for six gases (He(\square), H₂(\circ), CO₂(Δ), O₂(\blacktriangle), N₂(\bullet), and CH₄(\blacksquare)) and Maxwell model prediction(\blacklozenge) as a function of loading amount of TMSG in PTMSP.



This strongly reduced permeability is seemingly related to the reduced accessible free volume caused by the TMSG occupation of partial FFV in PTMSP. It is speculated that the organic filler TMSG can enter the interconnected FVE⁸⁻¹⁰ and to some extent occupy the “micropores”¹¹ in PTMSP. Such behavior was also reported in the study of PTMSP filled with low molecular weight polydimethylsiloxane (PDMS) by Nakagawa and coworkers.¹² In this study, the “pore-filling” hypothesis can be reasonably supported by the direct size comparison between the volume of the presumably spherical FVE in PTMSP^{9, 10} and the spherical TMSG molecule. Table 3.2 presents the estimated size for both, which indicates, that TMSG may be allowed to enter the partial FFV in PTMSP without disruption of polymer chain packing.

Table 3.2 Estimated volume of spherical TMSG and PTMSP FFV, respectively. The diameter of the TMSG molecule is about 10 Å, the PTMSP FFV radii expand from 1-9 Å from Hofmann et al.¹⁰

	Volume (Å ³)
TMSG	811
PTMSP FFV	5.6 – 3052

The analysis of the permeability decrease with TMSG content can further validate the assumption of the “pore-filling” in PTMSP with TMSG. In Figure 3.3, the decline in permeability for all six gases can be obviously divided into two stages. In the first stage, the permeability decreases radically with increasing TMSG loading, followed by a smooth decrease in permeability in the second stage. The turning point lies at the loading of around 27 vol. % TMSG. For example, about 250-fold loss in nitrogen permeability is observed at the loading of TMSG from 0 to 27 vol. %. In contrast, a relatively small decrease for nitrogen permeability (2.5-fold) takes place from 27 to 57 vol. % TMSG loading. A reasonable explanation for such behavior can be based on the hypothesis as well, that TMSG may firstly fill the larger interconnected FVE^{11, 13}, which contribute to the fast gas transport. After the available large free volume is occupied, the additional loaded TMSG may just reside between polymer chains, leading to an increased tortuosity for gas transport, this behavior is in line with the prediction of the Maxwell model.¹⁵ Srinivasan et al.¹¹ and Pinnau et al.¹³ assumed about 20 to 25% connected free volume is in PTMSP, and suggested most gas permeates through this interconnected FVE. In contrast, the other 75 to 80% dense polymer matrix contributes insignificantly to the gas permeation. This statement is consistent with the experimental results: around 27 vol. % loading TMSG can block the fast gas transport passage in PTMSP.

Such behavior further indicates that addition of TMSG can readily modify the FFV in PTMSP. To discuss this physical modification of FFV in PTMSP, the nitrogen permeability behavior in PTMSP/TMSG composite membranes is compared with that of four representative polyacetylenes derivatives with declined FFV (poly(1-trimethylsilyl-1-propyne) (FFV=0.29), poly(4-methyl-2-pentyne) (PMP) (FFV=0.28), poly[1-phenyl-2-[*p*-(trimethylsilyl)phenyl]acetylen-e] (PTMSDPA) (FFV=0.26) and poly(1-phenyl-1-propyne) (PPP) (FFV=0.22), which were reported by Toy and coworkers.¹⁵ In Figure

3.2, the nitrogen permeability is plotted as a function of the TMSG loading in PTMSP/TMSG composites. For comparison, the nitrogen permeability in four polyacetylenes as a function of the corresponding reciprocal FFV is also presented. Obviously, the simple process of filling PTMSP with TMSG leads to similar nitrogen permeabilities, which were obtained with the different polyacetylenes. In the polyacetylenes, the decrease in the nitrogen permeability is well correlated to the decrease in FFV.¹⁵ In PTMSP/TMSG composites, the similar relationship between the nitrogen permeability and the content of TMSG is observed as well. By analogy, it is reasonable to speculate, that the loading with TMSG can systemically reduce the FFV in PTMSP, consequently, reducing the permeability.

Besides a radical decrease in gas permeability in the PTMSP/TMSG composites, as clearly shown in Figure 3.1, the permeability decrease varies significantly from gas to gas. For instance, at the content of 27.2 vol.% TMSG in PTMSP, compared to the unfilled PTMSP, the permeability reduction is 35-fold for helium, 66-fold for hydrogen, 99-fold for carbon dioxide, 117-fold for oxygen, 248-fold for nitrogen, 312-fold for methane. The permeability decrease is apparently gas-size dependent. The rank of the permeability decrease of the gases is $\text{He} < \text{H}_2 < \text{CO}_2 < \text{O}_2 < \text{N}_2 < \text{CH}_4$, which is in a good agreement with the effective gas diameter order:¹⁶ $\text{He} (0.178\text{nm}) < \text{H}_2 (0.214\text{nm}) < \text{O}_2 (0.289\text{nm}) \approx \text{CO}_2 (0.302\text{nm}) < \text{N}_2 (0.304\text{nm}) < \text{CH}_4 (0.318\text{nm})$. Moreover, a consistent increase in permselectivity is observed for gas/ N_2 pairs (except methane/nitrogen because methane is larger than nitrogen) with increasing amount of TMSG in PTMSP, which is summarized in Table 3.3. It can be seen, PTMSP has almost no selectivity for He/ N_2 , but PTMSP with 45.8 vol.% TMSG displays almost a selectivity of 9. In order to visibly express the permselectivity change in the PTMSP/TMSG composites, the normalized permselectivity of the other five gases over nitrogen as a function of TMSG loading in PTMSP is plotted in Figure 3.3. The larger the size difference of the permeating gas-pair, the higher the increased permselectivity of the gas pair with increased loading of TMSG in PTMSP. Such behavior can be explained by the increased size selectivity in PTMSP/TMSG composites.

As generally observed, the size selectivity increases as permeability decreases in the PTMSP/TMSG membranes, which is in accordance with the well-known permeability/selectivity trade-off relationship.¹⁷ This behavior may be rationalized

from free volume consideration.¹ The decreased permeability and enhanced permselectivity exhibited by filling PTMSP with TMSG are believed to arise from the reduced, less selective interconnected FFV. Therefore, the small “conventional” free volume in PTMSP contributes to increase the size selectivity in the composites. Such behavior is typical for the low volume, conventional glassy polymers^{13, 18}

Table 3.3 Selectivities of various gases over nitrogen in PTMSP with various amounts of TMSG at 30 °C

Loading of TMSG in PTMSP (vol.%)	Gas/N ₂ selectivity				
	He	H ₂	CO ₂	O ₂	CH ₄
0.0	1.0	2.9	5.7	1.5	2.7
4.9	1.6	3.8	7.1	1.7	2.6
9.2	2.5	5.6	10.4	2.2	2.6
17.7	4.0	7.2	12.7	2.6	2.1
27.2	7.3	10.8	14.3	3.1	2.2
37.4	9.5	12.7	14.1	3.3	2.0
45.8	10.7	13.5	13.9	3.4	2.0
56.8	9.2	11.5	14.0	3.4	2.1

Figure 3.2 Nitrogen permeability (P(N₂)) in four disubstituted acetylene polymers (□) (PTMSP, PMP, PTMSDPA, PPP)¹⁵ and in PTMSP/TMSG composites (○) as a function of reciprocal fractional free volume (1/FFV) of the polymer¹⁵ and the loaded amounts of TMSG in vol.%, respectively. (1 barrer = 10⁻¹⁰ cm³ (STP) cm/(cm² s cmHg)).

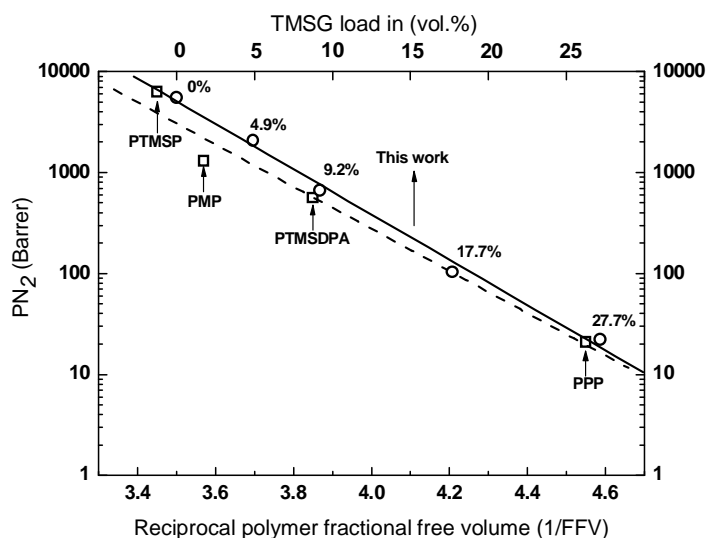
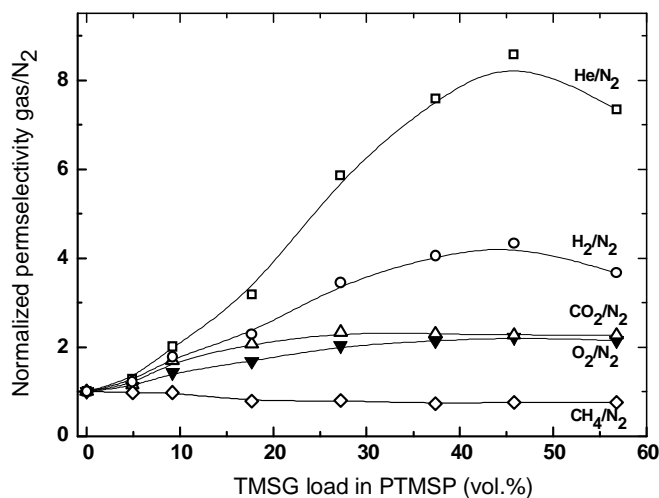
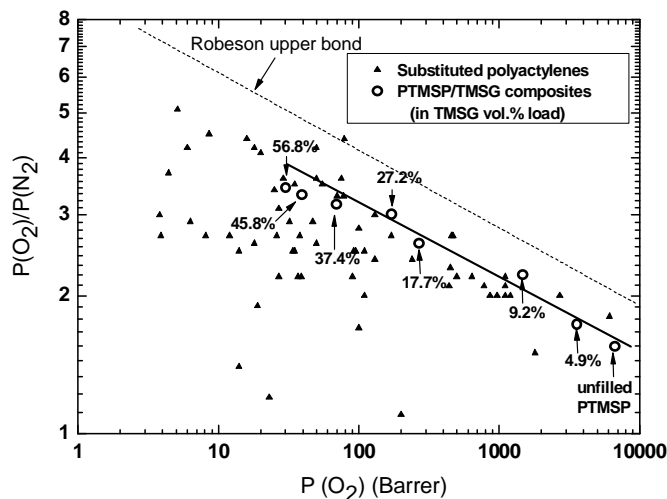


Figure 3.3 Normalized selectivities for five gases (He (\square), H₂ (\circ), CO₂ (Δ), O₂ (\blacktriangledown), CH₄ (\diamond)) over nitrogen in the PTMSP/TMSG composites as a function of loading amount of TMSG.



More specifically, the oxygen permeability and oxygen/nitrogen selectivity in PTMSP/TMSG composite membranes are compared. Figure 3.4 compares the correlation between oxygen permeability and oxygen/nitrogen selectivity for the substituted polyacetylenes¹⁹ and the PTMSP/TMSG composite membranes in this study. It clearly shows that the physical loading of TMSG in PTMSP can readily improve the selectivity of oxygen over nitrogen from 1.5 up to 3.5. The selectivity improvement, though, is along with a permeability decrease for O₂ from 8120 to 30 Barrer, which complies with the trade-off behavior relationship between the gas permeability and selectivity.¹⁷ Interestingly, in comparison with more than 50 synthesized polyacetylene polymers,¹⁹ PTMSP with various amount of TMSG exhibits a relatively good performance in terms of permeability and selectivity. Moreover, the optimal, tailored performance can be readily obtained via control of the TMSG loading compared to the time-consuming synthesis.

Figure 3.4 Relationship between oxygen permeability and its selectivity over nitrogen for substituted polyacetylenes (\blacktriangle)¹⁹ and PTMSP/TMSG composite membranes in this study (\circ). The upper bound line comes from Robeson.¹⁷



3.3.2 Diffusivity in PTMSP/TMSG

Since the permeation coefficient is a product of the diffusion and the solution coefficient, it is worthwhile to study both coefficients in order to get more insight in transport behavior of the PTMSP/TMSG composites. Table 3.4 presents the diffusion coefficients for He, H₂, CO₂, O₂, N₂, and CH₄ in PTMSP as a function of various contents of TMSG and the effective molecular diameter for each gas. The systematic decrease in diffusivity for all six gases is observed with increased contents of TMSG in PTMSP. Simultaneously, the diffusivity decrease is strongly related to the gas size difference. The small gas helium experiences the least loss in diffusivity; in contrast, the largest methane exhibits the largest loss. For example, in the PTMSP with 37 vol. % TMSG, helium diffusivity reduces by 5-fold compared to that in unfilled PTMSP, however, methane diffusivity reduces more than 100-fold. The gas diffusivity decline is well related to the gas size, which is ranked in the order of: CH₄ > N₂ > CO₂ ≈ O₂ > H₂ > He. In addition, the diffusivity change behavior is very similar to the permeability change in PTMSP/TMSG composites, which clearly indicates that the diffusivity plays a dominant role in the transport.

Table 3.4 Gas diffusion coefficients in a series of PTMSP/TMSG composite membranes at 30 °C in terms of the effective molecular diameter for six gases.

Gas	He	H ₂	CO ₂	O ₂	N ₂	CH ₄
Effective molecular diameters d_{eff} (nm)	0.178	0.214	0.302	0.289	0.304	0.318
Loading of TMSG in PTMSP (vol.%)	Diffusivity $\times 10^5$ (cm ² /s)					
0.0	25.2	29.4	3.2	4.5	3.5	3.02
4.9	19.9	16.4	1.65	2.24	1.47	1.21
9.2	14.1	10.5	0.83	1.07	0.68	0.46
17.7	5.9	3.7	0.22	0.3	0.16	0.09
27.2	4.3	2.0	0.09	0.15	0.08	0.04
37.4	3.6	1.5	0.06	0.11	0.06	0.03
45.8	3.2	1.4	0.05	0.1	0.05	0.02
56.8	3.4	1.5	0.07	0.13	0.07	0.03

It has been reported that major physicochemical factors, which control the gas diffusivity and selectivity of polymers are (1) cohesive energy density (CED) and (2) FFV, FVE size and size distribution and (3) gas–polymer interaction.²⁰ However, it is well-known that there are hardly any specific interactions of light gases with polymers at low gas pressures (<10 bar). It is also supposed that the CED of PTMSP/TMSG composites do not vary much by the physical addition of TMSG, because the special interactions between the hydrophobic filler TMSG and the hydrophobic polymer chains of PTMSP are absent. Thus, the gas diffusivity in the PTMSP/TMSG composite membranes depends mainly on the FFV. Theoretically, the diffusion coefficients straightforward reflect the mobility of molecule transport through the polymer.²¹ Cohen and Turnbull firstly formulated the mathematical relationship between the gas diffusion coefficient and the penetrate size combined with the polymer FFV, which is described in chapter 1.

In PTMSP, the extremely high FFV contributes to the high gas diffusivity.^{11, 13, 22} The decreased diffusivity in the PTMSP/TMSG composites obviously suggests less accessible FFV for gas transport, indicating that the filler TMSG occupies partial FFV in PTMSP. The observed improved diffusivity selectivity is mainly ascribed to the blocked interconnected FFV in PTMSP by TMSG. As a result, gas was forced to diffuse through the conventional FVE, where the size selectivity occurs as a conventional glassy, low free volume polymer.

According to Teplyakov and Meares' equation ¹⁶ (see chapter 1), Figure 3.5 presents the plots of the gas diffusivity as a function of the effective diameter in the PTMSP/TMSG composites. The intercept k_1 , slope k_2 and linear regression R parameters are summarized in Table 3.5. The linear relationship between the natural logarithm of gas diffusion coefficient and corresponding square of effective molecular size is proven (Regression value $R > 0.98$). As expected, it can be seen that the value of the slope (k_2) progressively increases with increase of TMSG loading, indicating the enhanced diffusivity selectivity. On the other hand, it is interesting to find that the intercept (k_1) systemically decreases with an increased content of TMSG, which is consistent with the gas diffusivity decrease. In other words, a large k_2 value always accompanies with a small value of k_1 and vice versa.

Figure 3.5 Plots of the natural logarithm of gas diffusivity as a function of square of its effective diameter in a series of PTMSP/TMSG composite membranes (TMSG loading in PTMSP: 0.0% (\square), 4.9% (\circ), 9.2% (Δ), 17.7% (∇), 27.7% (\diamond), 45.8% (\blacksquare), 56.8% (\bullet))

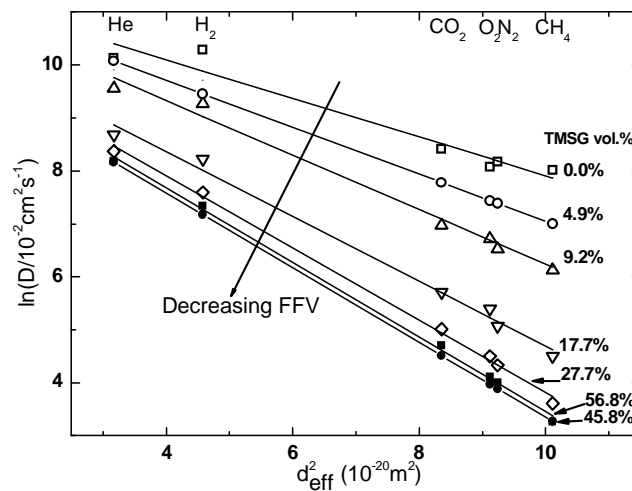


Table 3.5 Linear fitting parameters of k_1 , k_2 and regression R in the plots of the natural logarithm of gas diffusivity as a function of square of its effective diameter¹⁶ in a series of PTMSP/TMSG composite membranes.

Loading of TMSG in PTMSP (vol.%)	k_1	k_2	R
0	11.5573	0.3647	0.9744
4.9	11.4756	0.4427	0.9925
9.2	11.3866	0.5149	0.9949
17.7	10.8034	0.6113	0.9956
27.2	10.6268	0.6806	0.9988
37.4	10.4938	0.7035	0.9992
45.8	10.4017	0.7053	0.9991

3.3.3 Solubility in PTMSP/TMSG

From the permeability and diffusivity, the solubility is estimated according to Equation 1.1 (chapter 1). Table 3.6 exhibits the solubility coefficients for all six gases (He, H₂, CO₂, O₂, N₂ and CH₄) in PTMSP with various amounts of TMSG. With an increased TMSG content in PTMSP, a systematic decrease in gas solubility is observed. More than 50 % loading TMSG causes the solubility capacity of PTMSP to reduce by almost one order of magnitude for each gas. This solubility capacity is getting close to that of conventional glassy polymers.⁸ In addition, the solubility selectivity is almost unchanged. The gas solubility in a composite system can be roughly estimated by the additive model¹⁴ described by eq. 3.1:

$$S_m = S_0 \times (1 - \phi) + S_f \times \phi \quad (\text{eq. 3.1})$$

where S_m is the solubility in the polymer composite, ϕ is the filler volume fraction, S_0 is the gas solubility in the unfilled polymer, S_f is the gas solubility in the filler. Gas solubility in PTMSP is nearly 10 times higher than that in conventional glassy polymers, attributed to a large microporous structure for gas sorption.¹⁹ Therefore, the gas solution in TMSS can be neglected relative to that in PTMSP. Equation 3.1 can be simplified as eq. 3.2:

$$S_m = S_0 \times (1 - \phi) \quad (\text{eq. 3.2})$$

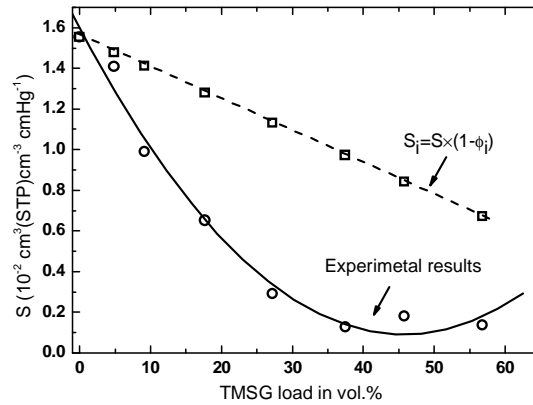
Figure 3.6 presents the nitrogen solubility coefficient in PTMSP/TMSG composites versus the TMSG loading. The prediction of the additive model is shown as comparison. The Figure clearly displays the negative departure for nitrogen solubility in comparison with the prediction of this model. The sorption coefficient depends primarily on three factors: (1) the penetrant condensability; (2) the polymer-penetrant

interactions; and (3) the free volume in glassy polymer matrix.²³ The penetrant condensability is an intrinsic property of each gas. Moreover, the interaction between the composite matrix and gas molecules is unaffected by the TMSG loading in PTMSP, supported by the unchanged solubility selectivity. Therefore, it is reasonable to suppose, that a negative departure from the prediction of the additive model in solubility for PTMSP/TMSG composites can be explained in terms of a reduction of free volume. PTMSP has an interconnected free volume (“microvoids”), which offer the high Langmuir solubility capacity for gas molecule in contrast to that of other conventional polymers.¹¹ The “pore-filling” by TMSG leads to greatly reduced Langmuir sorption capacity in non-equilibrium excess free volume in PTMSP.

Table 3.6 Effective force constants for six gases¹⁶ and their solubility coefficients in a series of PTMSP/TMSG composite membranes at 30 °C.

	He	H ₂	CO ₂	O ₂	N ₂	CH ₄
Effective force constants $(e/k)_{\text{eff}}$ (K)	9.5	62.2	213.4	112.7	83	154.7
Loading of TMSG in PTMSP (vol.%)	Solubility $\times 10^2$ (cm ³ (STP))/(cm ³ cmHg)					
0.0	0.226	0.541	9.773	1.805	1.555	4.913
4.9	0.072	0.483	8.843	1.6	1.41	4.483
9.2	0.12	0.354	8.35	1.387	0.989	3.83
17.7	0.07	0.202	5.95	0.888	0.651	2.535
27.2	0.037	0.119	3.523	0.469	0.291	1.265
37.4	0.032	0.098	2.77	0.356	0.126	0.904
45.8	0.03	0.083	2.295	0.297	0.18	0.745
56.8	0.025	0.072	1.9	0.238	0.137	0.584

Figure 3.6 The nitrogen solubility coefficient (\circ) in PTMSP/TMSG composites as a function of TMSG loading amount at 30 °C as comparison of the additive model (\square).

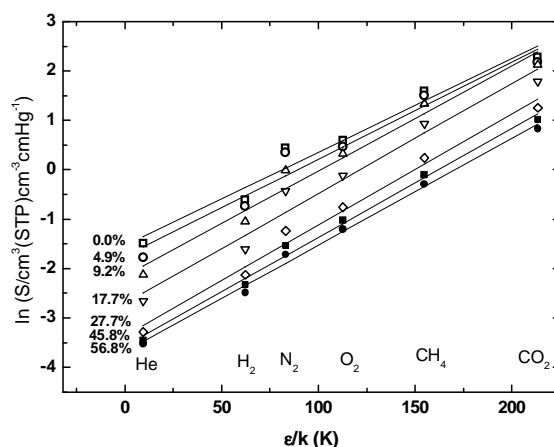


According to Teplyakov's equation (chapter 1), in Figure 3.7 the natural logarithm of gas solubility for six gases at 30 °C is plotted as a function of the square of its effective force constant in a series of PTMSP/TMSG composite membranes. From Figure 3.7 it is clearly read out, that the TMSG loading reduces the solubility in PTMSP for six gases in a similar way. This behavior suggests that no special interaction is introduced by incorporation of TMSG in PTMSP. In the Table 3.7 the intercept k_3 and the slope k_4 are presented. The slope k_4 is almost an invariable value (0.22), which is well in line with that of more than 50 homopolymers and copolymers fittings by Teplykov.¹⁶ Theoretically, this factor k_4 is independent of the nature of the polymer, which can be derived by the regular solution approach. A systematic increase in the intercept k_3 is observed with the increased loading of TMSG. As a result of the decreased FFV in PTMSP, less volume is provided for gas absorption. The unchanged solubility selectivity proves that all of the increase in permeability selectivity in PTMSP/TMSG composites is based on an increase in gas diffusivity selectivity.

Table 3.7 Linear fitting parameters of k_3 , k_4 and regression R in the plots of the natural logarithm of gas solubility at 30 °C as a function of square of its effective force constant ¹⁶ in a series of PTMSP/TMSG composite membranes.

Loading of TMSG in PTMSP (vol.%)	K_3	k_4	R
0	-1.5385	0.01893	0.9822
4.9	-1.7508	0.01967	0.9796
9.2	-2.1485	0.02125	0.9857
17.7	-2.7105	0.02229	0.9845
27.2	-3.3725	0.02255	0.9938
37.4	-3.5734	0.02206	0.9965
45.8	-3.6842	0.02159	0.9972

Figure 3.7 Plots of the natural logarithm of gas solubilities at 30 °C as a function of their effective force constants in a series of PTMSP/TMSG composite membranes (TMSG loading in PTMSP: 0.0% (\square), 4.9% (\circ), 9.2% (Δ), 17.7% (∇), 27.7% (\diamond), 45.8% (\blacksquare), 56.8% (\bullet)).



3.3.4 Activation energies of permeation in PTMSP/TMSG

The temperature dependence of permeability coefficients in PTMSP/TMSG composite membranes for the gases He, H₂, CO₂, O₂, N₂, and CH₄ were measured by the pressure-increase apparatus. Temperature was varied between 10 °C and 70 °C, and feed pressure was approximately 1 bar. The temperature-dependence of gas permeability can be expressed by the Arrhenius Equation (eq. 1.2 in chapter 1)

The activation energy of permeation E_P and the front factor P_0 derived from the slope of Arrhenius plots are presented in Table 3.8. With an increased content of TMSG in PTMSP, the activation energy of permeation E_P for each gas increases systemically. The same trend is observed in the front factor P_0 as well, which will be further

discussed later. PTMSP exhibits negative activation energy for most penetrants (excluding He) primarily due to the “microporous” structure.^{11, 13, 22} This microporous structure leads to considerably small activation energy for diffusion (E_D), since the heat of sorption (H_S) is always negative. The sum of activation energy of diffusion (E_D) and the heat of sorption (H_S) is the activation energy of permeation (E_P). Therefore, E_P in PTMSP is negative for most gases. The TMSG loading in PTMSP causes blocking of micropores in PTMSP. Hence, more diffusion jump energy for gas transport is required. For example, when the TMSG content in PTMSP is more than 28.5 vol.%, the E_P for each gas is comparable to that of a typical glassy polymer like polycarbonate. On the other hand, the opposite relationship between E_P and gas molecular size is observed in PTMSP and PTMSP/TMSG composites. In PTMSP, the larger gas has a relatively smaller E_P , in the order of E_P ($\text{CO}_2 < \text{CH}_4 < \text{O}_2 < \text{N}_2 < \text{H}_2 < \text{He}$). In contrast, in PTMSP containing 37.8 vol. % TMSG, the small gas requires lower activation energy to permeate than the large one. The E_P in this composite is in the reverse order compared to that of PTMSP: $\text{CO}_2 < \text{He} < \text{H}_2 < \text{O}_2 < \text{N}_2 < \text{CH}_4$. The more polar gas CO_2 has always the lowest activation energy of permeation due to its high sorption interaction with polymer matrix.²⁴

Table 3.8 Activation energy of permeation E_P and front factor P_0 for six light gases in a series of PTMSP/TMSG composite membranes.

Loading of TMSG in PTMSP (vol.%)	Activation energy of permeation E_P (kJ/mol) and front factor P_0											
	He		H ₂		CO ₂		O ₂		N ₂		CH ₄	
	E_P	P_0	E_P	P_0	E_P	P_0	E_P	P_0	E_P	P_0	E_P	P_0
0.0	0.5	4922	-2.1	4227	-11.7	205	-5.5	627	-3.5	819	-5.3	980
6.6	1.5	3532	-1.4	2489	-10.3	112	-4.8	338	-3.1	349	-6.3	229
14.4	5.1	3022	2.5	1869	-8.7	36	0.8	322	4.0	420	0.9	236
17.7	10.4	15311	9.3	16306	1.1	922	8.7	3860	13.4	8330	12.1	9958
21.2	11.8	20263	11.9	30487	6.8	4678	10.8	5664	14.9	9125	15.0	16801
28.5	13.7	29476	13.5	37090	8.7	5708	14.8	14760	17.5	15771	19.0	43412
37.8	17.7	99551	18.7	184759	16.5	76519	22.3	183237	28.7	625308	29.5	1716040

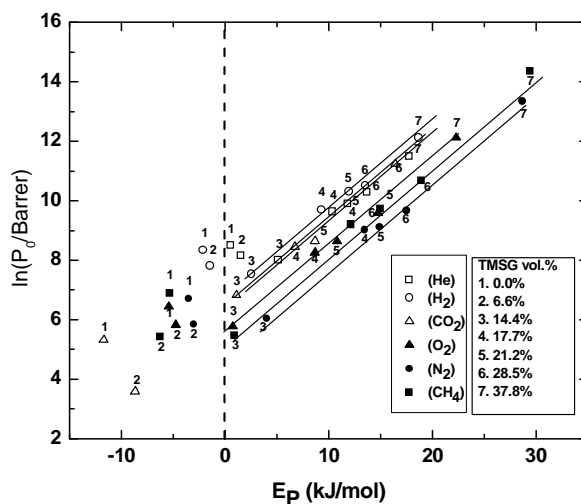
van Krevelen²⁵ observed that the “compensation effect” could be used to relate the activation energy of permeation to the front factor. (eq. 3.1 in chapter 1) The validity of this equation has been tested with the data given in Table 3.8, and the results are illustrated in Figure 3.8. In the PTMSP composite membranes with relatively high

TMSG loadings (TMSG loadings are 14.4, 17.7, 21.2, 28.5 and 37.8 vol.%), the E_p and $\ln P_0$ correlation fits well with the ‘compensation effect’. The linear regression parameters are summarized in Table 3.9. Regarding the values of a and b in Table 3.9, b seems to vary relatively little for all six gases and are very close to the value 0.2770 observed by van Krevelen.²⁵ For the parameter a , an interesting observation is that it shows a clear trend with the gas permeability, namely, the gas with high permeability has large a value. In the PTMSP/TMSG composite with considerable TMSG loading, the gas permeability as well as the fitting parameter a follows the same order: $\text{CO}_2 > \text{H}_2 > \text{He} > \text{O}_2 > \text{CH}_4 > \text{N}_2$. This also explained why van Krevelen observed an uncertain value of a in his work (the author thought the fitting parameter a was also gas type independent).

Table 3.9 “Compensation effect” linear regression parameters in PTMSP/TMSG membranes.

	A	b	R
He	6.6785	0.2721	0.9971
H ₂	6.9168	0.2792	0.9965
CO ₂	6.2930	0.3004	0.9979
O ₂	5.5663	0.2892	0.9976
N ₂	4.8414	0.2927	0.9968
CH ₄	5.2091	0.3062	0.9974

Figure 3.8 Correlation of activation energy of permeation E_p and the front factor $\ln P_0$ in PTMSP/TMSG composites for six gases [(He(\square), H₂(\circ), CO₂(Δ), O₂(\blacktriangle), N₂(\bullet), CH₄(\blacksquare)) at various amount of TMSG in PTMSP . The Arabic numbers represent the loading volume content of TMSG in PTMSP (1.(0.0%), 2.(6.6%), 3.(14.4%), 4.(17.7%), 5.(21.2%), 6.(28.5%), 7.(37.8%)).



Furthermore, it can be seen from Figure 3.10, that the points (given by E_P and $\ln P_0$) of pure PTMSP and PTMSP with low TMSG content (6.6 vol.%) are apart from the E_P - $\ln P_0$ line determined by the high TMSG loading composite membranes. Since a compensation effect means that the transport mechanism is similar among a series of polymers when Equation 1.3 is obeyed,²⁶ the results shown in Figure 3.10 suggests that the gas transport in PTMSP and high loaded PTMSP/TMSG composite membranes might follow different mechanisms. In PTMSP, the free volume appear to be connected and form the equivalent of a finely “microporous” material. In this regard, the gas permeation in PTMSP may fall in a transition region between the pore flow and solution-diffusion mechanisms.²⁷ When TMSG is incorporated into the PTMSP host, it might occupy the “fine micropores”. The PTMSP/TMSG composite membranes could be treated as a conventional glassy polymer, where the transport mechanism should be based on the solution-diffusion model.

3.4 Conclusions

This chapter describes the blending of the high free-volume polymer poly(1-trimethylsilyl-1-propyne) (PTMSP) with the small organic filler trimethylsilyl-glucose (TMSG). Gas permeability coefficients for helium, hydrogen, carbon dioxide, oxygen, nitrogen, and methane decreased drastically with the incorporation of TMSG. Simultaneously, the permselectivity increased. The permeability and selectivity change could be well correlated with the gas molecule size. The largest gas methane experienced the highest loss in permeability. Theoretically, the diffusion and solubility coefficients can be correlated to the penetrants effective diameter and its force constant, respectively. It could be shown, that the gas transport behavior in the PTMSP/TMSG-composites is predominantly governed by the decrease of the diffusion coefficients. From the gas transport properties in the PTMSP/TMSG composites, it is concluded that the filler TMSG can enter the large free volume elements (FVE) in PTMSP and blocks effectively the transport through the microvoids, improving the size selectivity. In addition, an increase in the activation energy of permeation E_P has been found with increasing TMSG content. This supports further the “pore-filling” assumption. The controlled addition of TMSG to PTMSP is a simple way of tailoring the permeability/selectivity behavior of high free volume polyacetylenes.

3.5 References

1. Merkel, T. C.; Freeman, B. D.; Spontak, R. J.; He, Z.; Pinnau, I.; Meakin, P.; Hill, A. J. *Chem. Mater.* **2003**, *15*, **109**.
2. Gomes, D.; Nunes, S.-P.; Peinemann, K.-V. *J. Membr. Sci.* **2005**, *246*, **13**.
3. Higuchi, A.; Yoshida, T.; Imizu, T.; Mizoguchi, K.; He, Zh. J.; Pinnau, I.; Nagai, K.; Freeman, B. D. *J. Polym. Sci.* **2000**, *38*, **1749**.
4. Lin, H. Q.; Freeman, B. D.
<http://www.netl.doe.gov/publications/proceedings/03/ucr-hbcu/Freeman.pdf>
5. Langsam, M.; Puri, P. S.; Anand, M.; Laciak, D. V. U.S. Patent 4,859,215, August 22, 1989 (Air Products and Chemicals, Inc.).
6. Mahajan, R.; Koros, W. J. *Ind. Eng. Chem. Res.*; **2000**, *39*, **2692**.
7. Roberto, A. K. Transmission and reflection of light in multiphase media. In *Polymer Blends: Formulation and Performance*; Paul, D.R. and Bucknall, C.B., Eds.; John Wiley & Sons; 2000; pp 301-304.
8. Wang, X.-Y.; Lee, K. M.; Lu, Y.; Stone, M. T.; Sanchez, I. C.; Freeman, B. D. *Polymer*, **2004**, *45*, **3907**.
9. Shantarovich, V. P.; Kevdina, I. B.; Yampolskii, Yu. P.; Alentiev, A. Yu, *Macromolecules* **2000**, *33*, **7453**.
10. Hofmann, D.; Heuchel, M.; Yampolskii, Y.; Khotimskii, V.; Shantarovich, V. *Macromolecules* **2002**, *35*, **2129**.
11. Srinivasan, R.; Auvil, S.R.; Burban, P.M. *J. Membr. Sci.* **1994**, *86*, **67**.
12. Nakagawa, T.; Fujisaki, S. *J. Membr. Sci.* **1994**, *94*, **183**.
13. Pinnau, I.; Toy, L. G. *J. Membr. Sci.* **1996**, *116*, **199**.
14. Barrer, R. M.; Barrie, J. A.; Raman, N. K. *Polymer* **1962**, *3*, **605**.
15. Toy, L. G.; Nagai, K.; Freeman, B. D.; Pinnau, I.; He, Z.; Masuda, T.; Teraguchi, M.; Yampolskii, Yu. P. *Macromolecules* **2000**, *33*, **2516**.
16. Teplyakov, V.; Meares, P. *Gas Sep. Purif.*, **1990**, *4*, **66**.
17. Robeson, L. *J. Membr. Sci.* **1991**, *62*, **165**.
18. Nunes, S.-P.; Peinemann, K.-V. Gas separation with membranes. In *Membrane technology in the chemical industry*; Nunes, S.-P.; Peinemann, K.-V., Eds.; Wiley-VCH: Weinheim, 2001; pp 39-67.
19. Nagai, K.; Masuda, T.; Nakagawa, T.; Freeman, B. D.; Pinnau, I. *Prog. Polym. Sci.* **2001**, *26*, **721**.
20. Jia, L.; Xu, J. *Polymer*, **1991**, *23*, **417**.

21. Cohen, M. H.; Turnbull, D. *J. Chem. Phys.* **1959**, *31*, **1164**.
22. Ichiraku, Y.; Stern, S. A.; Nakagawa, T. *J. Membr. Sci.* **1987**, *34*, **5**.
23. Petropoulos, J. H. Mechanisms and theories for sorption and diffusion of gases in polymers, in *Polymeric Gas Separation Membranes*, edited by Paul, P. R. and Yampol'skii, Y. P., CRC Press, **1994**
24. Thran, A.; Kroll, G.; Faupel, F. *J. Polym. Sci.* **1999**, *37*, **3344**.
25. Van Krevelen, D. W. *Properties of Polymers*, 3rd completely revised edition, Elsevier, **1997**
26. Freeman, B. D. *Macromolecules* **1999**, *32*, **375**.
27. Wijmans, J. G.; Baker, R. W. *J. Membr. Sci.* **1995**, *107*, **1**.

Chapter 4

Gas transport properties in an ethylcellulose composite membrane with nanosized organic filler trimethylsilyl-glucose

4.1 Abstract

This Chapter reports a novel mixed matrix membrane containing the organic filler trimethylsilyl-glucose (TMSG) with the size of around 1 nanometer into ethylcellulose (EC). The permeability, diffusivity and solubility coefficients of six gases (He, H₂, CO₂, O₂, N₂, and CH₄) are determined in these EC/TMSG composites with a series of TMSG loading using the time-lag method. Systemically increasing TMSG content in EC resulted in a distinct increase of all tested gas permeabilities. The increases of gas permeability as a function of TMSG loading amount experience two stages. As TMSG loading is less than 37 vol.%, a noticeably increased permeability with an almost unchanged selectivity is observed. For example, P(O₂) increases 1.7-fold at 37 vol.% TMSG in EC compared to that of unfilled one, while P(O₂)/ P(N₂) remains nearly constant. As TMSG is loaded more than 37 vol% in EC, the gas permeability radically increases. The oxygen permeability increases nearly 5-fold at 66 vol.% TMSG loading, the P(O₂)/ P(N₂) is slightly down to 2.8. Moreover, the larger penetrant benefits more permeability enhancement than the smaller one, as a result, the improved permeability and simultaneously improved permselectivity for larger gas over smaller gas (e.g. CO₂/H₂) are observed.

The temperature dependence of the permeability was also studied. The activation energy of permeation in EC/TMSG composites increases with increased TMSG content, although the permeability was also increased. The increase in the permeability with increased temperature is due to the increase of the front factor, which is proportional to the entropy change. These transport properties, together with glass transition temperature (*T_g*) measured by differential scanning calorimetry (DSC) analysis, suggest that the dominant reason for the permeability enhancement and permselectivity alteration is the increase in chain mobility by introducing of the TMSG filler.

4.2 Introduction

Mixed matrix membranes (MMMs) for gas separation have been not only the subject of research interest in the past 10 years,¹ but also are promising alternatives for the next generation membranes.² Generally, in MMMs, the incorporated inorganic fillers

consist of well defined porous structures such as zeolites, or carbon molecular sieves (CMS). The intrinsic pore sizes of these fillers have the extremely high molecular sieve ability. This super sieving property combined with the easy processibility of polymer has caused a large curiosity in the membrane research field. For example, Kulprathipanja et al.³ observed that the incorporation of silicalite into cellulose acetate improved O₂/N₂ selectivity from 3.0 to 3.6. Jia and Peinemann⁴ firstly reported the silicalite/PDMS mixed matrix membrane for slightly improved selectivities in O₂/N₂ and CO₂/CH₄ compared to those of the unfilled PDMS. Moreover, the CMS incorporated into two polyimides were reported by Vu et al..⁵ These composites even broke through the empirical Robeson's upper bound⁶ for CO₂/CH₄ and O₂/N₂. Those hybridizations seemed to provide a readily available means to obtain the optimal transport properties relative to the unfilled polymers. However, the unavoidable chemical incompatibility between polymer host and filler particle (especially regarding to the inorganic particle) leads to the inhomogeneous distribution of the filler and the unselective interface defect, which hinders the formation of the attractive composite materials.^{7,8}

Recently, one novel mixed matrix membrane with the nonporous, nano-sized inorganic particles like silica has been added to the super glassy polyacetylene polymer matrix, resulting in the improved gas permselectivity for hydrocarbons over incondensable gases such as methane. This phenomenon is attributed to increased fractional free volume (FFV) by disrupting the polymer chain packing.⁹⁻¹² This behavior was totally opposite to that of the conventional nonporous filler system.¹³ It was obvious, that this nonporous filler in those composites did not undertake the molecular sieve function as the conventional porous filler. Actually, this way of the FFV modification owing to alternation of polymer chain packing by filling special particle, offers another spectrum to fabricate a novel mixed matrix membrane with optimal performances.

In addition to the polymer FFV, the polymer chain mobility is another primary factor to control the molecule transport properties from a material viewpoint.¹⁴ In this study, we extend this idea to introduce one compatible organic filler trimethylsilyl-glucose (TMSG) into the polymer ethylcellulose (EC), in order to modify the polymer chain mobility. EC is selected in this study as the host for the TMSG mainly because it is polymer material with good membrane formation ability, medium gas separation capability, good flexibility, excellent durability and low cost.¹⁵ Additionally,

ethylcellulose is a practical membrane for industry application.¹⁶ In this article, the gas transport properties, including diffusivity, solubility, permeability, permselectivity and temperature dependence of permeability in this novel EC/TMSG mixed matrix membrane will be discussed.

4.3 Results and discussions

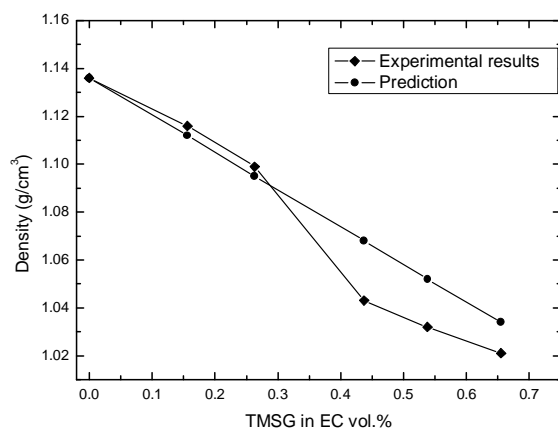
4.3.1 The density of EC/TMSG composites

Figure 4.1 displays the comparison of the estimated density by Equation 4.1 (expressed as (●)) and experimentally measured density by gravimetric analysis (expressed as (◆)) in a series of EC/TMSG composites as a function of TMSG content.

$$\rho = \frac{W_p + W_f}{\frac{W_p}{\rho_p} + \frac{W_f}{\rho_f}} \quad (\text{eq. 4.1})$$

where W_p and W_f refer to weight of polymer and filler, respectively. ρ_p and ρ_f refer to the density of polymer and filler, respectively. Clearly, an increased loading of TMSG in EC shows a trend of reduced composite density. This is in consistence with density difference between TMSG (0.96-0.98 g/cm³) and EC (1.14 g/cm³). A slightly positive deviation of measured density at less loading of TMSG and a relatively large negative deviation of measured density at more loading of TMSG in comparison with these calculated by the additive model are observed. This slightly positive deviation at low loading from the additive prediction seems to be in the range of the experimental uncertainty. Regarding to the negative deviation from the additive prediction at high loading, it might be due to the change of EC chain packing in a different behavior, when the measurement uncertainty is neglected.

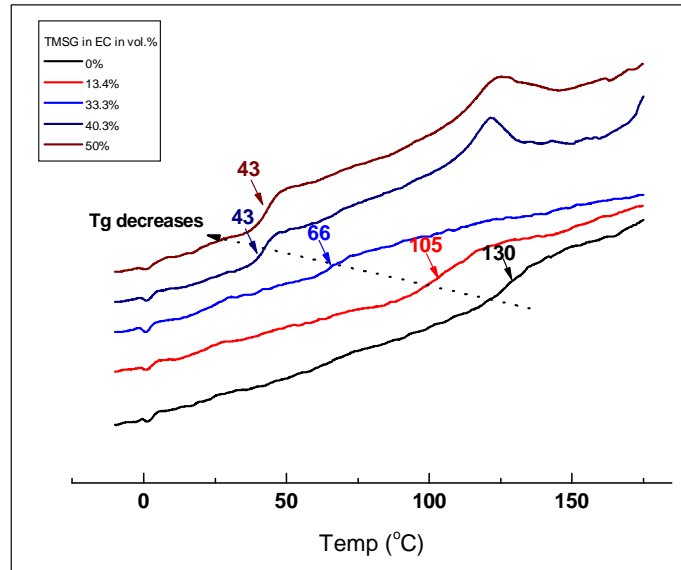
Figure 4.1 Density of EC/TMSG composites at R.T. as a function of TMSG loaded amount. The estimated density (expressed as (●)) and experimentally measured density (expressed as (◆)).



4.3.2 Glass transition temperature of EC/TMSG

Figure 4.2 presents DSC thermograms of a series of EC/TMSG composites. The average values of the thermal transitions T_g are also presented. Obviously, increasing TMSG content systematically decreases T_g in EC/TMSG composites. In other words, the ethylcellulose chain segmental dynamics are systematically enhanced. This behavior is different relative to inorganic filler, which has generally more impact on the polymer FFV than the polymer chain dynamics, because the specific interaction between filler and polymer chains is frequently absent.¹¹ This pronounced increase in EC chain mobility by TMSG might be due to the similar chemical structure between ethylcellulose and silylated-glucose, since both are based on glycoside. This similarity results in the compatible composite of EC/TMSG, which was further confirmed by the optical transparency. As a result, TMSG may efficiently separate EC chains, causing the chains more easily to slip. In addition, the increased chain mobility may be more pronounced compared to the offset effect in the presence of the weak hydrophobic interaction between TMSG and EC.

Figure 4.2 Glass transition temperatures of EC/TMSG composites as a function of TMSG loaded content.



4.3.3 Permeability and permselectivity

In Table 4.1, the effect of TMSG filler in EC on the permeability coefficients of six light gases (He, H₂, CO₂, O₂, N₂, and CH₄) is illustrated. The incorporation of TMSG in EC leads to a considerable increase in all tested gas permeabilities. For instance, in 26.4 vol.% TMSG loaded EC composite, permeabilities of N₂ and O₂ simultaneously increase by more than 50% in comparison with those of the unfilled one. As EC is loaded with 53.0 vol.% TMSG, the nitrogen permeability even increases by more than 3.5-fold. Based on the data in Table 4.1, the normalized gas permeability (P_i/P_0 , P_i refers to the permeability with various content of TMSG in EC, P_0 refers to the permeability of the unfilled EC) as a function of the loading content of TMSG is plotted in Figure 4.3, where the prediction of classical Maxwell model is also presented for comparison. The Maxwell model predicts the permeability decline of an increased path-length for penetrant in a polymer composite with an impermeable filler.¹³ It clearly demonstrates, that a reverse positive departure of the gas permeability is observed relative to the Maxwell model. In addition to the unusually increased gas permeability in the EC/TMSG composites, the permeability enhancement is gas dependent. A first impression is that the gas with larger size experiences a larger permeability enhancement. The permeability enhancement of six tested gases

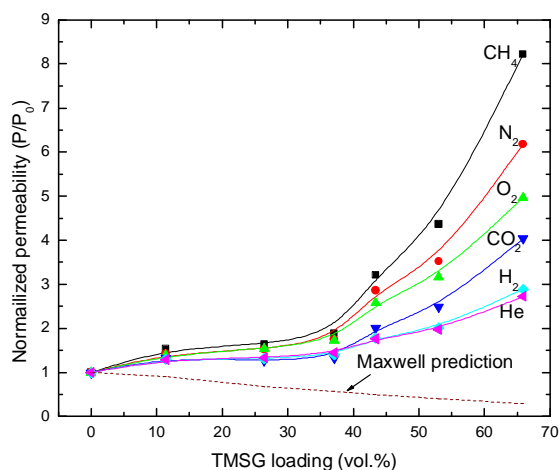
increases in the order of: He < H₂ < O₂ < CO₂ < N₂ < CH₄. For instance, at 66 vol.% TMSG loading, for the largest gas CH₄ the permeability enhancement is 8.2-fold, whereas, the smallest gas He experiences 2.7-fold increase in comparison with those of the unfilled EC.

Table 4.1 Gas permeability coefficients of the EC/TMSG composite membranes at 30 °C.

TMSG loading in EC (vol.%)	Sample Code	Permeability (Barrer*)					
		He	H ₂	O ₂	N ₂	CH ₄	CO ₂
0	1	40.2	56.0	11.8	3.48	7.11	70.9
11.4	2	51.9	72.6	16.8	4.92	10.9	94.0
26.4	3	53.5	73.3	18.2	5.31	11.7	90.0
37.1	4	58.0	78.2	20.3	6.10	13.4	93.8
43.4	5	70.9	99.3	30.5	9.94	22.8	142
53.0	6	79.2	113	37.3	12.3	31.0	176
65.9	7	109	162	58.6	21.5	58.5	286

*1 Barrer = 10⁻¹⁰ cm³(STP)·cm/(cm²·s·cmHg)

Figure 4.3 Normalized gas permeability coefficients for six gases (He, H₂, CO₂, O₂, N₂, and CH₄) and Maxwell model prediction as a function of loading amount of TMSG in EC.



Positive deviations from the Maxwell model have been rarely reported in the filled systems. In some organic-inorganic hybrid materials, the distinct permeation enhancement was observed, which is frequently attributed to the interface defect because of seemingly unsolved incompatibility between inorganic filler and polymer matrix. Such defect may produce a nonselective Knudsen diffusion.¹¹ For example, in the nylon-6/SiO₂ nanocomposite system, a slight addition of 5 wt.% of silica leads to a great increase of gas permeation in one order of magnitude higher than that of the

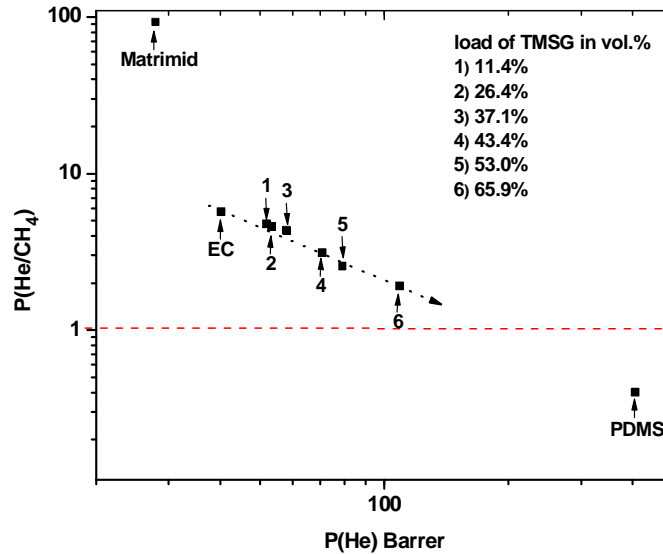
unfilled nylon membrane, and gas selectivity is in line with the Knudsen selectivity²¹. Recently, nanocomposite of high-permeability polymers (e.g. PTMSP and PMP) with silica were shown to have significantly increased permeability relative to the pure polymer while retaining selectivity. It was explained by that rigid PMP or PTMSP chains are unable to pack efficiently around the periphery of silica filler particles, resulting in a low-density in polymer-filler interfacial region and ‘a resultant increase in system free volume’.⁹⁻¹² In fact, the polymer-filler interface effect may be responsible for the enhanced FFV, since the filler (silica) and polymer (PTMSP or PMP) are intrinsically incompatible, which is indicated by the particle aggregation into clusters under the transmission electron microscopy (TEM). However, the solution-diffusion mechanism still remains in this interface. In this study EC/TMSG composites system, this mixed matrix membrane is miscible at molecular level, which is obviously supported by the optical transparency of this composite. Therefore, the ‘polymer-filler interface effect’ is undoubtedly not the dominant reason for the permeability enhancement.

The increased polymer chains flexibility seems be a reasonable explanation for this atypical manner in an increased permeability in the EC/TMSG composites. This is clearly indicated by the variation of glass transition temperature in this composite, which straightforwardly reflects the flexibility of polymer segments. The gas is transported through the densified polymer matrix based on the well-known solution-diffusion mechanism.¹⁶ The addition of TMSG into EC, which spaces the inter-chain apart and reduces the chain interaction, consequently enhances the possibility for gas molecule jump.

The increased polymer chains flexibility in EC/TMSG composites is further indicated by the noticeable difference in the permeability enhancement for the various penetrant with different size. In EC/TMSG composites, the permeability enhancement for larger gas methane is pronouncedly larger than that of smaller gas helium. This scenario is due to more permeability gain for methane than for helium, when polymer chain mobility increases. In addition, this behavior of this composite is getting close to that of rubber, which is more permeable to larger gas than smaller gas.⁶ Figure 4.4 summarizes the helium permeability and helium/methane selectivity for two representative polymer and EC/TMSG composites. The glassy polymer matrimide has a strong size selectivity ($P(\text{He})/P(\text{CH}_4)=90$); modest glassy polymer EC shows relatively weak helium selectivity ($P(\text{He})/P(\text{CH}_4)=5.2$); typical rubber polymer PDMS

even exhibits a reverse selectivity ($P(\text{He})/P(\text{CH}_4)=0.4$). EC/TMSG (66 vol.%) composite membrane exhibits minor selectivity ($P(\text{He})/P(\text{CH}_4)=1.8$). Such comparison clearly suggests, the permeability behavior of EC/TMSG composites gradually move to rubber polymer with increasing loading of filler TMSG.

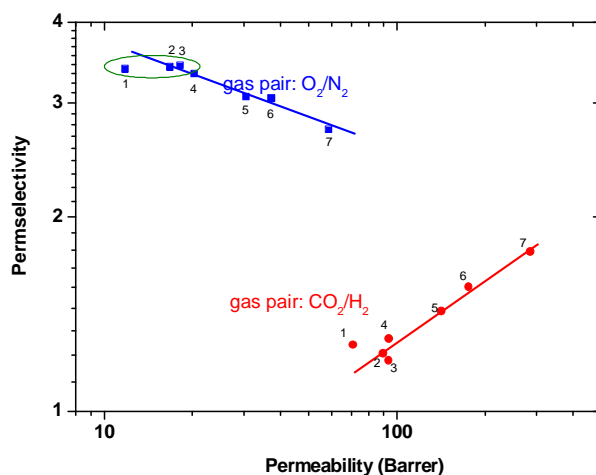
Figure 4.4 Relationship between helium permeability and its selectivity over methane for EC/TMSG composites and matrimid as well as PDMS. (Matrimid and PDMS data from reference ¹⁶)



Since the gas permeability enhancement in EC/TMSG composites is gas size relevant, and the gas with larger size will experience a great permeability enhancement, a resultant change in permselectivity is expected. Figure 4.5 shows the permeability and permselectivity relationship of O_2/N_2 and CO_2/H_2 gas pairs as a function of TMSG content in EC. For O_2/N_2 separation, the trade-off relationship between permeability and permselectivity is generally observed. At the relatively less loaded TMSG in EC (from 0 to 37 vol.%), the selectivity for O_2/N_2 remains almost constant ($P(\text{O}_2)/P(\text{N}_2)=3.4$, but the permeability increases considerably ($P(\text{N}_2)=3.48$ Barrer for EC, $P(\text{N}_2)=6.10$ Barrer for EC with 37 vol.% TMSG). This behavior for the increased permeability with the unchanged selectivity was similarly observed by Houde and Stern ²³, who studied the effect of ethoxyl content on the permeability and permselectivity of EC. They suggested, the unchanged selectivity for O_2/N_2 and increased permeability with increasing ethoxyl content is attributed to a slight increase in FFV. In this study, the unchanged O_2/N_2 and simultaneously increased

permeability is due to the increased polymer chain mobility to some extent. With continually enhanced loading of TMSG in EC, the permselectivity for O₂/N₂ slightly decreases from 3.4 to 3.0, accompanied with significantly enhanced permeability.

Figure 4.5 Relationship between P(O₂) and P(O₂)/P(N₂) as well as P(CO₂) and P(CO₂)/P(H₂) for EC/TMSG composites. Sample code is referred to Table 4.1.

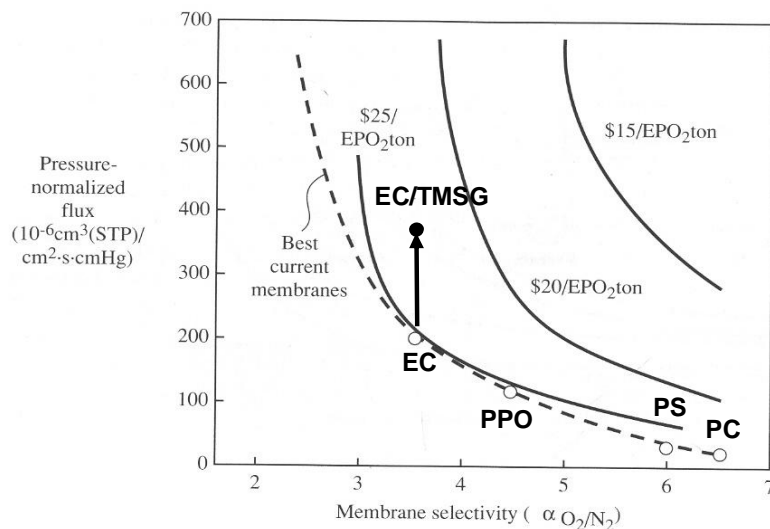


On the other hand, the EC/TMSG composites display both enhancements in gas permeabilities and selectivities for CO₂/H₂. For instances, in ethylcellulose containing 53 vol. % TMSG, permeability increase from 70.9 to 176 Barrer for CO₂ and from 56 to 113 Barrer for H₂. Simultaneously, the CO₂/H₂ selectivity increases from 1.27 to 2.01, which is also exhibited in Figure 4.5. This behavior is opposite to the empirically observed trade-off relationship between permeability and selectivity. This enhanced selectivity for CO₂/H₂ in EC/TMSG composites together with enhanced permeability are attributed to the increased chain mobility in EC/TMSG composites. The permeability enhancement of the larger molecule benefits more from the increased polymer dynamics than that of smaller one. The way of loading of TMSG in EC provides a simply means to improve so called reverse selectivity, which refers that larger penetrant (e.g., CO₂) permeates faster than smaller one (e.g., H₂).

From an application standpoint, asymmetric or composite membranes comprising a thin skin layer supported on a microporous substrate are often used in order to achieve a high permeability, which is desired to minimize membrane area and thus capital cost. With reference to this demand, the polymer to form the effective layer should have excellent thin-film processibility. Ethylcellulose is proven to be a successful candidate

to satisfy this requirement. Moreover, according to Baker's estimation,¹⁶ in order to reduce the process costs, high permeable membranes with a moderate permselectivity are required. Figure 4.6 shows the calculated oxygen production cost for 35-50% oxygen as a function of membrane performance referring to the combination of permeability and permselectivity in some of today's best membranes (ethylcellulose (EC), poly(phenylene oxide) (PPO), polysulfone (PS), and polycarbonate (PC)). It is clearly shown in Figure 4.6, that ethylcellulose is only one commonly used material close to \$25 equivalent pure oxygen (EPO₂), because of its good membrane formation and moderate selectivity. The EC/TMSG composites membrane seemingly offers a possibility to reach the cost-competitive aim of less than \$25 EPO₂. In the pilot-test, one asymmetric composite membrane with EC/TMSG has exhibited the oxygen flux of 1 m³/(m² h bar) and the selectivity of 3.1 for oxygen over nitrogen.

Figure 4.6 The calculated oxygen production cost for 35-50% oxygen as a function of membrane performance referring to the combination of permeability and permselectivity in some of today's best commercial membranes and EC/TMSG composites.



4.3.4 Diffusivity and solubility

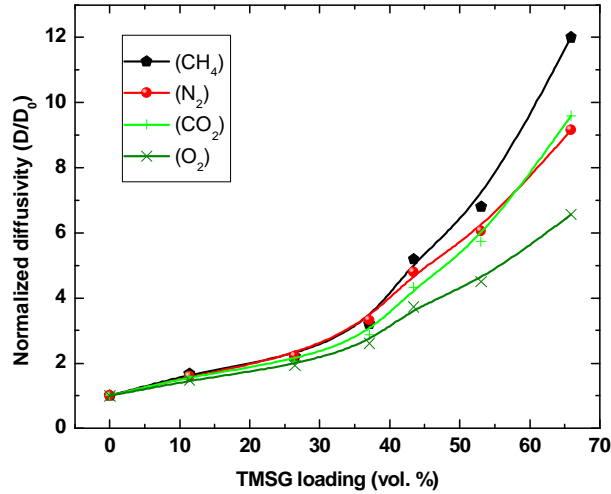
As the permeability is a product of the diffusivity and solubility, the following section discusses the influence of the addition of the TMSG on the diffusivity and solubility respectively. The diffusion coefficient of four light gases in EC membranes containing various content of TMSG are presented in Table 4.2. Helium and hydrogen are absent since the accuracy of the diffusion coefficients of these two small gases is

not good enough. The increased loading of TMSG in EC leads to a systematical increase in gas diffusivity. In order to present the diffusivity change behavior in EC/TMSG composites, Figure 4.7 plots the relative diffusivity (D_i/D_0) as a function of the TMSG loading, based on the data in Table 4.2. As it can be seen from this Figure 4.7, the gas diffusivity enhancement is in the order of $\text{CH}_4 > \text{N}_2 \approx \text{CO}_2 > \text{O}_2$, the gas with larger size (lower diffusivity) correspond to larger diffusivity increase and vice versa. For example, the CH_4 diffusivity in EC/TMSG membrane containing 65.9 vol. % TMSG is 12.0 times higher than that in the unfilled EC polymer. Comparatively, for the relative small gas O_2 , the diffusivity increases by 6.0-fold at the same condition. The low diffusivity of CO_2 in polymer membrane compared to that of O_2 is usually observed elsewhere and this may result from the fact that the CO_2 molecule is less spherical and more polar than the other gases.²⁵ However, in EC/TMSG composites membranes with and without TMSG loading, the CO_2 diffusivity is even lower than that of N_2 . This may be due to the specific interactions between polar groups in EC and the polar CO_2 molecules.²³

Table 4.2 Gas diffusivity coefficients in a series of EC/TMSG composite membranes at 30 °C.

TMSG loading in EC (vol.%)	O_2	N_2	CO_2	CH_4
	Diffusivity $\times 10^8 \text{ cm}^2/\text{s}$			
0	43	20	14	9
11.4	65	30	24	15
26.4	85	42	31	22
37.1	115	63	43	32
43.4	164	91	65	52
53.0	198	115	86	68
65.9	289	174	144	120

Figure 4.7 Normalized gas diffusivity coefficients for four gases (CO_2 , O_2 , N_2 , and CH_4) as function of TMSG loading in EC.



The diffusion change behavior in EC/TMSG composites is in well line with permeability change, which indicates, that all of the enhanced gas permeability in EC with increased TMSG content is dominated by the diffusion increase, and the size-relevant diffusivity enhancement directly leads to the decrease of size sieving ability of the composites. This behavior is in accordance with the well-known permeability-selectivity (diffusivity-selectivity) trade-off relationship.⁶ This increased diffusion behavior in EC/TMSG composites are different compared to that of conventional filler system.²⁶ In EC/TMSG, the systematical decrease in T_g is accompanied with an increased loading of TMSG, indicating an enhanced polymer chain mobility, which overwhelms the increased tortuosity by impermeable filler TMSG. Likewise, the increased diffusivity by the nonporous filler silica in polyacetylene polymers is also reported.⁹⁻¹² But, for those systems, the increased diffusivity is a result of increased FFV.

It is well recognized that the gas diffusivity is size dependence and it can be related with the empirical correlation (see Eq. 1.5 in chapter 1).²⁴ In Figure 4.8, the gas diffusivity is plotted as a function of the gas kinetic diameter (d_i) for N_2 , O_2 and CH_4 on the basis of eq. 1.5 and the diffusivity data listed in Table 4.2. The gas CO_2 is excluded in the fitting line because CO_2 molecule is less spherical and more polar than the other gases, which I have mentioned before. Helium and hydrogen are also

absent for the accuracy of the diffusion coefficients of these two small gases is too low. The fitting parameters k_1 and k_2 derived are listed in Table 4.3. The value of slope (k_2) is getting smaller with increasing TMSG loading in EC, which reflects the reduction of diffusion selectivity. In other words, the EC membrane has more mobility and more or less loses its size sieve selectivity when the small molecule TMSG is incorporated into the membrane matrix. The intercept (k_1) also shows a systemic decline. Interestingly, it finds a linear relationship between k_1 and k_2 as shown in Figure 4.9.

Table 4.3 Linear fitting parameters of K_1 , K_2 and regression R in the plots of the natural logarithm of gas diffusivity as a function of square of its effective diameter in a series of EC/TMSG composite membranes.

TMSG loading (vol. %)	0%	11.4%	26.4%	37.1%	43.4%	53.0%	65.9%
k_1	11.35	11.28	11.00	10.96	10.67	10.47	9.92
k_2	63.32	59.42	54.76	51.76	46.53	43.29	35.66
R	0.999	0.999	1	0.997	1	0.999	0.995

Figure 4.8 The plots of the natural logarithm of gas (O_2 , N_2 , CH_4) diffusivity as a function of square of its effective diameter in a series of EC/TMSG composite membranes.

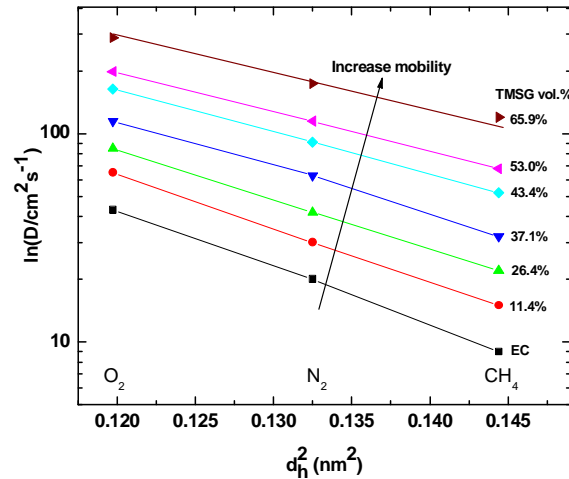
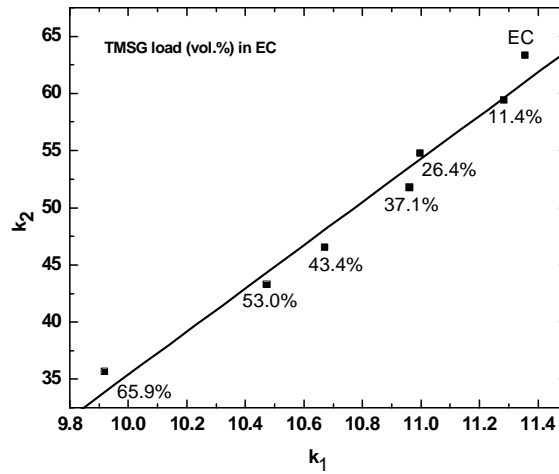


Figure 4.9 The relationship between k_1 and k_2 for EC/TMSG composites



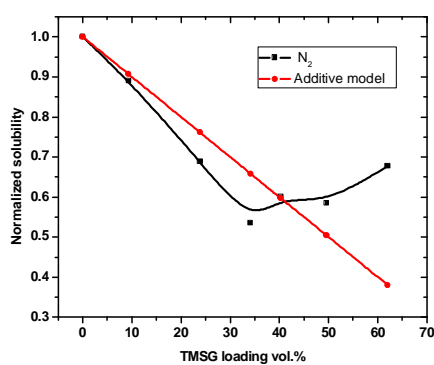
From the permeability and diffusivity coefficients, the solubility coefficients are estimated according to Equation 1.1. Table 4.4 exhibits the solubility coefficients for four light gases (CO_2 , O_2 , N_2 , and CH_4) in EC with various amounts of TMSG. With an increased TMSG content in EC, a decrease in gas solubility is observed, which further reveals that the dominant reason for the permeability enhancement is from diffusivity change. Moreover, the reduced solubility behavior is a strong evidence for the reasonable assumption that the sorption of the filler TMSG is negligible. The reduced gas sorption may be due to the reduction of the sorption sites in the polymer matrix by the filler, which can be theoretically estimated by the additive model²⁶ described by Equation 3.2 in chapter 3.

Figure 4.10 presents the nitrogen solubility coefficient in EC/TMSG composites as a function of TMSG loading content in comparison with the calculated additive model. The relatively low loading of TMSG (< 35 vol.%) in EC results in a decreased solubility, which is quite close to the prediction of the additive model, suggesting that the filler particle just occupies the sorption sites. However, the continuous loading TMSG in EC (> 35 vol.%) results in a slight increase of solubility. Excluding the experimental errors (the errors in the value of solubility could be high, since they combine the errors in the permeability and diffusivity from which solubility is calculated), this observation is still hard to explain.

Table 4.4 Gas solubility coefficients in a series of EC/TMSG composite membranes at 30 °C.

TMSG vol.% loading in EC	O ₂	N ₂	CO ₂	CH ₄
	Solubility $\times 10^2$ (cm ³ (STP)/(cm ³ cmHg))			
0	0.268	0.183	4.710	0.742
11.4	0.260	0.163	3.900	0.722
26.4	0.213	0.126	2.920	0.539
37.1	0.176	0.098	2.180	0.425
43.4	0.186	0.110	2.190	0.443
53.0	0.189	0.107	2.530	0.457
65.9	0.202	0.124	2.383	0.406

Figure 4.10 The nitrogen solubility coefficient in EC/TMSG composites as a function of TMSG loading amount at 30 °C in comparison with those of the additive model.



4.3.5 Temperature dependence of permeability

Table 4.5 displays the permeation activation energy and the front factor in EC/TMSG composites, which is calculated based on the Arrhenius equation (eq. 1.2 in chapter 1). It is of great interest to find that both the permeation activation energy and the front factor for each gas increase with increased loading of TMSG. In other words, the permeability and activation energy of permeation in EC/TMSG composites change in the same trend. This behavior is in contrast to the observation in poly(4-methyl-2-pentene) PMP/fumed silica nanocomposite, where a decrease of the permeation energies with an increased permeability were found.¹⁰ This was because the addition of the fumed silica altered the chain packing and thus reduced the required permeation energy. In our system, the increase of the permeation is due to the increase of the front factor. According to the Eyring's activated state theory,²⁸ the front factor is proportional to the entropy change. When TMSG is filled into the polymer matrix, the EC polymer chain mobility is increased. This means the polymer chains undergo rapid and chaotic motions. Penetrant gas molecules are able to participate in these

rapid molecule exchanges to execute frequent diffusion jumps.²⁸ When the front factor increases, the activation energy also increases, following the so called ‘compensation effect’ (partial offset of the effect of higher front factor by higher activation energy). This effect will be intensively discussed in chapter 7.

Table 4.5 Activation energy of permeation E_p and the natural logarithm of front factor P_0 for six gases in a series of EC/TMSG composite membranes. (E_p in unit: kJ/mol,

TMSG loading in EC (vol. %)	He		H ₂		CO ₂		O ₂		N ₂		CH ₄	
	E_p	$\ln P_0$	E_p	$\ln P_0$	E_p	$\ln P_0$	E_p	$\ln P_0$	E_p	$\ln P_0$	E_p	$\ln P_0$
0	16.42	10.14	15.59	10.13	7.31	7.09	16.59	8.98	21.4	9.66	19.89	9.76
24.1	16.43	10.43	15.79	10.51	9.94	8.39	17.48	9.77	22.90	10.79	20.94	10.71
40.7	18.70	11.40	19.19	11.89	16.90	11.15	22.52	11.83	26.97	12.43	27.49	13.39
54.1	19.50	11.63	20.45	12.27	24.36	13.94	25.76	13.01	27.84	12.71	31.10	14.76

$\ln P_0$: dimensionless)

4.4 Conclusions

The transport properties of the novel mixed matrix membrane with organic filler TMSG in EC has been studied. The EC/TMSG composites are compatible, which is indicated by the transparent appearance from optical observation and single T_g by DSC. The increased loading of TMSG in EC was observed to systemically enhance the gas transport, in contrast to permeation behavior in traditional filled polymer systems. The permeability enhancement is ranked in the order of penetrant size (He<H₂<CO₂<O₂<N₂<CH₄). In particular, at relatively lower loading of TMSG in EC the permeability increases, while the selectivity for oxygen/nitrogen remains nearly constant. At the relatively higher ratio loading, the trade-off relationship for permeability and permselectivity is observed. However, permselectivity increases simultaneously with the permeability enhancement for CO₂/H₂ in EC/TMSG system. The improved gas permeability appears to arise primarily from the increase in polymer chain mobility, which is straightforwardly indicated by the decrease of the T_g of those composites with the increasing TMSG content in EC. The gas permeability behavior in EC containing TMSG is well in accordance with the diffusivity enhancement. Activation energies of permeation for each tested gas in EC/TMSG increases with increasing TMSG content, although the gas permeabilities increase as well. This introduction of organic molecule TMSG has an effective impact on

dynamic behavior of polymer chain, which may provide another approach to finely tune the transport properties of polymer via the loading of TMSG.

4.5 References

1. Kulprathipanja, S. Mixed membrane development, *Annals of the NEW York Academy of Science* **2003**, 361-369.
2. Peinemann, K.-V. Next Generation Membrane Materials, Plenary Lecture at NAMS Annual Meeting, Honolulu (Hawaii, USA) **2004**
3. Kulprathipanja, S. Separation of polar gases from nonpolar gases, US-Patent 4,606,740 (1986)
4. Jia, M.; Peinemann, K.-V.; Behling, R.-D. *J. Membr. Sci.* **1991**, *57*, **289**.
5. Vu, D. Q.; Koros, W. J.; Miller, S. J. *J. Membr. Sci.* **2003**, *211*, **311**.
6. Robeson, L. *J. Membr. Sci.* **1991**, *62*, **165**.
7. Mahajan, R.; Koros, W. J. *Ind. Eng. Chem. Res.* **2000**, *39*, **2692**.
8. Mahajan, R.; Zimmerman, C. M.; Koros, W. J. In *Polymer Membranes for Gas and Vapor Separation: Chemistry and Materials Science*; Freeman, B. D., Pinnau, I., Eds.; American Chemical Society: Washington, DC, **1999**; pp 277-286.
9. Merkel, T. C.; Freeman, B. D.; Spontak, R. J.; He, Z.; Pinnau, I.; Meakin, P.; Hill, A. J. *Science* **2002**, *296*, **519**.
10. Merkel, T. C.; Freeman, B. D.; Spontak, R. J.; He, Z.; Pinnau, I.; Meakin, P.; Hill, A. J. *Chem. Mater.* **2003**, *15*, **109**.
11. Merkel, T. C.; He, Z.; Pinnau, I.; Freeman, B. D.; Meakin, P.; Hill, A. J. *Macromolecules* **2003**, *36*, **6844**.
12. Gomes, D.; Nunes, S. P.; Peinemann, K.-V. *J. Membr. Sci.* **2005**, *246*, **13**.
13. Barrer, R. M.; Barrie, J. A.; Raman, N. K. *Polymer* **1962**, *3*, **605**.
14. Cohen, M. H.; Turnbull, D. *J. Chem. Phys.* **1959**, *31*, **1164**.
15. Pinnau, I.; Freeman, B. D. Formation and Modification of Polymeric Membranes: Overview in *Membrane Formation and Modification*; Pinnau, I., Freeman, B. D. Eds.; ACS Symposium Series 744; American Chemical Society: Washington, D.C., 1999.
16. Nunes, S.-P.; Peinemann, K.-V. Eds., *Membrane Technology in the Chemical Industry*, Wiley-VCH, 2001.

17. Nouvel, C.; Ydens, I.; Degée, P.; Dubois, P.; Dellacherie, E.; Six, J. L. *Polymer* **2002**, *43*, **1735**.
18. Mormann, W.; Demeter, J. *Macromolecules* **1999**, *32*, **1706**.
19. Paul, D. R.; Bucknall, C. B. eds., *Polymer Blends: Formulation and Performance*, John Wiley & Sons, 2000.
20. Shishatskiy, M.; Yampol'skiy, Y.; Peinemann, K.-V. *J. Membr. Sci.* **1996**, *112*, **275**.
21. García, M.; Barsema, J.; Galindo, R. E.; Cangialosi, D.; Garcia-Turiel, J.; van Zyl, W. E.; Verweij, H.; Blank, D. H. A. *Polym. Eng. Sci.* **2004**, *44*, **1240**.
22. Meares, P. *J. Am. Chem. Soc.* **1954**, *76*, **3415**.
23. Houde, A. Y.; Stern, S. A. *J. Membr. Sci.* **1994**, *92*, **95**.
24. Teplyakov, V.; Meares, P. *Gas Sep. Purif.*, **1990**, *4*, **66**.
25. Thran, A.; Kroll, G.; Faupel, F. *J. Polym. Sci. B: Polym. Phys.* **1999**, *37*, **3344**.
26. Barrer, R. M. In *Diffusion in Polymers*; Crank, J.; Park, G. S. Eds.; Academic Press: London, 1968; pp 165-217.
27. Van Krevelen, D. W. *Properties of Polymers*, 3rd completely revised edition, Elsevier, **1997**.
28. Pixton, M. R.; Paul, D. R. "Relationships between Structure and Transport Properties for Polymers with Aromatic Backbones" Ch. 3 in "Polymeric Gas Separation Membranes," D. R. Paul and Y. P. Yampol'skii, Eds., CRC Press, Boca Raton, FL, 1994.

Chapter 5

Gas transport properties in PTMSP and EC composite membranes with organic filler trimethylsilylsaccharides with different molecular weight

5.1 Abstract

This chapter aims to investigate systematically the gas transport behavior in two glassy polymers. One is the rigid, high fractional free volume (FFV) poly(1-trimethylsilyl-1-propyne) (PTMSP) and the other is the relatively flexible, considerably lower FFV ethylcellulose (EC). Both polymer systems are filled with a series of various molecular weight (Mw) trimethylsilylsaccharides (TMSS), trimethylsilyl-glucose (TMSG) (Mw= 180), trimethylsilyl-dextran-1 (TMSD1) (Mw= 900-1200), and trimethylsilyl-dextran-500 (TMSD500) (Mw= 350-550 k).

The consistent trend of decreasing gas permeability, diffusivity, and solubility with increasing loading of the TMSS fillers was observed in the PTMSP/TMSS system. In addition, the extent of reduction of gas permeability, diffusivity, and solubility in these composites is closely related to the Mw of TMSS fillers at an equivalent loading of various TMSS in the PTMSP matrix. For example, the PTMSP permeability to nitrogen reduced 227-fold, 43-fold, and 4-fold, respectively, when filled with constant 27.2 % TMSG, TMSD1, and TMSD500. The diffusivity decreased 45-fold, 21-fold, and 3-fold, and the solubility decreased 5.0-fold, 2.0-fold, and 1.3-fold, respectively. The decreases in permeability, diffusivity and solubility are directly related to the decrease of FFV in PTMSP caused by the incorporation of the various Mw fillers. In contrast to the decrease of permeability observed in the PTMSP/TMSS system, a systematic increase of gas permeability and diffusivity was obtained for the EC/TMSS system with increasing loading of TMSS fillers. However, no consistent change of solubility was observed in EC/TMSS. Moreover, the gas diffusivity increase for the EC/TMSS system correlated well with the Mw of the TMSS fillers, in contrast to the permeability increase. For example, when TMSG, TMSD1, and TMSD500 were used as fillers, the permeability to nitrogen of EC composites with 32.1 % fillers increased 1.75-fold, 1.81-fold, and 1.64-fold, respectively, compared to that in unfilled EC. The diffusivity increased 3.32-fold, 1.84-fold, and 1.31-fold, and the solubility increased -1.87-fold, 0-fold, and 1.25-fold, respectively. All applied TMSS fillers led to an increase of gas diffusivity, which can be attributed to increased chain mobility. The chain mobility changes in EC/TMSS resulted in changes of the

excess FFV of EC, and therefore altered the gas solubility. The increase extent of chain mobility was the highest with the lowest Mw TMSS.

5.2 Introduction

In chapter 3 and 4, the gas transport behavior is strongly influenced by the FFV and chain mobility in high FFV PTMSP and low FFV EC, respectively. It will be interesting to further study the effect of filler size on gas transports. In fact, a couple of reports sporadically discussed the filler size effect. For example, Merkel et al.¹ found out that the permeability increases in the polyacetylene (poly(4-methyl-2-pentyne) (PMP)) with the incorporation of eight different size particles (primary particle diameter 7-500 nm) with different surface chemistries. Recently, Andrady et al.² incorporated silica (primary particle size: 7-40 nm) modified with hexamethyldisilazane or dimethyldichlorosilane into the rigid PTMSP. They also found a pronounced correlation between relative permeability and primary particle diameter of the filler. In contrast, a decreased permeability was observed in the flexible PDMS loaded with decreasing zeolite particle size.³

In addition to the filler-size related permeability change, the rigidities of the filler and the polymer matrix also have an influence on the transport properties of the filled system. As far as reported, all flexible organic fillers in PTMSP led to a decreased permeability, compared to pure PTMSP. In contrast, rigid inorganic fillers such as fumed silica in PTMSP increased the permeability. The rigidity of the polymer is indicated by opposite permeability changes for flexible PDMS³ and rigid PTMSP² filled with rigid particles, i.e., zeolites and fumed silica.

To extend the studies of chapter 3 and 4, in this study, the high FFV and rigid PTMSP is filled with two larger molecular weight of TMSS (trimethylsilylsaccharides (i.e. trimethylsilyl-dextran-1 (TMSD1) (Mw= 900-1200) and trimethylsilyl-dextran-500 (TMSD500) (Mw= 350-550 k))) relative to the TMSG (Mw= 180) analogue. Besides, these two TMSS fillers have also been added to the low FFV, more flexible EC for comparison. The impact of various Mw of TMSS fillers in two different polymer matrices on the free volume and chain mobility is comprehensively discussed, associated to the gas transport properties.

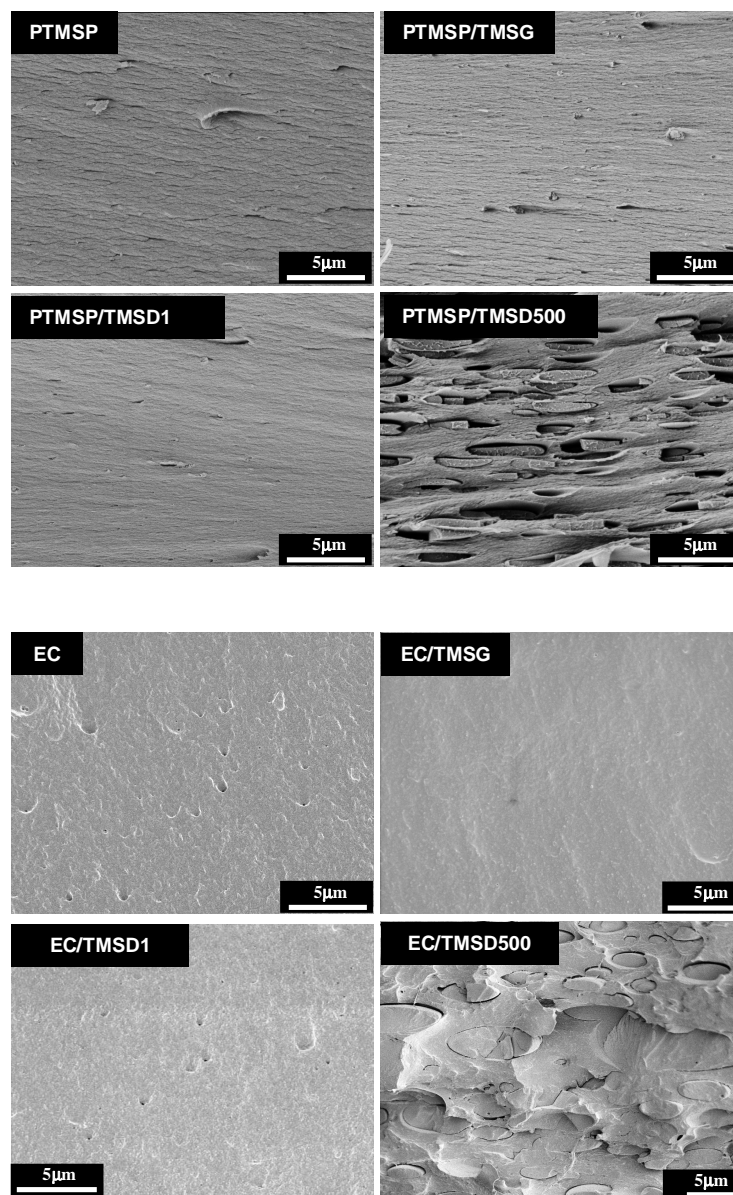
5.3 Results and discussion

5.3.1 Phase behavior via optical observation and scanning electron microscopy (SEM)

All EC/TMSG, EC/TMSD1, PTMSP/TMSG, and PTMSP/TMSD1 composite films are transparent and flawless via optical observation, indicating an excellent miscibility between the polymers (PTMSP and EC) and the low Mw fillers (TMSG and TMSD1). In contrast, the EC/TMSD500 and PTMSP/TMSD500 composite films are opaque, suggesting phase separation. The evaluation of the miscibility of composite material via the optical observation has been discussed elsewhere.⁴

Figure 5.1 presents SEM cross-section of fractures of PTMSP and EC films containing various Mw TMSS fillers at an equivalent loading content (i.e., EC/TMSS (32.1 vol.%) and PTMSP/TMSS (27.2 vol.%)). The homogenous morphologies are observed in low Mw fillers (TMSG and TMSD1) in EC and PTMSP composites. In contrast, the high Mw TMSD500 in both polymer matrices displays heterogeneous morphologies. In the EC/TMSD500 composite, the ellipsoid TMSD500 microphase is dispersed in a continuous EC matrix. The length of the major axis for the TMSD500 ellipses varies approximately from 4 to 10 μm ; the length of the minor axis varies roughly from 1 to 3.7 μm . The geometric shape factor of eccentricity for these TMSD500 ellipses in EC is nearly constant (3.1 ± 0.34). In the PTMSP/TMSD500 composite, the TMSD500 microphase forms more elongated ellipses like platelets, which distributes in a continuous PTMSP matrix similar to that observed for EC. The length of the TMSD500 microphase is in the range of 3–5 μm , and its height is in the range of 0.4–0.7 μm . The ratio of the length/height is nearly constant (7.5 ± 1.2). The different elongations of the filler TMSD500 in EC and PTMSP composites might be attributed to the complex interplay between the matrix and the dispersed phase, and might be also due to the different casting concentration of EC and PTMSP composite. Interestingly, a similar phase behavior was also observed for PTMSP/poly(1-phenyl-1-propyne) (PPP) composites investigated by Toy et al.,⁵ where PPP ellipsoids were observed to disperse in a continuous PTMSP matrix via TEM.

Figure 5.1 SEM photographs of the fracture cross-section of two series of composite materials (EC/TMSS (32 %) and PTMSP/TMSS (27 %)).



Such phase behavior can be explained as following. Theoretically, the phase behavior in a mixture system can be determined by the Gibbs free energy change, which combines the enthalpy change and entropy change in the mixture.⁶ From the enthalpy change point of view, it seems to be reasonable to exclude the surface chemistry dissimilarity for the three saccharide-based fillers, since they have been hydrophobized with trimethylsilyl groups via the silylation with hexamethyldisilazane. Moreover, these TMSS fillers might give rise to an insignificant contribution to the

combinatorial enthalpy change, because the hydrophobic nature of the trimethylsilyl-agent just provides a weak interaction. From the entropy change point of view, as the M_w of the TMSS filler is decreased, the combinatorial entropy change becomes more important and eventually may overcome an unfavourable combinatorial enthalpy change and lead to a homogenous mixture.

5.3.2 Differential scanning calorimetry

At a constant content of TMSS (32.1 vol.%) loading in EC, a decrease of T_g in both EC/TMSG (64 °C) and EC/TMSD1 (100 °C) composite relative to that of unfilled EC (130 °C), which directly reflects increased polymer chain mobility, is observed. Moreover, the low M_w TMSG has more impact to improve the mobility of polymer chain than a relatively high M_w TMSD1. This difference is due to: 1) TMSG has smaller size relative to TMSD1; 2) TMSG (liquid at 30 °C) has a higher mobility than TMSD1 (solid at 30 °C). On the other side, single T_g for both of EC/TMSG and EC/TMSD1 composites further indicates a good compatibility between the polymer host and the filler, which is in good agreement with the results of the SEM and optical observation.

For the EC/TMSD500 composite, a single T_g (130 °C) appears because the glass transition temperatures of TMSD500 and EC are identical by accident (around 130 °C). In fact, the immiscible behavior for EC/TMSD500 is confirmed by SEM, which unveils that the EC chain mobility behavior is unaffected by the filler TMSD500 opposite to those in EC/TMSG and EC/TMSD1 composites.

5.3.3 The transport properties of PTMSP/TMSS system

5.3.3.1 Permeability

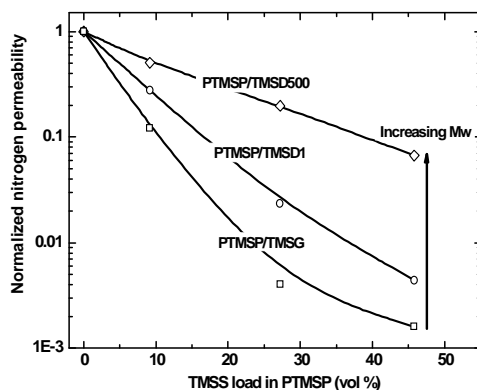
In Table 5.1, the permeability of six gases (He, H₂, CO₂, O₂, N₂, and CH₄) in PTMSP filled with TMSD1, and TMSD500 as a function of various loading contents are illustrated. The gas transport data of the PTMSP/TMSG composites is directly obtained from chapter 3. Obviously, the incorporation of TMSS in PTMSP leads to a systematic decrease in gas permeability. In addition, the declined gas permeability seems to be related to the M_w of TMSS at comparable loading content. For instance, in PTMSP loaded with 27.2 vol. % various M_w TMSS, nitrogen permeability decreases to a large extent, compared to that of unfilled PTMSP ($P_{(N_2)}=5490$ Barrer), e.g., PTMSP/TMSG: 250-fold decrease ($P_{(N_2)}=22$ Barrer), PTMSP/TMSD1: 43-fold decrease ($P_{(N_2)}=128$ Barrer), and PTMSP/TMSD500: 5-fold decrease ($P_{(N_2)}=1087$

Barrer). In order to visibly express the permeability change behavior, Figure 5.2 plots the normalized nitrogen permeability as a function of the loading content of various Mw TMSS. It clearly displays that the filler size is a crucial factor to affect the permeability decrease.

Table 5.1 Gas permeabilities of the PTMSP/TMSD1, and PTMSP/TMSD500 composite membranes at 30 °C.

Composites	loading (vol.%)	permeability ($10^{-10} \text{ cm}^3 \text{ (STP) cm/ (cm}^2 \text{ s cmHg)}$)					
		He	H ₂	CO ₂	O ₂	N ₂	CH ₄
PTMSP/TMSD1	9.2	2260	5307	11855	2719	1516	3753
	27.2	494	925	1695	342	128	284
	45.8	168	253	331	75	24	50
PTMSP/TMSD500	9.2	3475	8060	17450	4295	2780	7100
	27.2	1745	3816	7882	1897	1087	2858
	45.8	781	1567	2899	703	365	936

Figure 5.2 Normalized nitrogen permeability coefficients for PTMSP/TMSG (□), PTMSP/TMSD1 (○), and PTMSP/TMSD500 (◇) as a function of loading amount of respective TMSS filler in PTMSP.



In PTMSP/TMSG, the drastically decreased permeability is closely related to the reduced excess large free volume in PTMSP by filled with TMSG, discussed in chapter 3. Similarly, the considerable permeability loss in the homogenous PTMSP/TMSD1 composite can also be explained by the same mechanism, i.e., “pore filling”. However, the size of TMSD1 is difficult to be estimated because of the complex TMSD1 branch and nonspherical structure. But, the size of TMSD1 with no less than 5 glycoside repeat units is significantly larger than that of TMSG with a single repeat unit. Therefore, it seems to be likely that the partial TMSD1 molecule fits PTMSP micropores rather than the whole molecule, leading to the partial blockage of the FFV in PTMSP.

This assumption is indirectly supported by the fact that the permeability decreases more in PTMSP/TMSD1 than in PTMSP/TMSG at an equivalent filler loading. In PTMSP/TMSG, the drastic permeability decline in PTMSP had a turning point at the loading of around 27 vol % TMSG (e.g. $P(N_2)=22$ Barrer), indirectly indicating roughly 27 vol % interconnected fractional free volume in PTMSP. At equivalent loading content of TMSD1 in PTMSP, the nitrogen permeability is 128 Barrer. Empirically, the nitrogen permeability in most of the low FFV glassy polymers is below 50 Barrer.⁷⁻⁹ This value is higher than that in the low FFV polymers, indicating the partially presence of the large FFV in PTMSP/TMSD1 (27 vol. %). In other words, 27 vol. % TMSD1 loading may only partially block PTMSP micropores.

Comparatively, the drastically decreased permeability in the filled PTMSP system with different Mw PDMS fillers was also reported by Nakagawa et al.,¹⁰ who attributed the reduced permeability to the postulated “pore filling” in PTMSP by PDMS. However, in contrast to the PTMSP/TMSG system, the high Mw PDMS had a stronger impact on gas permeability decline in PTMSP relative to the low Mw PDMS. It has been explained by Nakagawa et al.,¹⁰ that high Mw PDMS just filled the large microvoids in PTMSP, but low Mw PDMS occupied small and large microvoids in PTMSP. This difference might result from the different membrane preparation processes. The incorporation of PDMS in PTMSP was performed by an immersion process,¹⁰ whereas, in this study, the polymer solution-casting process is employed, which is described in the film preparation (see chapter 2).

Concerning the PTMSP/TMSD500 composite, the assumption of “pore filling” seems to be not appropriate, since the size of TMSD500 (dextran500: Mw= 350-550 k) is apparently too large to fit into the FFV in PTMSP. In addition, the SEM reveals that TMSD500 forms micrometer size platelets dispersed in the PTMSP matrix. The gas transport in this type of heterogeneous composite can be well predicted by the modified Maxwell’s model,¹¹ which describes the gas permeability in a more permeable continuous matrix containing a dispersed, less permeable and ellipsoidal filler. Equation 5.1 expresses this correlation.

$$P_m = P_c \left[1 + \frac{(1 + 2W/L)\phi_d}{\frac{P_d/P_c + 2W/L}{P_d/P_c - 1} - \phi_d} \right] \quad (\text{eq. 5.1})$$

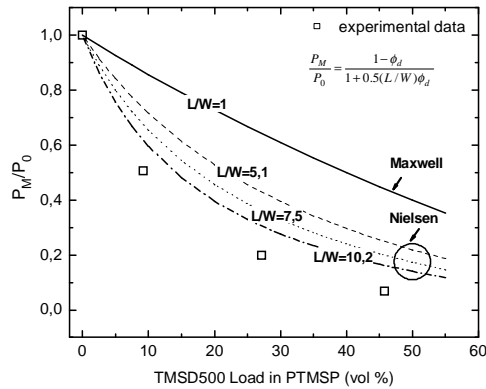
where P_m , P_c , and P_d are the composite, continuous, and disperse phase permeabilities,

respectively, and ϕ_d is the dispersed-phase volume fraction. Here, L and W is the length and width of the dispersed phase platelet, respectively. Due to the fragile property of TMSD500, which might result from its highly branched structure, the measurement of gas permeability for a free-standing TMSD500 film is experimentally unfeasible. However, PTMSP has the largest gas permeability known until now (at least more than 2 orders of magnitude higher than conventional, low FFV glassy polymers).¹² Therefore, it can be assumed that the dispersed TMSD500 phase is nearly impermeable to gas compared to the PTMSP phase. Hence, eq. 5.1 can be simplified, and expressed with the Nielsen's equation,¹³ as described by eq 5.2,

$$P_m = P_c \times \frac{(1-\phi_d)}{[1+(L/2W)\times\phi_d]} \quad (5.2)$$

Figure 5.3 shows a favorable agreement between the Nielsen's model predictions with the experimental results. The geometric factor L/W ranges from 5.1 to 10.2, which is obtained from measuring the dimension of dispersed phase TMSD500 in the continuous phase PTMSP in SEM. The average value of $L/W = 7.5$ displays slight deviation from the prediction of this model, which might be due to the uncertainty of the dimension variation of TMSD500 phase during the fractural process indicated by the SEM. Moreover, this uncertainty might be due to the negligence of permeability of TMSD500 phase in PTMSP.

Figure 5.3 Normalized nitrogen permeability (P_m/P_0) (\square) in PTMSP/TMSD500 as function of TMSD500 loading content in PTMSP, in comparison of that of Maxwell model prediction¹¹ and Nielsen model¹³ prediction with consideration of geometric factor (L/W) of dispersion phase of TMSD500 in the continuous PTMSP phase. The geometric factor L/W is 1 (sphere) for the Maxwell model, and > 1 (nonsphere) for Nielsen model. The geometric factors are obtained from direct measurement the dispersion phase of TMSD500 in SEM. The $L/W = 5.1, 7.5,$ and 10.2 is the smallest value, average value, and largest value, respectively, from the experiment.



In brief retrospect, the consistent tendencies in permeability decrease for various Mw TMSS fillers are observed in the PTMSP/TMSS system. In addition, the various Mw TMSS fillers result in permeability decreases to various extents. The relative size of the free volume of PTMSP and TMSS filler is crucial for the permeability decline.

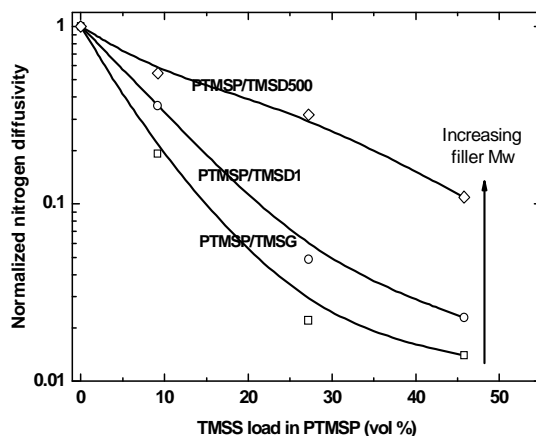
5.3.3.2 Diffusivity and solubility

Gas diffusivities (CO_2 , O_2 , N_2 , and CH_4) in PTMSP/TMSD1 and PTMSP/TMSD500 are summarized in Table 5.2, which excludes He and H_2 because of their experimental uncertainties. Figure 5.4 plots the normalized nitrogen diffusivity as a function of loading content of various Mw TMSS. Similar to the permeability change, the consistent decrease in gas diffusivity accompanied with increased loading of TMSS fillers and the decrease of filler Mw dependent diffusivity are observed. For example, at 27.2 vol % filler content in PTMSP, nitrogen diffusivity reduction is 44-fold for PTMSP/TMSG ($0.08 \times 10^{-5} \text{ cm}^2/\text{s}$), 21-fold for PTMSP/TMSD1 ($0.17 \times 10^{-5} \text{ cm}^2/\text{s}$) and 3-fold for PTMSP/TMSD500 ($1.11 \times 10^{-5} \text{ cm}^2/\text{s}$), compared to that of unfilled PTMSP ($3.5 \times 10^{-5} \text{ cm}^2/\text{s}$). The drastic decrease of diffusivity PTMSP/TMSD1 composites is undoubtedly due to the “pore-filling” as previously discussed. However, in PTMSP/TMSD500 (27.2 vol. %), the nitrogen diffusivity is in the same order as that in PTMSP. This might be result from an increased gas diffusion path length in PTMSP by the less permeable TMSD500 dispersed phase rather than from the PTMSP FFV change.

Table 5.2 Gas diffusivities of the PTMSP/TMSD1, and PTMSP/TMSD500 composite membranes at 30 °C, which are derived based on eq. 2.2 in chapter 2.

composites	loading (vol. %)	diffusivity $\times 10^5$ (cm^2/s)			
		CO_2	O_2	N_2	CH_4
PTMSP/TMSD1	9.2	1.22	1.84	1.25	0.85
	27.2	0.23	0.34	0.17	0.10
	45.8	0.08	0.16	0.08	0.04
PTMSP/TMSD500	9.2	1.46	2.43	1.91	1.31
	27.2	1.00	1.60	1.11	0.90
	45.8	0.38	0.61	0.38	0.29

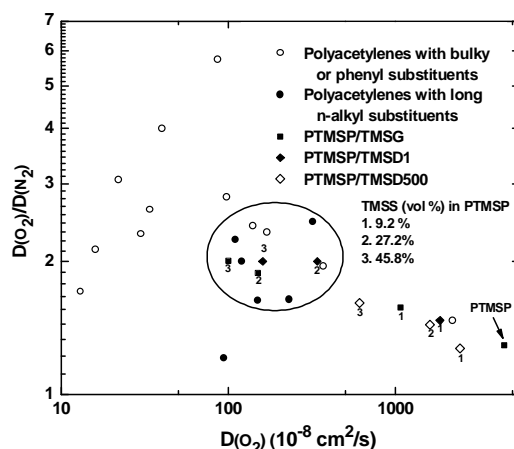
Figure 5.4 Normalized nitrogen diffusivity coefficients for PTMSP/TMSG (\square), PTMSP/TMSD1 (\circ), and PTMSP/TMSD500 (\diamond) as a function of loading amount of respective TMSS filler in PTMSP.



Noticeably, the polyacetylene family exhibits a wide range of difference in diffusivity primarily due to the different polymer chain packing by the variously substituted groups.¹² It is interesting to directly compare the gas diffusivity behavior in the PTMSP/TMSS system with that in substituted polyacetylenes. Figure 5.5 presents the correlation between oxygen diffusivity and oxygen/nitrogen diffusivity selectivity for 19 substituted polyacetylenes (data from Masuda et al.¹⁴), which consist of three substituted groups (e.g., a bulky group, a long n-alkyl group, and a phenyl group). It can be clearly read out from Figure 5.5, that the behavior of $D(O_2)$ and $D(O_2)/D(N_2)$ in PTMSP with 27.2 % and 45.8 % small TMSS fillers (e.g., TMSG and TMSD1) are fairly similar to those in polyacetylenes with long n-alkyl group. Compared to the bulky and rigid phenyl groups, the flexible nature of long n-alkyl groups may lead to increased localized chain mobility in polyacetylenes. On the one hand, it will reduce the diffusion jump energy, resulting in increased diffusivity. On the other hand, the resultant good polymer chain packing will decrease the fractional free volume, and consequently decreasing diffusivity. This phenomenon is also observed in polyacetylene with a series of different alkyl chain length by Pinnau et al.¹⁵ Similarly, in this study, in PTMSP filled with TMSG and TMSD1 the drastically decreased FFV results in a strong gas diffusivity decrease and simultaneous diffusivity-selectivity increase. On the other hand, the small and relatively mobile fillers TMSG and TMSD1 may increase the local gas diffusion to some extent, but weaken the diffusivity-selectivity. Regarding to the effect of localized chain mobility on gas

transport properties, Singla et al. ¹⁶ has studied a series of glassy polymers. Further discussion on it is beyond the scope of this article.

Figure 5.5 Relationship between oxygen diffusivity and its selectivity over nitrogen for PTMSP/TMSG (■), PTMSP/TMSD1 (◆), and PTMSP/TMSD500 (◇) composite membranes in this study. For comparison, this relationship for substituted polyacetylenes ¹⁴ with various side groups, i.e., polyacetylenes with bulky or phenyl substituents (○) and polyacetylenes with long n-alkyl substituents (●) are included.



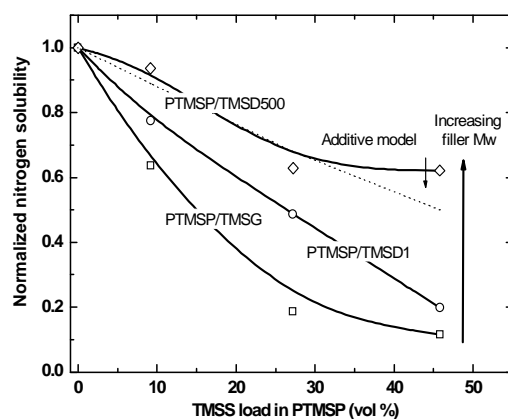
The calculated gas solubility in PTMSP/TMSD1 and PTMSP/TMSD500 based on eq. 1.1, is presented in Table 5.3. The increased loading of different Mw TMSS in PTMSP also leads to a consistent trend of gas solubility decrease. In addition, the small size filler TMSG causes a more significant solubility reduction in PTMSP compared to the large size filler TMSD500. For example, at 27.2 vol. % loading of TMSS in PTMSP, the nitrogen solubility reduces by 5.4-fold for PTMSP/TMSG ($0.291 \times 10^{-2} \text{ cm}^3 \text{ (STP) / (cm}^3 \text{ cmHg)}$), 2.1-fold for PTMSP/TMSD1 ($0.76 \times 10^{-2} \text{ cm}^3 \text{ (STP) / (cm}^3 \text{ cmHg)}$), and 1.6-fold for PTMSP/TMSD500 ($0.98 \times 10^{-2} \text{ cm}^3 \text{ (STP) / (cm}^3 \text{ cmHg)}$), respectively, compared to the unfilled PTMSP ($1.56 \times 10^{-2} \text{ cm}^3 \text{ (STP) / (cm}^3 \text{ cmHg)}$). The relative diffusivity change is higher than the relative solubility change, which suggests that the diffusivity variation in PTMSP/TMSS system is mainly responsible for the permeability change.

Table 5.3 Gas solubilities of the PTMSP/TMSD1, and PTMSP/TMSD500 composite membranes at 30 °C, which are derived based on eq. 1.1 in chapter 1.

composites	loading (vol. %)	Solubility $\times 10^2 \text{ cm}^3 \text{ (STP)} / (\text{cm}^3 \text{ cmHg})$			
		CO ₂	O ₂	N ₂	CH ₄
PTMSP/TMSD1	9.2	9.8	1.5	1.2	4.4
	27.2	7.3	1.0	0.76	2.9
	45.8	4.0	0.48	0.31	1.3
PTMSP/TMSD500	9.2	12.0	1.8	1.5	5.4
	27.2	7.9	1.2	0.98	3.2
	45.8	7.6	1.2	0.97	3.3

The gas solubility in a composite system can be roughly estimated using additive model. Figure 5.6 presents the experimentally determined nitrogen solubility in PTMSP/TMSS composites as a function of filler content, as well as the prediction of the additive model based on eq. 3.2 in chapter 3. It is obvious that the solubilities in both of PTMSP/TMSG and PTMSP/TMSD1 composites have a negative departure from this model. These departures might be attributed to the postulated “pore-filling” in PTMSP by TMSG and TMSD1, leading to less open micropores in PTMSP for gas absorption, and a strongly reduced gas solubility which was discussed in chapter 3. However, the nitrogen solubility in PTMSP/TMSD500 is fairly close to the prediction of the additive model. This behavior can be reasonably explained by the fact that PTMSP intrinsic micropores are nearly intact in the PTMSP/TMSD500 composite with microscopic phase separation. Resultantly, gas solubility in this composite is just the sum of gas sorption in the two phases.

Figure 5.6 Normalized nitrogen solubility coefficients in PTMSP/TMSG (\square), PTMSP/TMSD1 (\circ), and PTMSP/TMSD500 (\diamond) composites as a function of TMSS loading amount at 30 °C, in comparison of the additive model, as shown in a dash line.



5.3.4 Transport properties of EC/TMSS Composites

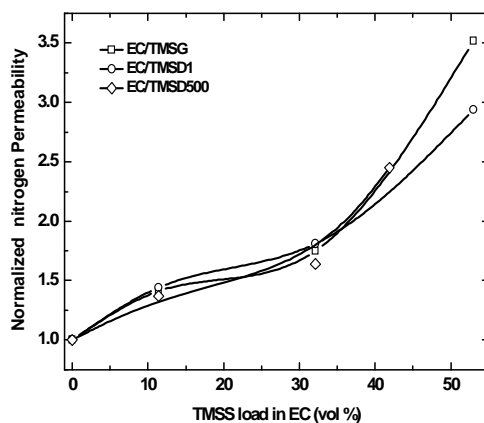
5.3.4.1 Permeability

In Table 5.4, the permeability of six gases (He, H₂, CO₂, O₂, N₂, and CH₄) in EC filled with various Mw TMSS are illustrated. Figure 5.7 plots the normalized nitrogen permeability as a function of the loading content of various Mw TMSS in EC. In contrast to the permeability decrease in PTMSP/TMSS system, a consistent trend of permeability increase in EC/TMSS is observed. In addition, the permeability increase seems to be not well related to the filler's Mw compared to that in PTMSP/TMSS system. For example, as EC is loaded with 32 vol.% TMSG, TMSD1, and TMSD500, respectively, the increase of nitrogen permeability is fairly constant, i.e., EC/TMSG: 1.75-fold (6.1 barrer), EC/TMSD1: 1.81-fold (6.3 barrer), and PTMSP/TMSD500: 1.64-fold (5.7 barrer) compared to that in unfilled EC (3.5 barrer).

Table 5.4 Gas permeabilities of the EC/TMSG, EC/TMSD1, and EC/TMSD500 composite membranes at 30 °C.

composites	loading (vol. %)	permeability ($10^{-10} \text{ cm}^3 \text{ (STP) cm} / (\text{cm}^2 \text{ s cmHg})$)					
		He	H ₂	O ₂	N ₂	CH ₄	CO ₂
EC/TMSG	0.0	40.2	56.0	11.8	3.5	7.1	70.9
	11.4	51.9	72.6	16.8	4.9	10.9	94.0
	32.1	58.0	78.2	20.3	6.1	13.4	93.8
	53	79.2	113	37.3	12.3	31.0	176
EC/TMSD1	11.4	50.4	71.5	15.4	5.1	10.2	90.6
	32.1	65.8	91.9	22.1	6.3	13.6	112.7
	53	87.6	123.8	31.3	10.2	21.2	154.1
EC/TMSD500	11.4	48.8	69.2	14.5	4.8	9.1	89.7
	32.1	56.0	77.3	17.1	5.7	10.0	95.4
	41.9	79.6	111.9	27.6	8.5	17.6	147

Figure 5.7 Normalized nitrogen permeability coefficients for EC/TMSG (□), EC/TMSD1 (○), and EC/TMSD500 (◇) as a function of loading amount of respective TMSS filler in EC.



In the conventional, low FFV glassy polymer EC (FFV: 0.15), the “pore-filling” behavior cannot take place, since even the smallest filler TMSG (~1 nm) is too large to fit the FFV in EC. This is supported by the fact that the average diameter of FFV in conventional, glassy polymer is around 0.2 nm.¹⁸ Furthermore, It seems to be implausible that both of flexible TMSS fillers disrupt EC chain packing like the rigid FS in PTMSP, where the increased FFV results in the increased permeability.

The FFV approach does not seem to be a key factor for the permeability increase in EC/TMSG and EC/TMSD1. However, the increased permeability is obviously mainly attributed to the increased polymer chain mobility, revealed by the decreased T_g accompanied with the loading of TMSG and TMSD1 in EC. In other words, TMSG and TMSD1 in EC seem to act as plasticizers, which can efficiently separate the EC chains and cause the polymer chains to slip more easily. As a result, the opportunity for gas molecule diffusion jump increases more readily in the “plasticized” chains relative to that in the rigid chain.¹⁹ Therefore, an increased gas permeability is observed in both of composites.

However, in EC/TMSD500, the increased gas permeability might not be a consequence of plasticization, which is indicated by the microphase separation for EC/TMSD500 with SEM. The gas transport through this type of heterogeneous medium is a result of collective transport in the EC and TMSD500 phases. The increased gas permeability in EC filled with TMSD500 can be explained by a higher permeability in the TMSD500 phase relative to that in EC phase. This speculation is based on: 1) the same repeat units of TMSD500 and EC, i.e. glycoside; 2) their same backbone structure, but, the highly branched TMSD500 may have a looser packing structure than a relatively linear EC, resulting in a higher FFV in TMSD500; 3) their same backbone structure, but, the side group of trimethylsilyl in TMSD500 is more flexible relative to the ethyl side group in EC, resulting in a higher, localized mobility in TMSD500 compared to that in EC.

5.3.4.2 Diffusivity

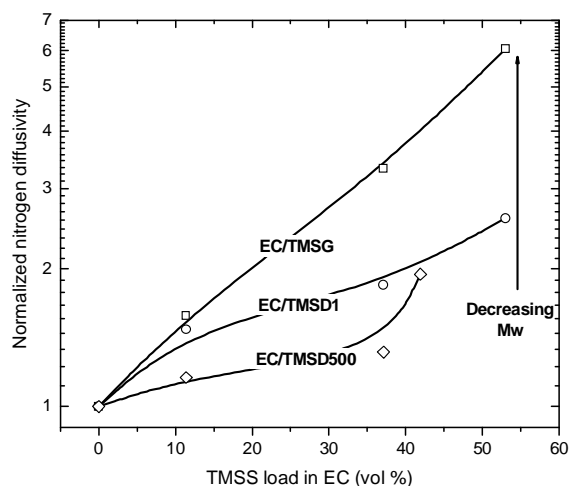
Table 5.5 present the diffusion coefficients of four gases (CO₂, O₂, N₂, and CH₄) in EC/TMSS composites. Figure 5.8 plots the normalized nitrogen diffusivities for EC with TMSG, TMSD1, and TMSD500 as a function of their loading contents. With increasing loading of TMSS in EC the diffusivity increases systematically. In addition, the diffusivity increase is dependent on the Mw of TMSS in EC, in contrast to the permeability, which seems to be independent on the Mw of TMSS fillers. The

diffusivity increases with decreasing Mw of TMSS. For example, at a constant 32 % loading of TMSS fillers, the nitrogen diffusivity increases 3.2-fold in EC/TMSG ($63 \times 10^{-8} \text{ cm}^2/\text{s}$), 1.7-fold in EC/TMSD1 ($35 \times 10^{-8} \text{ cm}^2/\text{s}$), 1.2-fold in EC/TMSD500 ($25 \times 10^{-8} \text{ cm}^2/\text{s}$) compared to that of unfilled EC ($20 \times 10^{-8} \text{ cm}^2/\text{s}$).

Table 5.5 Gas Diffusivities of the EC/TMSG, EC/TMSD1, and EC/TMSD500 composite membranes at 30 °C.

composites	loading (vol.%)	diffusivity $\times 10^8 (\text{cm}^2/\text{s})$			
		CO ₂	O ₂	N ₂	CH ₄
EC/TMSG	0	14	43	20	9
	11.4	24	65	30	15
	32.1	43	115	63	32
	53	86	198	115	68
EC/TMSD1	11.4	19	54	28	12
	32.1	28	78	35	18
	53	38	103	49	26
EC/TMSD500	11.4	18	48	22	11
	32.1	20	57	25	13
	41.9	30	78	37	18

Figure 5.8 Normalized nitrogen diffusivity coefficients for EC/TMSG (□), EC/TMSD1 (○), and EC/TMSD500 (◇) as a function of loading amount of respective TMSS filler in EC.



The impacts on the EC chain mobility by various Mw TMSS fillers cause the corresponding changes in gas diffusivities at an equivalent filler loading. The extent of gas diffusivity increase in EC/TMSS is well related to the declined T_g at 32 vol.% filler loading, which is ranked in the order of: EC/TMSG < EC/TMSD1 < EC/TMSD500. Furthermore, the effect on EC chain mobility by a series of TMSS fillers can also be recognized from gas molecule diffusivity-selectivity. It is well-

known, that an increase in polymer chain mobility will generally lead to a reduction in molecule diffusivity-selectivity. For example, the flexible rubbery polymer PDMS has a very low diffusivity-selectivity. The small molecule O_2 ($d_{\text{eff}} = 0.289$ nm) has a higher diffusivity than the relatively large CH_4 ($d_{\text{eff}} = 0.318$ nm) in the glassy polymer EC ($D(O_2)/D(CH_4) = 4.8$). At equivalent 52 vol.% loading of small TMSS fillers in EC, the O_2/CH_4 diffusivity-selectivity reduction in EC/TMSG, EC/TMSD1, and EC/TMSD500 is about 40 %, 16 %, and 8 %, respectively. Obviously, this diffusivity-selectivity reduction is well correlated to the extent of EC chain mobility increase by various TMSS fillers. In contrast to the EC/TMSS system, the increased molecule diffusivity-selectivity in PTMSP/TMSS is caused by the various extents of blockages of weak size-selective micropores in PTMSP.

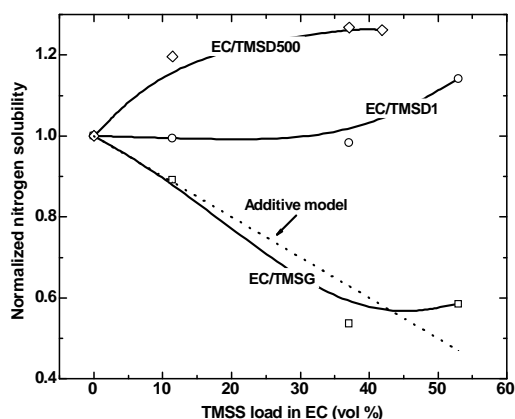
5.3.4.3 Solubility

The calculated solubility data are displayed in Table 5.6. Figure 5.9 presents the relative nitrogen solubility in EC/TMSS systems as a function of filler content. Compared to the consistent trend of the solubility decrease in PTMSP/TMSS systems, no uniform trend of solubility change in EC/TMSS is observed. In the EC/TMSG composite, the gas solubility decreases as TMSG content increases, which is quite consistent with the prediction of the additive model. However, another more plausible explanation is the decreased gas solubility in EC/TMSG attributed to a decreased “excess FFV” in EC/TMSG composite. It is generally known, that a surplus in FFV (i.e., excess FFV) in glassy polymers exists owing to restricted polymer segmental mobility in the glassy state compared to rubbery polymer in an equilibrium state.²⁰ Therefore, gas solubility in a glassy polymer is generally somehow higher than that in rubbery polymer. As TMSG in EC acts as a plasticizer, the plasticized EC polymer chain will relax more easily, leading to a reduced “excess FFV”, and consequently a reduced gas absorption. This similar behavior in EC/TMSG and PTMSP/TMSG further reveals that the “excess free volume” is a critical factor for gas absorption.

Table 5.6 Gas solubilities of the EC/TMSG, EC/TMSD1, and EC/TMSD500 composite membranes at 30 °C.

composites	loading (vol.%)	solubility $\times 10^2$ (cm ³ (STP))/(cm ³ cmHg)			
		CO ₂	O ₂	N ₂	CH ₄
EC/TMSG	0	4.7	0.27	0.18	0.74
	11.4	3.9	0.26	0.16	0.72
	32.1	2.2	0.17	0.10	0.43
	53	2.5	0.19	0.11	0.46
EC/TMSD1	11.4	4.9	0.28	0.18	0.83
	32.1	4.1	0.28	0.18	0.76
	53	4.0	0.31	0.21	0.83
EC/TMSD500	11.4	5.1	0.30	0.22	0.85
	32.1	4.7	0.30	0.23	0.84
	41.9	4.9	0.35	0.23	0.98

Figure 5.9 Normalized nitrogen solubility coefficients in EC/TMSG (□), EC/TMSD1 (○), and EC/TMSD500 (◇) composites as a function of TMS loading amount at 30 °C, in comparison of the additive model, as shown in a dash line.



Concerning gas absorption behavior in the EC/TMSD1 composite, the nitrogen solubility is constant in EC filled with a small portion of TMSD1 (11 vol % and 32 vol %). With a further increased content of TMSD1, the solubility increases slightly by about 10 %. The filler TMSD1 plasticizes the EC polymer chain less than TMSG, indicated by the T_g comparisons. Resultantly, the reduced “excess FFV” in EC by TMSD1 is less than that in EC/TMSG. In addition, compared to the rubber-like TMSG, a glassy oligomer TMSD1 might introduce extra “excess FFV” in this composite at 30 °C, which will more or less compensate the reduced “excess FFV” caused by the plasticization effect.

In the EC/TMSD500 composite, increased gas solubility is observed with the

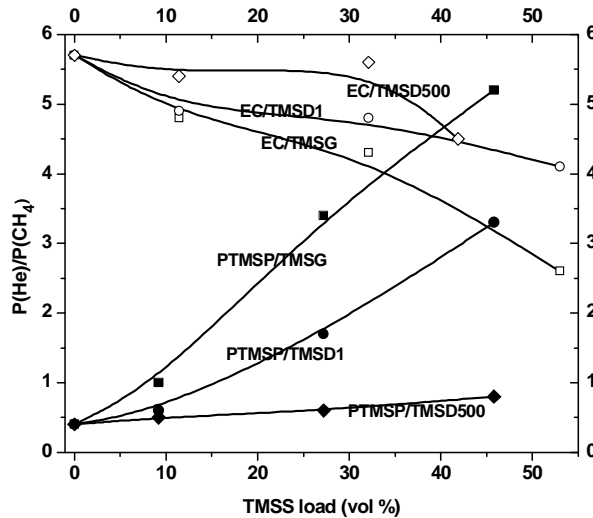
increased loading of TMSD500. Contrary to the impact on the “excess FFV” in EC by low Mw analogies TMSG and TMSD1, the solubility change in EC/TMSD500 might be just the sum of the solubilities in both EC and TMSD500 phases, which is similar to that in PTMSP/TMSD500 composites. Since the microsized phase separation in EC/TMSD500 and PTMSP/TMSD500 is revealed by SEM, the increased gas solubility for this composite might be due to the fact that TMSD500 has a higher gas sorption than EC.

5.3.5 Permselectivity

5.3.5.1 He/CH₄ permselectivity in the PTMSP/TMSS and EC/TMSS systems

The unusual, large FFV in PTMSP causes a weaker gas-size dependent selectivity compared to conventional, low FFV polymers.¹² For example, the permeability of the small gas He ($d_{\text{eff}} = 0.178$ nm) is even 2.5-fold lower than that of the large gas CH₄ ($d_{\text{eff}} = 0.318$ nm) in PTMSP. In contrast, in the low FFV, glassy polymer ethylcellulose, the $P(\text{He})$ is 5.7-fold faster than the $P(\text{CH}_4)$. The permeability change as function of gas diameter is extraordinarily sensitive to polymer FFV and chain mobility change. In order to clearly visualize the impacts of the free volume change in PTMSP and the chain mobility variation in EC on the gas size-selectivity behavior by the loading of various Mw TMSS fillers, Figure 5.10 plots the He/CH₄ selectivity as function of loading content of TMSG, TMSD1, and TMSD500 in PTMSP and EC. The high Mw filler TMSD500 in PTMSP and EC insignificantly alters the He/CH₄ selectivity, which is in good agreement with the observation of phase separation by SEM. Therefore, nearly undisturbed FFV in the continuous PTMSP phase and almost unchanged chain mobility in the continuous EC phase are the result. Additionally, the lowest Mw filler TMSG in both systems has the strongest influence on the variation of the He/CH₄ selectivity, compared to higher Mw TMSS fillers at the equivalent filler loading. In the opposite way, the He/CH₄ selectivity systematically increases in PTMSP with increasing loading of TMSG and TMSD1, which serves as another indirect evidence of the “pore filling.

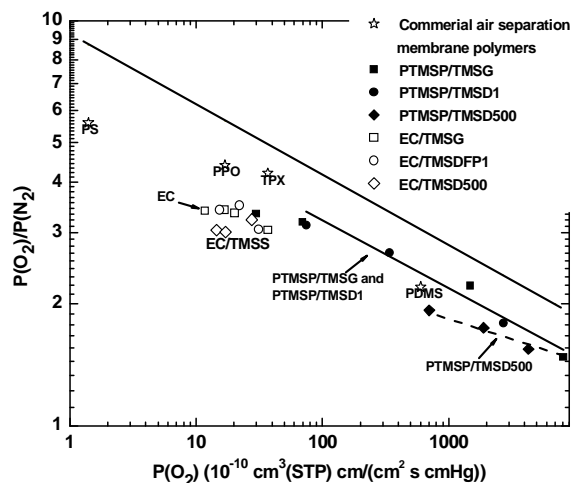
Figure 5.10 Selectivity of He/CH₄ in EC/TMSG (□), EC/TMSD1 (○), EC/TMSD500 (◇), PTMSP/TMSG (■), PTMSP/TMSD1 (●), and PTMSP/TMSD500 (◆) composites as a function of loading amount of respective TMSS filler.



5.3.5.2 O₂/N₂ permselectivity in PTMSP/TMSS and EC/TMSS systems

It is worthwhile to review the oxygen/nitrogen separation in PTMSP/TMSS and EC/TMSS systems, since air separation is the largest market in gas separation. In Figure 5.11, the O₂/N₂ selectivity and O₂ permeability for PTMSP/TMSS and EC/TMSS composites is presented. Four commercial air separation membrane materials ²¹ (PDMS, poly(4-methyl-1-pentene) (TPX), poly(2,6-dimethyl-1,4-phenylene oxide) (PPO), and polysulfone (PS)) are also included, in addition to the well-known Robeson's upper bond. ²² The PTMSP/TMSD1 composites also show a similar O₂/N₂ separation performance relative to PTMSP/TMSG. However, in PTMSP/TMSD500, the decreased permeability cannot be sufficiently compensated by the increased selectivity compared to those in other two analogues composites. Compared to the fastest permeability polymer PDMS, the transport properties in PTMSP/TMSG and PTMSP/TMSD1 is noticeably located more close to the Robeson's upper bond.

Figure 5.11 Relationship between oxygen permeability and its selectivity over nitrogen for EC/TMSG (\square), EC/TMSD1 (\circ), EC/TMSD500 (\diamond), PTMSP/TMSG (\blacksquare), PTMSP/TMSD1 (\bullet), and PTMSP/TMSD500 (\blacklozenge) composite membranes in this study. For comparison, this relationship for several commercial air separation membranes ²¹ (e.g., poly(dimethylsiloxane) [PDMS], poly(4-methyl-1-pentene) [TPX], poly(2,6-dimethylphenylene oxide) [PPO], and polysulfone [PS]). The upper bound line comes from Robeson. ²²



Ethylcellulose was one of the first successful polymers for commercial air separation membranes. ^{21, 23} The addition of TMSS fillers into EC leads to a significant permeability increase with only a slight selectivity loss. With a permeability of 50 Barrer and an O₂/N₂-selectivity of more than 3, the EC/TMSS composite might be an attractive low cost material for oxygen enrichment.

5.4 Conclusion

In the rigid, high free volume PTMSP filled with TMSS, gas permeability, diffusivity, and solubility decreased consistently with increasing filler content. Low Mw fillers (e.g., TMSG and TMSD1) led to a stronger reduction of gas transport parameters compared to the high Mw filler TMSD500. The small fillers caused a reduction of the free volume. Consequently, permeability, diffusivity and solubility were reduced. The large filler TMSD500, on the other hand, was too large to occupy the free volume elements of PTMSP. A microsized phase separation could be observed by SEM. In this composite, the reduced permeability could be attributed to the combined permeability in both PTMSP and TMSD500 phases.

Contrary to the PTMSP/TMSS system, the TMSS filled EC (low FFV) showed a higher gas permeability than the pure polymer. Additionally, no clear correlation

between M_w of the filler and permeability increase could be observed. The low M_w fillers TMSG and TMSD1 led to a decreased T_g and an increase of gas diffusivity, which can be explained by an increase in chain mobility (plasticization effect). Moreover, the plasticization simultaneously leads to a reduction of “excess FFV” in the glassy polymer EC, resulting in a decrease of gas sorption. Similar to the PTMSP/TMSD500 composite, the high M_w filler TMSD500 did not change the polymer chain mobility and the FFV, which is also supported by SEM observation and T_g measurements. The increased permeability, diffusivity, and sorption can be explained by the combination of the transport properties of the EC and TMSD500 phases.

5.5 References

1. Merkel, T. C.; Freeman, B. D.; Spontak, R. J.; He, Z.; Pinnau, I.; Meakin, P.; Hill, A. J. *Science* **2002**, *296*, **519**.
2. Andraday, A. L.; Merkel, T. C.; Toy, L. G. *Macromolecules* **2004**, *37*, **4329**.
3. Tantekin-Ersolmaz, S. B.; Atalay-Oral, C.; Tatlier, M.; Erdem-Senatarlar, A.; Schoeman, B.; Sterte, J. *J. Membr. Sci.* **2000**, *175*, **285**.
4. Roberto, A. K. Transmission and reflection of light in multiphase media. In *Polymer Blends: Formulation and Performance*; Paul, D. R. and Bucknall, C. B. Eds.; John Wiley & Sons; **2000**; pp 301-304.
5. Toy, L. G.; Freeman, B. D.; Spontak, R. J.; Morisato, A.; Pinnau, I. *Macromolecules* **1997**, *30*, **4766**.
6. Merfeld, G. D. and Paul, D. R. Polymer-polymer interactions based on mean field approximations, Paul, D. R. and Bucknall, C. B. Eds.; John Wiley & Sons; **2000**; pp 55-91.
7. Hwang, S. T.; Choi, C. K.; Kammermeyer, K. *Separation Science* **1974**, *9*, **461**.
8. Pauly, S. Permeability and diffusion data. In: *Polymer Handbook, 4th edition*; Brandrup J.; Immergut E. H.; Grulke E. A. Eds.; John Wiley & Son; **1999**; VI/543-VI/569.
9. Park, J. Y.; Paul, D. R. *J. Membr. Sci.* **1997**, *125*, **23**.
10. Nakagawa, T.; Fujisaki, S., Nakano, H.; Higuchi, A. *J. Membr. Sci.* **1994**, *94*, **183**.
11. Petropoulos, J. H. Membrane with non-homogenous sorption and transport

- properties *In Polymer Membranes*; Gordon M., Eds.; Springer Verlag; 1985; pp 93-142.
12. Nagai, K.; Masuda, T.; Nakagawa, T.; Freeman, B. D.; Pinnau, I. *Prog. Polym. Sci.* **2001**, *26*, **721**.
 13. Nielsen, L. E. *J. Macromol. Sci. (Chem.)* **1967**, *A1(5)*, **929**.
 14. Masuda, T.; Iguchi, Y.; Tang, B.-Z.; Higashimura, T. *Polymer* **1988**, *29*, **2041**.
 15. Pinnau, I.; Morisato, A.; He, Z. *Macromolecules* **2004**, *37*, **2823**.
 16. Singla, S.; Beckham, H. W.; Rezac, M. E. *J. Membr. Sci.* **2002**, *208*, **257**.
 17. Merkel, T. C.; Freeman, B. D.; Spontak, R. J.; He, Z.; Pinnau, I.; Meakin, P.; Hill, A. J. *Chem. Mater.* **2003**, *15*, **109**.
 18. Hofmann, D.; Heuchel, M.; Yampolskii, Y.; Khotimskii, V.; Shantarovich, V. *Macromolecules* **2002**, *35*, **2129**.
 19. Crank, J., Park, G. S., *Diffusion in Polymers*, London, Academic U.K., 1986.
 20. Van Krevelen, D. W. *Properties of Polymers*, 3rd completely revised edition, Elsevier, 1997.
 21. Nunes, S.-P.; Peinemann, K.-V. Gas separation with membrane. In *Membrane technology in the chemical industry*; Nunes, S.-P.; Peinemann, K.-V., Eds.; Wiley-VCH: Weinheim, 2001; pp 39-67.
 22. Robeson, L. *J. Membr. Sci.* **1991**, *62*, **165**.
 23. Baker, R. W. *Ind. Eng. Chem. Res.* **2002**, *41*, **1393**.

Chapter 6

Gas transport properties in ethylcellulose nanocomposite membranes with various nanosized silylated glucose

6.1 Abstract

In this chapter, the six gases (He, H₂, CO₂, O₂, N₂, and CH₄) permeability, diffusivity and solubility coefficients in ethylcellulose (EC) filled with a series of loading of various silyl-agents glucose (i.e., trimethylsilyl-glucose (TMSG), triethylsilyl-glucose (TESG), triisopropylsilyl-glucose (TIPSG), and diphenylmethylsilyl-glucose (DPMSG)) were determined at 30 °C with the time-lag method. In addition, the transport properties in EC with a representative plasticizer dioctylphthalate (DIPH) and one glucoside based derivate pentacetate-glucose (PAG) are included for comparison. With alkyl-silylated glucose and DIPH in EC, increased diffusivity and permeability are observed. In contrast, the introduction of DPMSG and PAG results in a decreased diffusivity and permeability. At the equivalent filler loading, TMSG exhibits the highest permeability and diffusivity increase, compared to TIPSG, and DIPH. Similarly, the loading of all of fillers lead to a decreased gas solubility, however, TMSG gives the least solubility loss relative to other fillers. In the EC/silylated-glucose, the gas permeation properties are related to the variation of excess fractional free volume (FFV) and local chain mobility. The increased alkyl chain length attached on the silane leads to more flexibility (i.e., increase diffusivity), but less excess FFV (i.e., decrease diffusivity). The overall gas transport properties are the combination of both factors. In the oxygen/nitrogen separation, the EC/TMSG exhibits an improved performance relative to the unfilled EC. This simple physical introduction of trimethylsilyl (TMS) group produces a similar effect to the chemical modification of polymer with TMS group.

6.2 Introduction

The physical incorporation of low molecule weight organic additives into membrane provides a simple way for modifying the gas separation properties of membrane materials. Maeda and Paul ¹⁻⁴, Ruiz-Treviño and Paul ⁵⁻⁶, Larocca and Pessan ⁷ have systematically studied the gas transport properties in three practical membranes, i.e. polysulfone (PSF), polyphenyloxide (PPO), and polyetherimide (PEI) with incorporation of various organic additives. Normally, it has been found that the

addition of these fillers into glassy polymers reduces the gas permeability and enhances the selectivity, which can be interpreted by the retarded local chain mobility, reduced fractional free volume and the loss of excess free volume.¹⁻⁷ However, no improvement in the separation performance has been reported.⁴ Since the performances of the filled composites are tightly related to the filler properties, such as FFV and mobility, it is necessary to carefully design and synthesize new fillers in order to obtain novel composite membrane materials.

Previous structure/properties studies have provided some empirical rules for designing polymeric membrane materials. Several works revealed that the silyl groups often favored high gas permeability with minimal sacrifice in selectivity.⁸⁻¹³ For instance, it was found that the substitution of trimethylsilyl (TMS) group at the ortho ether site of polysulfone (PSF) significantly increased the oxygen permeability from 1.1 to 7.1 Barrer compared to the unmodified one (PSF), and slightly decreased the oxygen/nitrogen selectivity from 5.8 to 5.5.¹⁰ Hence, it is interesting to study the composite membranes filled with low molecular fillers containing silyl groups. In the chapter 1, a comprehensive summary of gas transport properties in TMS-substituted polymer membranes is outlined.

In the present work, the gas transport properties in ethyl cellulose (EC) membrane is studied containing four various silylated-glucose fillers, i. e., trimethylsilyl-glucose (TMSG), triethylsilyl-glucose (TESG), triisopropylsilyl-glucose (TIPSG), and diphenylmethylsilyl-glucose (DPMSG). EC is selected as the host membrane mainly because it is a polymer material with medium gas separation performance, good membrane formation ability, good flexibility, excellent durability and low cost.¹⁴⁻¹⁶ In addition, EC is one of the membrane materials used for the industrial oxygen/nitrogen separation.¹⁷ Glucose is used as the carrier for the silyl group because it has the same structure as the repeat unit of EC (i.e., glycoside), that will give a compatible composite. Moreover, glucose containing five hydroxyl groups could provide high opportunities in silyl group substitution.

6.3 Results and discussion

6.3.1 Permeability and permselectivity

Table 6.1 illustrates the effect of filler incorporation on the permeability coefficients of six light gases (He, H₂, CO₂, O₂, N₂, and CH₄) in EC composite membranes. For the four silylated glucose fillers, the incorporation TESG and TIPSG leads to an increase in gas permeability compared with unmodified EC. The permeability

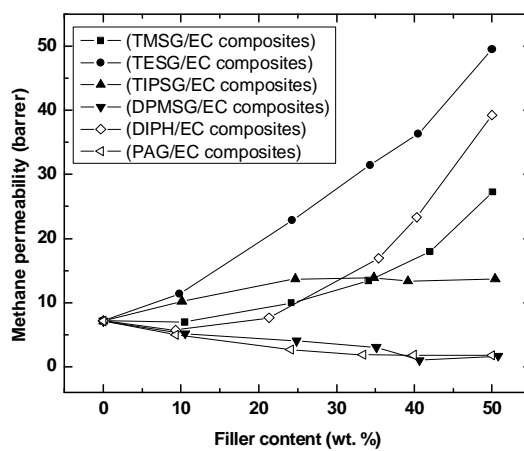
increase is more pronounced for TMSG filler than TIPSG (For example, at c.a. 24 wt.% filler loading, $P(N_2) = 8.98$ Barrer in EC/TESG, $P(N_2) = 5.86$ Barrer in EC/TIPSG, comparatively, $P(N_2) = 3.48$ Barrer in unfilled EC). In contrast, the addition of DPMSG filler drastically decreases the permeability (For example, $P(N_2) = 1.85$ Barrer in EC/DPMSG (24.9 %)). For the TMSG containing composite membranes, the permeability maintains nearly unchanged at low content of loading (For example, $P(N_2) = 3.10$ Barrer in EC/TMSG (10.5 %)), and then turns to increase with continuously increasing loading. For the other two fillers (i.e, DIPH and PAG), the addition of DIPH decreases the gas permeability at low DIPH loading and then a fast increase takes place, similar to that of EC/TMSG. The EC/PAG composite membranes show monotonic reduction of gas permeability with increasing PAG content, like the EC/DPMSG composite. To visibly express the relative permeability change in the EC composites with various fillers, in Figure 6.1, the methane permeability is plotted as a function of filler content for all the six fillers studied. It clearly shows that the gas transport behavior in EC composite membranes is significantly affected by various fillers.

Table 6.1 Gas permeability coefficients in EC and EC composite membranes incorporated with various silylated glucose fillers, DIPH and PAG.

Filler (wt.%)	P(He)	P(H ₂)	P(O ₂)	P(N ₂)	P(CO ₂)	P(CH ₄)
No additive	40.2	56.0	11.8	3.48	70.9	7.11
TMSG (10.5)	38.0	50.8	11.1	3.10	63.9	6.94
TMSG (24.2)	49.9	67.5	15.8	4.82	77.6	9.95
TMSG (34.1)	56.5	75.9	19.8	6.23	92.0	13.4
TMSG (42.0)	63.0	87.0	24.8	7.86	113.6	17.9
TMSG (50.1)	78.3	107.8	34.7	11.2	162.3	27.3
TESG (9.8)	45.2	66.0	16.6	4.94	91.9	11.3
TESG (24.3)	55.0	85.0	26.5	8.98	133.5	22.8
TESG (34.3)	60.9	96.2	34.4	12.0	170.2	31.4
TESG (40.5)	68.0	104.1	38.5	14.3	189.3	36.3
TESG (50.0)	72.8	121.0	49.3	18.8	235.0	49.5
TIPSG (10.1)	46.9	63.0	15.4	4.85	83.4	10.2
TIPSG (24.7)	46.3	66.1	18.5	5.86	94.0	13.7
TIPSG (34.8)	46.7	65.0	18.5	6.47	92.0	13.9
TIPSG (39.2)	45.9	62.9	17.8	5.93	86.3	13.3
TIPSG (50.4)	45.5	62.6	18.1	6.00	85.1	13.7
DPMSG (10.5)	31.5	42.0	8.63	2.50	51.0	5.15
DPMSG (24.9)	23.8	31.8	6.57	1.85	38.4	4.02
DPMSG (35.1)	21.3	25.8	4.77	1.45	28.0	3.03
DPMSG (40.7)	18.7	21.2	2.34	0.58	10.4	0.98
DPMSG (50.8)	20.4	24.6	3.57	0.95	18.1	1.67
DIPH(9.31)	31.98	42.14	9.18	3.46	51.19	5.7
DIPH (21.3)	28.05	38.20	10.37	3.46	58.70	7.61
DIPH (35.4)	33.03	49.09	18.01	6.23	108	16.91
DIPH (40.3)	40.17	59.97	23	8.53	142.50	23.31
DIPH (50.0)	48.26	73.83	34.48	13.16	217.05	39.26
PAG (9.31)	36.99	47.86	9.07	2.91	51.52	4.95
PAG (24.1)	30.70	34.21	5.62	1.89	29.29	2.65
PAG (33.4)	26.15	29.35	4.47	1.39	n.a.	1.85
PAG (39.9)	26.27	27.97	4.23	1.22	22.28	1.81
PAG (50.0)	26.27	27.39	4.99	1.43	22.34	1.75

Permeability unit: barrer, 1 barrer = 10^{-10} cm³ (STP) cm/ (cm² s cmHg).

Figure 6.1 Permeability coefficients for CH₄ as a function of filler content in EC composite membranes incorporated with various silylated glucose fillers and two commercial fillers DIPH and PAG.

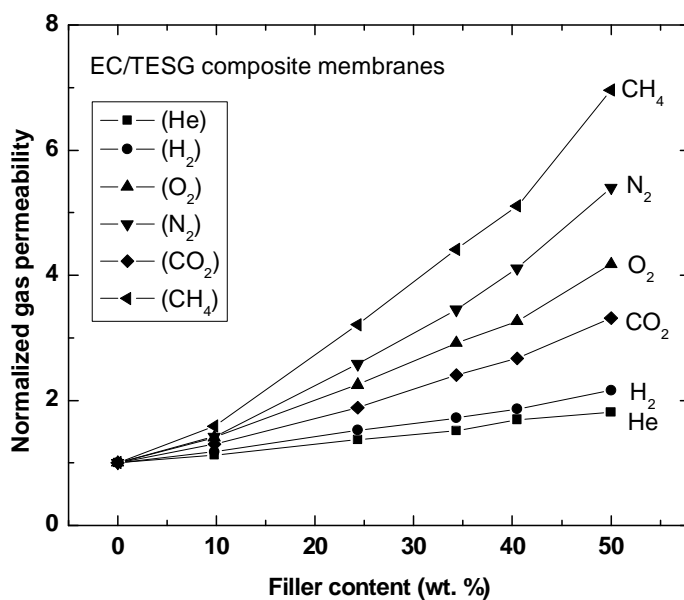


The enhanced gas permeability in EC/TMSG (with TMSG content starting from 24.2 %), EC/TESG, and EC/TIPSG composites may be explained mainly by the improved local mobility with the incorporation of the fillers. Firstly, the addition of filler in glassy polymers normally results in a decreased glass transition temperature (T_g). It has been observed that the T_g decreases from 130 °C for unfilled EC to 64 °C for the EC/TMSG composite at TMSG content of 34.2 %. It suggests that the fillers act as plasticizers, which can efficiently separate the EC chains and cause the polymer chains more easily to slip. This plasticization effect can also be further supported by the fact that the equivalent loading of the TESG leads to a noticeable higher increase in the gas permeability compared to the TMSG and TIDSG fillers because of the more flexible ethyl group than methyl and isopropyl groups in the filler side chain. In addition, the silyl groups themselves like TMS group, which are bulky and able to generate many molecular scale voids,⁹⁻¹² should also play another important role in boosting gas permeability. In contrast, the declined gas permeability in the EC/DPMSG composite can be ascribed to the presence of planar phenyl group with dense packing. Additionally, the stiff phenyl group, compared to alkyl groups, could even restrict chain mobility, resulting in the decreasing permeability.

Generally speaking, the incorporation of TMSG, TESG, and TIDSG fillers in EC membranes increases the permeability of all penetrants. However, it can be found in Table 6.1, that the permeability of small molecules He and H₂ increases to a lesser

extent as compared to the other four larger gases. For example, Figure 6.2 presents the plots of the normalized permeability (calculated as the ratio of the permeability in filled EC to the unfilled EC) in EC/TESG composites for all six gases as a function of filler content. It can be easily read out that the permeability enhancement of six tested penetrants increases in the order of: He < H₂ < CO₂ < O₂ < N₂ < CH₄, which is the same rank as the molecular sizes. This behavior can be explained as the following. For the diffusion of small gases like helium and hydrogen, as stated by Meares¹⁸, the cooperative oscillation of the polymer segment might be sufficient for performing a jumping process. However, for the diffusion of larger gases, the complete rotation of polymer segment may be required. Hence, as the polymer local chain mobility increases, larger gas takes the advantage to enhance the diffusion coefficient than small gas. This is also in agreement with the fact that the rigid glassy polymer exhibits high size selectivity and flexible rubbery polymer losses its diffusion selectivity based on the penetrant size. In addition, this similar trend of penetrant size dependent permeability change is also observed in EC/TMSG, EC/TIPSG, and EC/DIPH, indicating the identical transport behavior as above mentioned.

Figure 6.2 Normalized gas permeability coefficients for He, H₂, O₂, N₂, CO₂, and CH₄ as a function of filler content in EC/TMSG composite membrane.



It is worthwhile to study the effect of filler loading on the gas selectivity. As it is pointed out previously, the incorporation of DPMSG and PAG decreases the

permeability and increases the selectivity, following the trade-off rule.¹⁹ On the other hand, the loading of TMSG, TMSG, TIPSG, and DIPH filler into EC membrane leads to increased gas permeability. The improved permeability is at the expense of decreased selectivity for most of the gas pairs. However, for some pairs, i.e., CO₂/H₂, and CH₄/N₂, the selectivity increases at the same time when gas permeability increases for the reason that the larger gas has larger permeability increase as discussed above. For instance, the CO₂ permeability increases from 62 to 170 Barrer for EC/TMSG composite membrane (with 34.3 % TMSG loading), as compared to the unmodified EC. Meantime, the selectivity of CO₂/H₂ increases from 1.1 to 1.8.

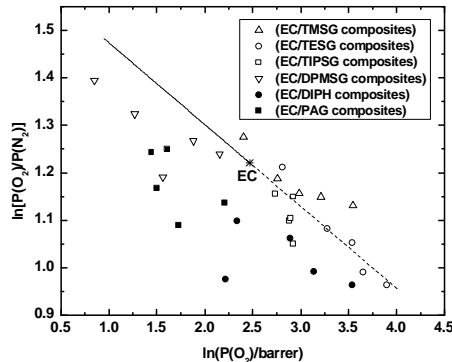
EC is one of the polymers interesting for the commercially used O₂/N₂ separation. Hence, it is worthwhile to further study the O₂/N₂ separation performance in filled EC composite membranes. Figure 6.3 plots O₂/N₂ selectivity as a function of oxygen permeability in the form of natural logarithm for the EC composite membranes containing various fillers. The dash line in this figure is presented to evaluate the influence of the filler incorporation on the O₂/N₂ separation performance compared to the unfilled EC. The dash line is determined as:

$$P_{O_2} / P_{N_2} = \beta P_{O_2}^{-0.1724}$$

$$\beta = \exp[\ln P_{O_2,EC} + 0.1724 \ln(P_{O_2} / P_{N_2})_{EC}] \quad (\text{eq. 6.1})$$

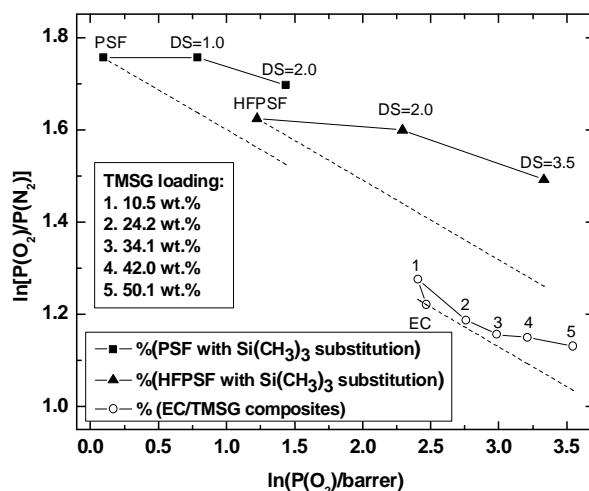
In fact, Equation 6.1 identifies the line that crosses the point of unmodified EC is parallel to the Robeson plot for O₂/N₂ gas pair using equation of $P_{O_2} / P_{N_2} = 9.2 P_{O_2}^{-0.1724}$.¹⁹ It is reasonable to state that the points above the dash line suggest an improvement in the gas separation performance.

Figure 6.3 Relationship between oxygen permeability and O₂/N₂ selectivity for EC composite membranes incorporated with various silylated glucose fillers and two commercial filler DIPH and PAG.



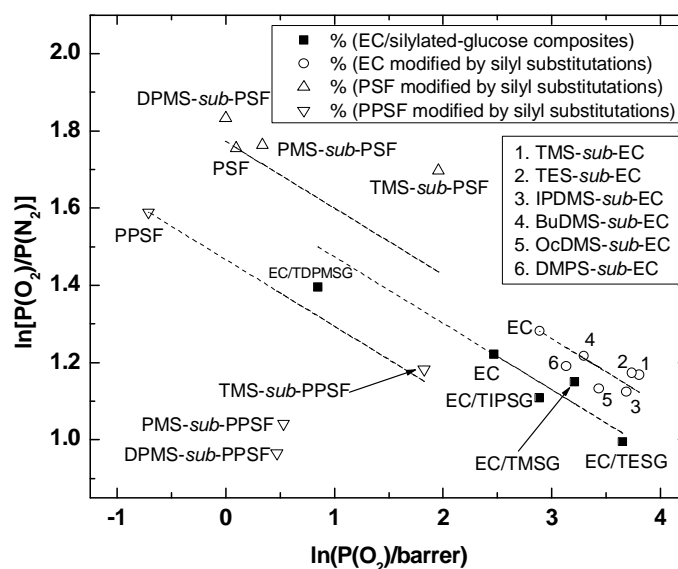
It can be observed from Figure 6.3 that the silylated-glucose fillers exhibit a good performance in terms of permeability and selectivity, in comparison with the two commercial fillers PAG and DIPH. Considering PAG is the acetate substituted glucose, it clearly suggests the better performance of the silylated glucose comes mainly from the presence of the silyl groups. On the other hand, the introducing of the silylated groups doesn't always lead to better O₂/N₂ separation performance as compared to the unmodified EC. The incorporation of TIPSG and TDPMSG even diminishes the O₂/N₂ separation performance. The EC/TESG composite membranes basically maintain the O₂/N₂ separation performance, but one can tailor the permeability/selectivity properties in a relatively wide range. It is interesting to find out that the EC/TMSG composite membranes exhibit better performances as compared to the original EC membrane, especially at high TMSG loading. This behavior is in a good agreement with the previous studies, which have shown that the chemical substitution of TMS groups in a polymer chain can generally improve the separation performance because of its unique, bulky and flexible properties.⁸⁻¹³ For example, in the studies of the transport properties of the two TMS substituted polysulfones, Lee et al. have also found the improvement in the separation performance is more significant with increase of degree of substitution (DS) of the TMS group.¹¹ In Fig. 6.4, the effect of the TMSG contents on the performance of the composite membranes is illustrated, together with the effect of the DS of TMS group in PSF and hexafluoropolysulfone (HFPSF) on the properties of the chemical modified membranes. The dash lines in Figure 6.4 are used to compare the performance of the modified and unmodified membranes that are determined by Equation 6.1. Figure 6.4 clearly shows that increasing the amount of the TMS group leads to a better separation performance, no matter that the TMS group is introduced by the chemical or physical modifications.

Figure 6.4 Relationship between oxygen permeability and O_2/N_2 selectivity for EC/TMSG composite membranes with different TMSG content and for TMS substituted PSF¹⁰ and HFPSF¹⁰ at different degree of substitution.



As mentioned previously, various silyl groups can be introduced into the membrane materials by two different methods, i.e., chemical modification by direct substitution and physical modification by incorporation of silylated fillers in this study. Hence, it is interesting to further compare these two methods with the introduction of various silyl groups. In Fig. 6.5, the oxygen/nitrogen separation performance in four systems is compared: 1) EC/silylated-glucose composite membranes (containing around 40 wt. % silylated glucose fillers); 2) silylated EC;¹³ 3) silylated PSF;¹⁰ and 4) silylated phenylpolysulfone (PPSF)¹⁰ with various silyl groups. The degree of silylation of various silyl groups in PSF and PPSF is around 2.0¹⁰. For the silylated derivatives of EC, the substitution degree is quite low (around 0.31)¹³. It is worthwhile to mention that the gas transport data in the EC membrane reported by Khan et al.¹³ are different from those of the EC membrane. It might be due to the different ethoxy content in the two studies (48 wt.% in Khan et al's work¹⁶ vs. 46 wt. % in this study), since it was reported that the gas transport properties in EC membranes were greatly affected by the ethoxy content¹⁴⁻¹⁵. Similarly, in Fig. 6.5, four dash lines are presented to evaluate the influence of the chemical substitution of various silyl groups and physical incorporation of silylated glucose fillers on membranes gas separation performance in relative to the unmodified membranes.

Figure 6.5 Relationship between oxygen permeability and O_2/N_2 selectivity for EC composite membranes incorporated with various silylated glucose fillers and for EC¹³, PSF¹⁰ and HFPSF¹⁰ substituted with various silyl groups.



Legend: TMS-sub-EC: Trimethylsilyl-ethylcellulose; TES-sub-EC Triethylsilyl-ethylcellulose ; IPDMS-sub-EC: Dimethylisopropylsilyl-ethylcellulose; BuDMS-sub-EC: Dimethyl-tert-butylsilyl-ethylcellulose; OcDMS-sub-EC: Dimethyl-n-octylsilyl-ethylcellulose; DMPS-sub-EC: Dimethylphenylsilyl-ethylcellulose

From Figure 6.5, firstly, it can be seen that the introducing of TMS groups in the membrane materials, either by chemical method or physical method, can improve the separation performance (e.g., TMS-sub-PSF vs PSF, TMS-sub-PPSF vs PPSF, TMS-sub-EC vs EC, EC/TMSG vs EC). Secondly, the substitution of TES group in EC membrane also leads to a slightly better performance. Comparatively, the physical incorporation of TMSG has no help to improve the separation performance. Thirdly, the substitution of *iso*-propyldimethylsilyl (IPDMS) group in EC membranes have slightly decreased separation performance, which is similar to the physical incorporation of TIPS-glucose in EC membrane. Fourthly, except that the increased separation performance has been observed in diphenylmethylsilyl (DPMS) substituted PSF and phenylmethylsilyl (PMS) substituted PSF, the decreased separation performance in other chemically or physically modified phenylsilyl has been observed. In brief summary, Fig. 6.5 reveals that the substitution of silyl groups may improve or deteriorate the membrane separation performance, depending on the structure of the silyl groups, and also on the polymer class. Interestingly, the introducing of the TMS

groups into membrane materials normally leads to the improved gas separation performance. Finally, it is fair to say that the physical modification of EC membrane can modify the gas transport properties in a comparable way as the chemical modification.

6.3.2 Diffusivity and solubility

Since the permeability is a product of diffusivity and solubility, further studies on these two terms can provide insight into the gas transport in those composite membranes. Table 6.2 presents the diffusion and sorption coefficients for N₂, O₂, CO₂, and CH₄ in all the EC/fillers composites. Helium and hydrogen are absent since the accuracy of the diffusion coefficients of these two small gases is not good enough. The rank for the diffusivity for the four penetrants is: O₂ > N₂ > CO₂ > CH₄. The lower diffusivity of CO₂ compared to that of N₂ in EC and EC based composite membranes could be due to the specific interactions between polar groups in EC and polar CO₂ molecules. In fact, the same order of CO₂ diffusion coefficients is also observed in the studies in EC ¹³ and EC derivatives ¹⁶ by several authors.

Table 6.2 Gas diffusion and sorption coefficients in EC and EC composite membranes incorporated with various silylated glucose fillers, DIPH, and PAG.

Filler (wt.%)	D(O ₂)	D(N ₂)	D(CO ₂)	D(CH ₄)	S(O ₂)	S(N ₂)	S(CO ₂)	S(CH ₄)
No additive	43	20	14	9	0.268	0.183	4.710	0.74
TMSG (10.5)	50	24	20	13	0.22	0.13	3.27	0.52
TMSG (24.2)	84	40	29	22	0.19	0.12	2.67	0.45
TMSG (34.1)	112	58	41	32	0.18	0.11	2.22	0.42
TMSG (42.0)	140	77	57	45	0.18	0.10	1.98	0.34
TMSG (50.1)	184	102	85	62	0.19	0.11	1.91	0.44
TESG (9.8)	75	39	26	19	0.22	0.13	3.53	0.58
TESG (24.3)	142	79	55	48	0.19	0.11	2.43	0.47
TESG (34.3)	186	110	78	70	0.19	0.11	2.18	0.45
TESG (40.5)	213	130	91	82	0.18	0.11	2.07	0.44
TESG (50.0)	267	161	123	108	0.19	0.12	1.90	0.46
TIPSG (10.1)	72	36	26	19	0.21	0.13	3.16	0.54
TIPSG (24.7)	112	60	45	34	0.17	0.10	2.07	0.40
TIPSG (34.8)	119	59	52	38	0.16	0.11	1.77	0.37
TIPSG (39.2)	116	63	49	36	0.16	0.09	1.77	0.37
TIPSG (50.4)	121	65	54	39	0.15	0.09	1.59	0.35
DPMSG (10.5)	44	20	16	11	0.20	0.13	3.22	0.46
DPMSG (24.9)	48	24	20	15	0.14	0.08	1.93	0.27
DPMSG (35.1)	44	24	20	14	0.11	0.06	1.38	0.22
DPMSG (40.7)	23	10	9	5	0.10	0.06	1.15	0.22
DPMSG (50.8)	23	10	10	4	0.15	0.10	1.78	0.37
DIPH (9.31)	53	26	18	13	0.174	0.099	2.797	0.431
DIPH (21.3)	62	33	24	20	0.168	0.106	2.463	0.371
DIPH (35.4)	111	65	50	45	0.162	0.096	2.180	0.378
DIPH (40.3)	165	100	78	71	0.139	0.085	1.822	0.330
DIPH (50.0)	230	153	115	109	0.150	0.086	1.894	0.360
PAG (9.31)	43	21	13	10	0.209	0.139	3.829	0.506
PAG (24.1)	39	21	10	8	0.143	0.089	2.980	0.326
PAG (33.4)	35	18	n.a.	6	0.128	0.078	n.a.	0.295
PAG (39.9)	34	19	8	7	0.123	0.066	2.802	0.265
PAG (50.0)	98	18	8	7	0.051	0.080	2.826	0.269

Diffusion coefficient in the unit of 10^{-8} cm²/s,

Sorption coefficient in the unit of 10^{-2} cm³ (STP)/(cm³ cmHg).

The effect of filler incorporation on gas diffusivity is illustrated in Figure 6.6, where the methane diffusion coefficient is plotted as a function of various filler content. It shows that the incorporation of the TMSG and DIPH filler noticeably increases the diffusivity of methane. DIPH is a typical plasticizer, the long *n*-alkyl group in the filler structure could be responsible for the diffusivity improvement since it is well recognized that the substitution of long *n*-alkyl group in polymer structure can largely increase the chain mobility.²⁰ The incorporation of TMSG filler can also increase the

chain mobility, the same as DIPH filler. However, in addition, the TES groups may create molecular scale voids,¹³ which favor higher diffusivity. Figure 6.6 also shows that the introduction of the TMSG and TIPSG notably increases the diffusivity, although to a less extent as compared to TESG. A possible reason for this behavior is that the bulky TMS and TIPS groups in side chain of the fillers can not increase the chain mobility as effectively as TESG. Although the loading of DPMSG filler results in decreased permeability (as shown in Table 6.1), it slightly increases the gas diffusivity when the filler content is rather low. However, the increase of the diffusivity is quite insignificant because of the presence of planar and nonflexible phenyl group in DPMSG filler. With further increasing the content of the DPMSG filler, the diffusivity decreases. This may due to the aggregation of the fillers at high filler loading. Similarly, the addition of PAG fillers results in a monotonically decreased diffusivity, in contrast to the silylated-glucose in these filled EC composite membranes. It indicates an antiplasticization effect.

The diffusivity change is gas type dependence, for instance, Fig. 6.7 illustrates the normalized gas diffusivity of O₂, N₂, CO₂, and CH₄ as a function of filler content in EC/TEG composite membranes. Maximum improvement in the diffusivity is observed for CH₄, the largest gases. Then, CO₂ and N₂ follow to a similar level. The O₂ diffusivity increases to the least extent. This behavior could be rationalized by the fact that the larger molecule benefits more from the increased chain mobility in performing the diffusion jump as discussed previously (see 6.3.1). In addition, the improvement in diffusivity of the CO₂ may be also partially ascribed to the specific interaction between the EC membrane and CO₂ molecule with the incorporation of the TEG filler.

Figure 6.6 Diffusion coefficients for CH₄ as a function of filler extent in EC composite membranes incorporated with various silylated glucose fillers and two commercial fillers DIPH and PAG.

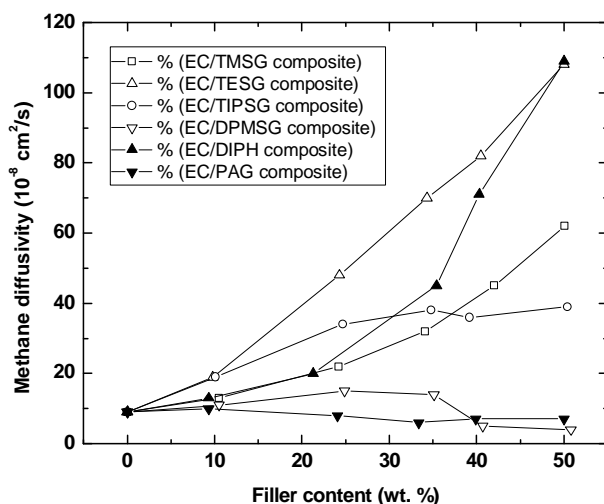


Figure 6.7 Normalized gas diffusion coefficients for O₂, N₂, CO₂, and CH₄ as a function of filler content in EC/TESG composite membrane.

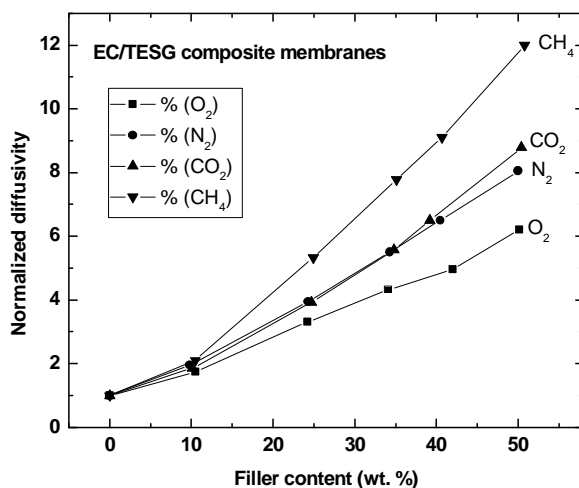


Table 6.2 shows that the incorporation of fillers in EC membranes decreases the solubility for O₂, N₂, CO₂, and CH₄. This should be attributed to the loss in the excess free volume caused by the incorporation of low molecular weight additives, which has been clarified theoretically and experimentally.²¹⁻²² On the other hand, one can find that different fillers decrease the sorption coefficients to different extents. Figure 6.8 demonstrates the change of the solubility for methane with the incorporation of

various fillers. As a general trend, for the four silylated glucose fillers, the introduction of DPMSG in EC reduces the solubility more strongly than TMSG, TESG, and TIPSG. This behavior can be rationalized if one is considering that the spherical alkyl-silylated glucose relative to the planar structure of phenyl-silylated glucose can generate more molecular scale voids,¹⁵ which could partially compensate the loss in excess free volume. The solubility reduction caused by PAG and DIPH is more than by TMSG, TESG, and TIPSG, and less than by DPMSG. In Fig. 6.9, the solubility decrease of different gases in EC/TESG composite membranes is presented. It can be observed that the gas CO₂ with higher critical temperature (i.e., with larger solubility) suffers larger solubility decrease, compared to other gases.

Figure 6.8 Sorption coefficients for CH₄ as a function of filler extent in EC composite membranes incorporated with various silylated glucose fillers and two commercial filler DIPH and PAG.

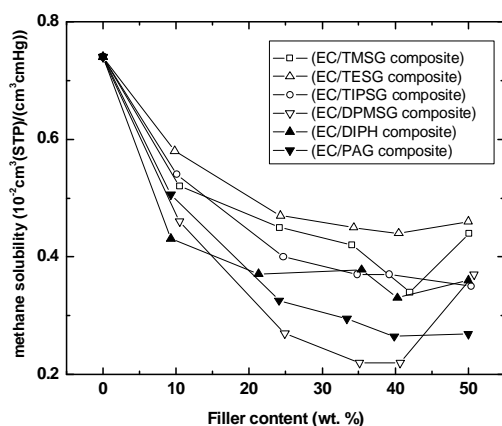
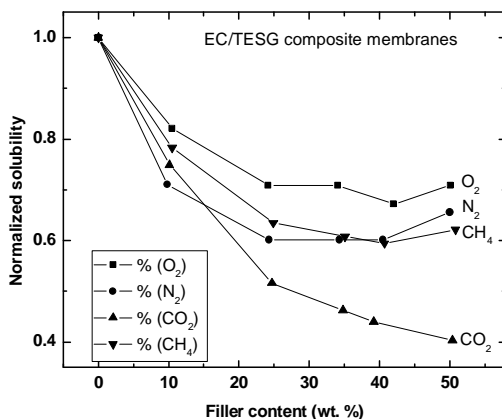


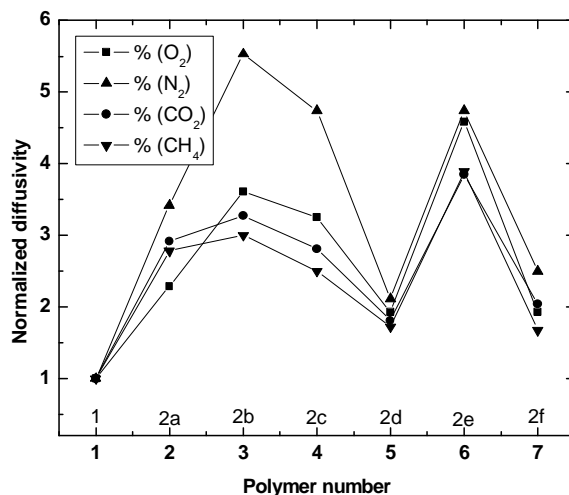
Figure 6.9 Normalized gas sorption coefficients for O₂, N₂, CO₂, and CH₄ as a function of filler content in EC/TESG composite membrane.



Khan et al. have studied the effect of substitution of various silylated groups on the gas diffusion and sorption coefficients.¹³ Based on the data reported by the authors, Fig. 6.10 and 6.11 show the normalized diffusivity and solubility in various silylated EC membranes respectively. At the first sight, it is interesting to find that the substitution of silyl groups increases in diffusivity coefficients and it decreases the sorption coefficients at most cases, similar to that observed in the EC composites containing silylated-glucose. Take gas CH₄ as example, the substitutions of TMS (2a), TES (2b), and IPDMS (2c) groups increased diffusivity more than DMPS (2f) group. Likewise, in the EC/silylated-glucose composite membranes, the incorporation of TMSG, TESG, and TIPSG leads to more diffusivity increase as compared to the incorporation of DPMSG filler (see Figure 6.6). In addition, for all investigated gases, the incorporation of TESG filler in EC shows the highest gas diffusivity increase compared to other analogues groups, similar to chemically modified TES-sub-EC compared to other analogues groups. However, when compare the extent of diffusivity increase in the substitutions of TES (2b) (see figure 6.10), the largest molecule CH₄ has the lowest diffusivity increase. This behavior is different compared with the observed findings of the EC/TESG composite membranes, where the O₂ diffusivity increase is the lowest (see Figure 6.7).

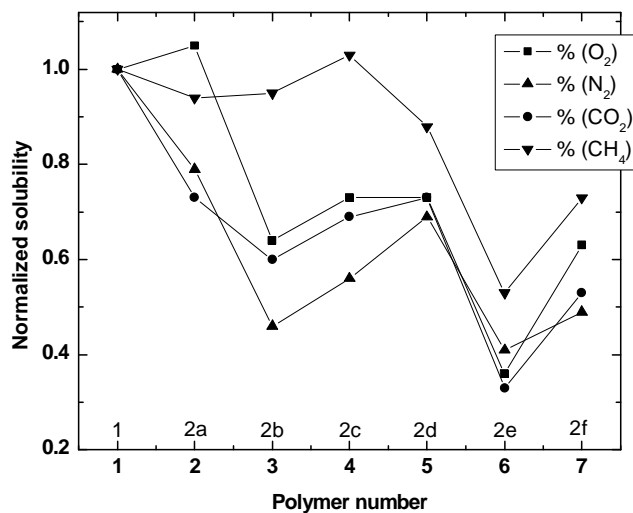
For CH₄ solubility change, the substitutions of TMS (2a), TES (2b), and IPDMS (2c) groups decreased solubility less than DMPS (2f) group. Likewise, in the EC/silylated-glucose composite membranes, the incorporation of TMSG, TESG, and TIPSG leads to less solubility decrease as compared to the incorporation of DPMSG filler (see Figure 6.8). However, when compare the extent of solubility decrease in the substitutions of TES (2b) (see figure 6.11), the largest molecule CH₄ has the lowest solubility decrease. This behavior is different compared with the observed findings of the EC/TESG composite membranes, where the O₂ solubility decrease is the lowest (see Figure 6.9).

Figure 6.10 Effect of various silyl group substitutions in EC membrane ¹³ on the gas diffusion coefficients for O₂, N₂, CO₂, and CH₄.



Legend: 1: Ethylcellulose; 2a: Trimethylsilyl-ethylcellulose; 2b: Triethylsilyl-ethylcellulose; 2c: Dimethylisopropylsilyl-ethylcellulose; 2d: Dimethyl-tert-butylsilyl-ethylcellulose; 2e: Dimethyl-n-octylsilyl-ethylcellulose; 2f: Dimethylphenylsilyl-ethylcellulose

Figure 6.11 Effect of various silyl group substitutions in EC membrane ¹³ on the gas sorption coefficients for O₂, N₂, CO₂, and CH₄.



6.4 Conclusion

The silylated-glucose filled EC composite membranes showed higher diffusivity and lower solubility as compared to the unmodified EC, which has been also observed in the chemically silyl-substituted EC. This behavior could be explained by the increased

chain mobility and loss of excess free volume by the incorporating of these low molecular weight additives. The alkyl-silylated-glucose (i.e., TMSG, TMSG, and TIPSG) fillers containing flexible and bulky silyl groups increased gas diffusivity more significantly and decreased solubility to a less extent, as compared to DPMSG with the presence of nonflexible and planar phenyl group. This phenomenon has been also observed in the chemically silyl-substituted EC (TMS-, TES-, IPDMS-sub-EC vs DMPS-sub-EC). Obviously, the changed gas permeability in EC composite membranes with silylated glucose is mainly attributed to the diffusivity change.

The results showed that silylated glucose filler exhibited better performance in O₂/N₂ separation than the two commercial fillers DIPH and PAG. Moreover, EC/TMSG composites showed the best O₂/N₂ separation performance as relative to other EC/silylated-glucose fillers. The improvement of separation performance in EC/TMSG is more pronounced with increasing TMSG content. The loading of 50 % TMSG in EC membrane increased the O₂ permeability from 11.8 to 34.7 Barrer, and just slightly decreased O₂/N₂ selectivity from 3.39 to 3.10.

6.5 References

1. Maeda, Y.; Paul, D. R. *J. Polym. Sci., Part B: Polym. Phys.* **1987**, *25*, **957**.
2. Maeda, Y.; Paul, D. R. *J. Polym. Sci., Part B: Polym. Phys.* **1987**, *25*, **981**.
3. Maeda, Y.; Paul, D. R. *J. Polym. Sci., Part B: Polym. Phys.* **1987**, *25*, **1005**.
4. Maeda, Y.; Paul, D. R. *J. Membr. Sci.* **1987**, *30*, **1**.
5. Ruiz-Trevino, F. A.; Paul, D. R. *J. Appl. Polym. Sci.* **1997**, *66*, **1925**.
6. Ruiz-Trevino, F. A.; Paul, D. R. *J. Appl. Polym. Sci.* **1998**, *68*, **403**.
7. Larocca, N. M.; Pessan, L. A. *J. Membr. Sci.* **2003**, *218*, **69**.
8. Khotimskii, V. S.; Filippova, V. G.; Bryantseva, I. S.; Bondar, V. I.; Shantarovich, V. P.; Yampolskii, Y. P. *J. Appl. Polym. Sci.* **2000**, *78*, **1612**.
9. Finkelshtein, E. Sh.; Makovetskii, K. L.; Gringolts, M. L.; Rogan, Yu. V.; Golenko, T. G.; Starannikova, L. E.; Yampolskii, Yu. P.; Shantarovich, V. P.; Suzuki, T. *Macromolecules* **2006**, *39*, **7022**.
10. Kim, I.-W.; Lee, K. J.; Jho, J. Y.; Park, H. C.; Won, J.; Kang, Y. S.; Guiver, M. D.; Robertson, G. P.; Dai, Y. *Macromolecules* **2001**, *34*, **2908**.
11. Lee, K. J.; Jho, J. Y.; Kang, Y. S.; Dai, Y.; Robertson, G. P.; Guiver, M. D.; Won, J. *J. Membr. Sci.* **2003**, *212*, **147**.

12. Lee, K. J.; Jho, J. Y.; Kang, Y. S.; Won, J.; Dai, Y.; Robertson, G. P.; Guiver, M. *D. J. Membr. Sci.* **2003**, *223*, **1**.
13. Khan, F. Z.; Sakaguchi, T.; Shiotsuki, M.; Nishio, Y.; Masuda, T. *Macromolecules* **2006**, *39*, **6025**.
14. Houde, A. Y.; Stern, S. A. *J. Membr. Sci.* **1994**, *92*, **95**.
15. Houde, A. Y.; Stern, S. A. *J. Membr. Sci.* **1997**, *127*, **171**.
16. Li, X.-G.; Kresse, I.; Xu, Z.-K.; Springer, J. *Polymer* **2001**, *42*, **6801**.
17. Baker, R. W. *Ind. Eng. Chem. Res.* **2002**, *41*, **1393**.
18. Meares, P. *J. Am. Chem. Soc.* **1954**, *76*, **3415**.
19. Robeson, L. *J. Membr. Sci.* **1991**, *62*, **165**.
20. Pinnau, I.; Morisato, A.; He, Z. *Macromolecules*, **2004**, *37*, **2823**.
21. Vrentas, J. S.; Duda, J. L.; Ling, H.-C. *Macromolecules* **1988**, *21*, **1470**.
22. Ruiz-Trevino, F. A.; Paul, D. R. *J. Polym. Sci., Part B: Polym. Phys.* **1998**, *36*, **1037**.

Chapter 7

Temperature dependence of gas transport in ethylcellulose composite membranes filled with trimethylsilyl-saccharose

7.1 Abstract

This chapter investigates systemically the effect of the addition of low molecular weight filler trimethylsilyl-saccharose (TMSSA) on the temperature dependence of gas transport in ethylcellulose (EC) composite membranes. The activation energies of permeation and diffusion (E_P and E_D), and heat of solution (ΔH_S) are obtained following the Arrhenius - van't Hoff rule by fitting permeability (P), diffusivity (D), and solubility (S) data measured at 20, 30, 40, and 50 °C with a pressure increasing time-lag apparatus. It finds ΔH_S became less negative with increasing TMSSA content, due to the gradual loss of excess free volume. However, there is no consistent change of E_D . The E_D value of the composite membranes first decreases with the addition of TMSSA and then begins to increase with further additions of TMSSA. This could be explained by the opposite effect of changes in excess free volume and chain mobility. E_P variation is also in line with E_D , for the reason that E_P is mainly governed by E_D than by ΔH_S . The present work also studies the compensation relationship between the activation energies and the natural logarithm of pre-exponent factor in permeability and diffusivity i.e., $\ln P_0 = \alpha_P + \beta_P E_P$ and $\ln D_0 = \alpha_D + \beta_D E_D$, and the compensation relationship between the heat of solution and the natural logarithm of the pre-exponent factor in solubility i.e., $\ln S_0 = \alpha_S + \beta_S \Delta H_S$. These relationships in a number of rubbery and glassy homopolymers are also compared. It shows that the EC/TMSSA composite membranes exhibited different behavior in term of the compensation relationship due to special local environment around the permeating molecule. It is concluded that the study of the compensation effect provided a useful insight into the polymer structure.

7.1 Introduction

Polymeric membranes incorporated with low molecular weight fillers have been studied as gas separation materials for a long time.¹⁻¹⁰ The effect of filler addition on flexibility and volumetric behavior in these composite membranes were also extensively investigated by several authors.¹¹⁻¹³ It suggests the incorporation of the low molecular weight fillers may lead to a loss in (excess) free volume, and meantime improve or retard chain flexibility in the polymer matrix (plasticization or

antiplasticization). Consequently, it results in a reduction in gas solubility, an increase or decrease in gas diffusivity, respectively. The whole permeability change is independent of the relative extent of the change of solubility and diffusivity. However, a few studies of the effect of filler addition on the temperature dependence of gas transport are reported until now.^{1, 2} This study attempts a step to cover this gap by systemically studying temperature dependence of gas transport in trimethylsilyl-saccharose (TMSSA) filled ethylcellulose (EC) composites membranes, which has shown interesting results for O₂/N₂ separation in technical application.¹⁴ It is also expected that this study could provide insight into the impact of membrane properties caused by filler incorporation, such as the reduction in excess free volume and increase in chain flexibility, since transport properties are well correlated to both of properties.

On the other hand, gas transport properties are a useful tool to study polymer structure. For instance, in a review article, Hiltner et al. have demonstrated that the gas molecules transport could be a useful structure probe for volumetric property in polymeric materials.¹⁵ In EC/TMSSA composite matrices, it expects that there were different motional modes as compared to typical rubbery or glassy homopolymers. Firstly, TMSSA filler may act as a plasticizer to enhance the motion of EC chain, like EC/TMSG in Chapter 4. Secondly, the addition of TMSSA filler also introduces short-time motional mode, which may facilitate the diffusion jump.¹⁶ Hence, it would be interesting to study $\ln D_0$ vs. E_D relationship in composite membranes containing low molecular weight filler.

In some solution/sorption process such as gas solvation in liquid and gas/vapor adsorption/desorption in microporous materials, enthalpy-entropy compensation (or the compensation between pre-exponent factor and activation energy) has been found and extensively discussed.¹⁷⁻²¹ But, for the gas solution/sorption in polymeric medium, few relevant studies and discussions in this topic were found.²²⁻²⁵ An interesting observation is that, Yampolskii and co-authors noted that enthalpy-entropy combination showed good linear relationship for gas sorption in glassy polymers.^{22, 23} There are also some studies about the relationship between the pre-exponential factor and the activation energy of permeation,^{26, 27}. However, controversy still remains in this topic. For instance, van Krevelen²⁶ found good linear relationships between E_P and $\ln P_0$ for small molecules gases permeating in several rubbery polymers and glassy polymers, but linear relationship is less accurate for glassy polymers.²⁹ In the chapter

3, it was found that the $\ln P_0$ vs. E_P relationship in the PTMSP/TMSG composite was affected by both gas and polymer properties. Hence, it seems to be interesting to re-evaluate $\ln P_0$ and E_P relationship in this system. It is also interesting to study $\ln D_0$ vs E_D , and $\ln S_0$ vs ΔH_S relationships in EC/TMSSA composite membranes. A wide range of rubbery and glassy polymers studied in literatures are compared as well.

7.3 Results and discussion

7.3.1 Effect of TMSSA loading on activation energies and heat of solution.

The introducing TMSSA filler into EC membrane increases gas permeability, diffusivity, and in contrast, decreases solubility. This behavior is quite similar as what has been observed in EC composite membranes filled with TMSG, which is interpreted by increased chain mobility, and reduced excess free volume. This has been is discussed in Chapter 4 and 6. The same explanations can also be valid for EC/TMSSA system, since TMSSA is analogues to TMSG in structures.

Table 7.1 presents E_P and $\ln P_0$ data in EC/TMSSA composite membranes for six gases (He, H₂, O₂, N₂, CO₂, and CH₄). It can be seen that, in EC/TMSSA composite membranes, the order of E_P values for different gases generally follows:

$$\text{CO}_2 < \text{H}_2 \leq \text{He} < \text{O}_2 < \text{N}_2 \approx \text{CH}_4$$

CO₂ has the lowest E_P due to much more negative ΔH_S resulting from its higher critical temperature compared to other five gases. The E_P values for H₂ and He are close to O₂ because He and H₂ have lower E_D (because of their smaller sizes) and less negative ΔH_S (i.e., the less condensabilities). CH₄ has almost the largest E_P values because it has the largest molecule size, and hence the largest E_D among these six gases.

Table 7.1 Activation energy of permeation (E_P) and natural logarithm of pre-exponent factor ($\ln P_0$) for six light gases in EC/TMSSA composite membranes

	He		H ₂		O ₂		N ₂		CO ₂		CH ₄	
	E_P	$\ln P_0$	E_P	$\ln P_0$	E_P	$\ln P_0$	E_P	$\ln P_0$	E_P	$\ln P_0$	E_P	$\ln P_0$
EC	15.95	10.02	15.87	10.29	17.81	9.48	20.46	9.25	6.68	6.85	20.93	10.16
EC*	/	/	6.9	6.78	6.3	5.02	8.1	4.42	3.3	5.54	8.7	5.32
EC/TMSSA1	14.86	9.77	13.29	9.47	15.50	8.83	18.35	8.72	6.57	6.97	17.78	9.22
EC/TMSSA2	15.24	10.11	13.93	9.91	14.63	8.75	18.68	9.11	5.71	6.82	17.40	9.39
EC/TMSSA3	16.38	10.65	15.45	10.58	18.32	10.31	22.44	10.69	9.67	8.41	21.75	11.21
EC/TMSSA4	20.36	12.31	22.23	13.31	27.51	14.03	30.72	14.08	19.92	12.48	33.11	15.82

The units are kJ mol⁻¹ for E_P and barrer for P_0 .

*The results reported by Li et al.,³¹

Table 7.1 also shows that the E_P values first decrease with the introduction of TMSSA and then turn to increase with further additions of TMSSA. This could be explained

by the opposite changes in E_D and ΔH_S caused by filler incorporation, which will be discussed later. It is necessary to mention here that for EC/TMSSA2, EC/TMSSA3, and EC/TMSSA4, the increase of E_P in these three membranes are accompanied with an increase in permeability. Similarly, it can be found that incorporation of plasticizer into polymers usually increases E_P values, and also increases the permeability at the same time ^{1,2} (TMSSA could be considered as a kind of plasticizer). Similarly, larger E_P , accompanied by higher P values were normally found for a polymer in rubbery state than those in glassy state as firstly noted by Meares, ³² and data collected by Pauly.³³ It is worthwhile to stress that the higher permeability in these studies should be a result of higher P_0 values (since larger E_P values resulting in lower permeability). The relationship between $\ln P_0$ and E_P in EC/TMSSA composite membranes and in a number of other rubbery and glassy polymers will be further discussed later.

Table 7.2 shows E_D and $\ln D_0$ values of O₂, N₂, CO₂, and CH₄ in EC/TMSSA composite membranes. For each EC/TMSSA membrane, it can be seen E_D values are ranked as:

$$O_2 < N_2 < CO_2 < CH_4.$$

Clearly, the gas activation energy of diffusion is well in line with the gas size. The higher E_D values of CO₂ relative to those of N₂ (kinetic diameters of 3.30 vs. 3.64 Å and Lennard-Jones collision diameters of 3.941 vs. 3.798 Å for CO₂ vs. N₂) ³⁴ in EC/TMSSA should be ascribed to less spherical CO₂ molecule, and what is more important, the specific interactions between polar CO₂ molecules and EC.³⁵

Table 7.2 Activation energy of diffusion (E_D) and natural logarithm of pre-exponent factor ($\ln D_0$) for four gases in EC/TMSSA composite membranes

	O ₂		N ₂		CO ₂		CH ₄	
	E_D	$\ln D_0$	E_D	$\ln D_0$	E_D	$\ln D_0$	E_D	$\ln D_0$
EC	31.41	-2.20	31.73	-2.85	32.55	-2.81	38.85	-0.78
EC*	10.4	-10.53	13.1	-10.14	12.6	-10.69	17.4	-9.55
EC/TMSSA1	25.63	-4.14	26.67	-4.44	29.65	-3.61	32.66	-2.81
EC/TMSSA2	23.57	-4.58	26.73	-4.04	28.78	-3.54	32.74	-2.35
EC/TMSSA3	27.83	-2.71	28.53	-3.13	29.74	-2.94	34.13	-1.54
EC/TMSSA4	32.65	-0.59	33.82	-0.78	36.38	-0.07	39.92	1.03

The units are kJ mol⁻¹ for E_D and cm² s⁻¹ for D_0 .

*The results reported by Li et al., ³¹

It can also be seen from Table 7.2 that EC/TMSSA4 has the largest E_D values for each gas. Then the unfilled EC membrane follows. The E_D values for EC/TMSSA1,

EC/TMSSA2, and EC/TMSSA3 are similar, and are noticeably lower than those for EC/TMSSA4 and EC. This observation could be rationalized in the frame work of Brandt's model.³⁶ In this model, the author proposed that the activation energy of diffusion has two contributions: (a) an intramolecular term due to the resistance of the molecular chains to bending; and (b) an intermolecular term to overcome the repulsion of the bending segments by their neighbors. The intramolecular energy is related to internal rotation and the intermolecular energy is connected to internal pressure of the polymer (or cohesive energy density). Based on this model, a simplified equation²⁸ to estimate E_D could be given as:

$$E_D = \varphi_\alpha (d_A - d_s)^2 + \varphi_\beta (d_A - d_s) \quad (\text{eq. 7.1})$$

where d_s is defined to be "proximately equal to the linear distance perpendicular to the chain axis through which a chain may move freely";³⁶ d_A is the diameter of the penetrant; and φ_α and φ_β basically represents the effect of chain flexibility and internal pressure on E_D , respectively. The real meaning of φ_α and φ_β can refer to ref 28.

As mentioned above, the addition of TMSSA filler into EC membrane increases flexibility, leading to a loss in excess free volume, resulting in a decrease of both φ_α ($\varphi_\alpha \rightarrow 0$ for flexible polymer)²⁷ and d_s values. For the EC/TMSSA composites with low content TMSSA loading, the contribution of reduction in intramolecular energy caused by the enhanced chain mobility might predominate. Hence, noticeable lower E_D values in EC/TMSSA1, EC/TMSSA2, and EC/TMSSA3 are observed. With further increase filler content, like in EC/TMSSA4 membrane, the effect of increased intermolecular energy should be more significant due to significant loss (or even vanishing) of excess free volume. Therefore, E_D values in EC/TMSSA4 are ever higher than those in EC. From the above mentioned analysis, the effect of filler (or plasticizer) on activation energy of diffusion is complex. As an evidence, it can be found in Beck and Tomka's work that, EC composite membranes (degree of substitution (DS) of 2.2) containing 10, 20, and 30 wt. % glycerol tributyrate (GTB) have similar E_D values of O₂ (31.3, 30.4, and 30.2 kJ mol⁻¹).⁷ However, E_D values seems to be slightly affected by filler contents in EC composite membranes (DS of 1.7) incorporated with diethyl tartrate (DET). For instant, the composite membranes with 10, 20, 30, and 40 wt. % DET have E_D values of 32.9, 35.9, 38.4, and 38.1 kJ

mol⁻¹, respectively.⁷ However, the authors did not provide E_D values for pure EC in this study. Therefore, it is hard to further analyze the effect of plasticizer on E_D in their systems.

Table 7.3 shows ΔH_S and $\ln S_0$ values of O₂, N₂, CO₂, and CH₄ in EC/TMSSA composite membranes. It shows that the values of ΔH_S for different gases are ranked as follows

$$CO_2 \prec CH_4 \prec O_2 \prec N_2.$$

This is also the same trend as gas critical temperature. It can also be found that ΔH_S values increase monotonously (to be less negative) with the addition of TMSSA. The same effect of filler addition on ΔH_S were also observed in three EC/plasticizer systems investigated by Beck and Tomka.⁷ So, it is clear that the incorporation of low molecular weight fillers leads to a loss in excess free volume, which has been clarified both theoretically and experimentally.^{12, 13} As pointed out by Petropoulos, sorption in preformed or partially preformed microcavities is more exothermic than sorption in the polymeric matrix.²⁸ Therefore, with the addition of TMSSA filler (or other plasticizers) into EC membrane, the excess free volume decreases gradually, leading to a corresponding increase in ΔH_S (to be less negative).

Table 7.3 Heat of solution (ΔH_S) and natural logarithm of pre-exponent factor ($\ln S_0$) for four gases in EC/TMSSA composite membranes.

	O ₂		N ₂		CO ₂		CH ₄	
	ΔH_S	$\ln S_0$	ΔH_S	$\ln S_0$	ΔH_S	$\ln S_0$	ΔH_S	$\ln S_0$
EC	-13.61	-11.35	-11.27	-10.92	-25.87	-13.37	-17.91	-12.08
EC*	-4.4	-7.59	-5.5	-8.66	-9.9	-7.03	-8.8	-8.2
EC/TMSSA1	-10.13	-10.06	-8.32	-9.87	-23.09	-12.45	-14.88	-11.00
EC/TMSSA2	-8.95	-9.69	-8.05	-9.88	-23.06	-12.67	-15.35	-11.29
EC/TMSSA3	-9.50	-10.00	-6.09	-9.21	-20.07	-11.67	-12.37	-10.27
EC/TMSSA4	-5.14	-8.40	-3.10	-8.16	-16.46	-10.47	-6.80	-8.24

The units are kJ mol⁻¹ for ΔH_S and cm³ (STP) cm⁻³ cmHg⁻¹ for S_0 .

*The results reported by Li et al.,³¹

Furthermore, the activation energies and heat of solution in pure EC membrane obtained in the present work are compared with those reported by Li and co-workers.³¹ The data E_P , E_D , and ΔH_S cited directly from their work are presented in Tables 7.1, 7.2, and 7.3, respectively for comparisons. It can be seen that the values of E_P and E_D reported by Li et al. are much lower, and the ΔH_S values are much higher (less negative) than this work. However, P , D and S data at room temperature in both

works are quite close. According to the E_P , E_D and ΔH_S ; and P , D and S data (at 25 °C) provided by Li et al., $\ln P_0$, $\ln D_0$ and $\ln S_0$ are estimated and listed in Tables 7.1, 7.2 and 7.3, respectively. Again, one can see that values of $\ln P_0$ and $\ln D_0$ according to Li et al are obviously lower, and $\ln S_0$ values are much higher than this study. This can be explained as the following. Since the sets of $\ln P_0$ and E_P ; $\ln D_0$ and E_D ; and ΔH_S and $\ln S_0$ data should give similar P , D , and S data (at least at room temperature), it is clear that, higher activation energy (or heat of solution) must be compensated by higher pre-exponent factor, and vice versa. The above discussion reveals the reason why sometimes it was argued that the “compensation effect” is a result of the experimental errors (for instance, discussions in refs 21, 30 and 37). In other words, experimental errors may lead to the cause of compensation. However, the compensation relations could be a result of the enthalpy-entropy compensation. The physical meaning and validation of the enthalpy-entropy relationship is beyond the scope of the present work. For more information in this topic, readers can refer to ref 30. It should be kept in mind that one should be cautious in dealing with compensation relations. As stated by Liu and Guo, the compensation relations “are complicated with so many artifacts and misunderstandings”.²⁹

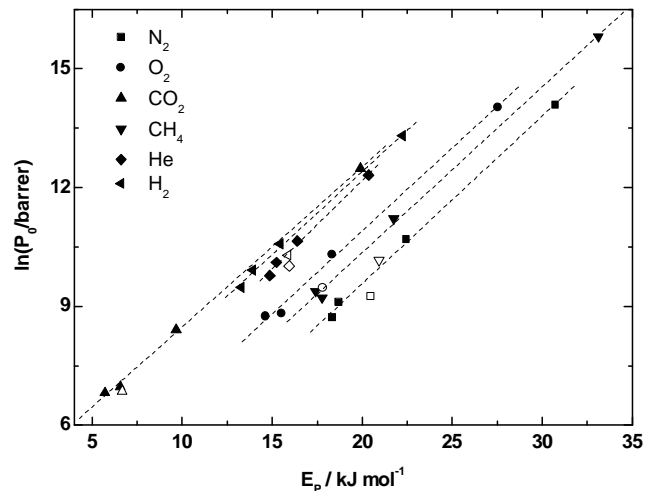
Besides the work of Li et al., there are also several E_P , E_D , and ΔH_S data available for EC membrane or EC based composite membranes. For instance, He et al. reported E_P value of 15.5 kJ mol⁻¹ for O₂, and 19.4 kJ mol⁻¹ for N₂ (the authors only presented E_P values for these two gases).³⁸ Beck and Tomka reported ΔH_S values of around -10 kJ mol⁻¹ of O₂ in pure EC.⁷ The above results seems to be close to these in this study. Besides, the E_D , and ΔH_S values of O₂ for EC membranes containing different plasticizers are in the ranges from 30 to 39 kJ mol⁻¹, and from -11 to -4 kJ mol⁻¹, respectively. These values also seem to be reasonable when considering that E_D and ΔH_S are affected by filler (or plasticizer) types.

7.3.2 Compensation effect

Figure 7.1 (see data in Table 7.1) illustrates $\ln P_0$ vs. E_P relationship for six light gases in pure EC (hollow points) and EC composite membranes (solid points). The points (either hollow or solid) with same shape represent one type of gas. For instance, the hollow and solid circle refers to O₂. From this figure, it can be seen that a good linear relationship between $\ln P_0$ and E_P is found for each gas for TMSSA filled EC films (except EC). What is more, the six lines are primarily parallel, and the intercept values are ordered as CO₂, H₂, He, O₂, CH₄, and N₂, the same trend as the permeation

coefficients of the six gases in EC/TMSSA composite membranes. And it can also be seen from Figure 7.1 that, for each gas, the point of pure EC is normally below the line defined by TMSSA filled EC composite membranes. The above $\ln P_0$ vs E_p behaviors are close to that have been noted in PTMSP/TMSG composite membranes in Chapter 3, where a good linear relationship between $\ln P_0$ and E_p for each gas in PTMSP composite membranes with TMSG filler content larger than 14.4 vol. % is observed, and the intercepts of six fitting lines are ranked as CO_2 , H_2 , He, O_2 , CH_4 , and N_2 . However, what is totally different in PTMSP/TMSG composite membrane, the addition of TMSG filler leads to a significant increase in E_p and drastically decrease in permeability. In contrast, in EC/TMSSA system, at least for EC/TMSSA2, EC/TMSSA3, and EC/TMSSA4, larger E_p values are accompanied by higher permeability. This unusually behavior could be understood when $\ln P_0$ vs. E_p behavior in EC/TMSSA composite membranes is further compared to the behavior in a number of other pure component rubbery and glassy polymers as described below.

Figure 7.1 Correlation of natural logarithm of pre-exponential factor ($\ln P_0$) and activation energy of permeation (E_p) for six gases in EC/TMSSA composite membranes. The points of either hollow or solid with same shape represent one type of gas.



In Figure 7.2 (see data in Table 7.1), $\ln P_0$ vs. E_p relationship is shown for six gases, which is clearly distinguished in four types of polymeric materials, i.e., EC/TMSSA composite membranes, rubbery polymers, “flexible” glassy polymers, and “rigid”

glassy polymers. The division of flexible and rigid glassy polymers follows their $\ln D_0$ vs. E_D behavior which is somewhat arbitrary and not precise³⁹ The rubbery polymers presented for comparison include poly(diene)s³⁴ (data collected by Pauly), poly(siloxane)s^{40, 41} and poly(alkyl (meth)acrylate)s⁴² (in molten or rubbery state). The glassy polymers contain poly(carbonate)s,^{43, 44} poly(arylene ethers)s,⁴⁵⁻⁴⁷ and poly(phenylene sulfone imide)s⁴⁸. And the rigid glassy polymers includes poly(amideimide)s,⁴⁸ poly(aryl ether sulfone)s,⁴⁹ poly(aryl ether ketone)s,⁵⁰ and polypyrrolones.⁵¹ For simplification of graphics, the data points referring to these polymers have been not been specified.

In Figure 7.2, it can be seen that the points of rubbery polymers, and those of flexible glassy polymers are definitely distinguished from each other (the two dash lines are presented for better view by eyes). And it can be found that the data corresponding to rigid glassy polymers are somewhat scattering, however, normally below the line referring to flexible glassy polymer. It can be seen that poly(phenylmethylsiloxane) (PPhMS) shows different behavior as compared to other rubbery polymers (Figure 7.2 (E) and 7.2 (F), the author⁴⁰ didn't report the data for He, H₂, O₂ and N₂). Although PPhMS is a rubbery polymer ($T_g = -28$ °C),⁴⁰ the points for this polymer are falling in the lines referring to flexible glassy polymers. This should be due to the presence of bulky, planar, and nonflexible phenyl group. This phenomena supports the explanation that the "local environment around the permeating molecule"⁵¹ is more crucial for the permeation (diffusion) process. In fact, in the study of the $\ln D_0$ vs. E_D relationship, it has already been noted this special behavior of the PPhMS polymer.¹⁵ The above observations suggest that the $\ln P_0$ vs. E_P relationship is mainly controlled by $\ln D_0$ vs. E_D behavior. However, the $\ln P_0$ vs. E_P relationship is also affected by $\ln S_0$ vs. ΔH_S relationship, albeit relative slightly. Except the two points corresponding to PPhMS in Fig. 7.2 (E) and (F), all other data exhibit quite good linear relationship. The obtained fitting equation is $\ln P_0 = 7.2858 + 0.2622 \times 10^{-3} E_P$ (the units are barrer for permeability, and J mol⁻¹ for activation energy).

Figure 7.2 Correlation of natural logarithm of pre-exponential factor ($\ln P_0$) and activation energy of permeation (E_p) in rubbery, flexible and rigid glassy polymers (data from refs 35, 42-54), as well EC/TMSSA composite membranes for different gases He (Figure 7.2 (A)), H₂ (Figure 7.2 (B)), O₂ (Figure 7.2 (C)), N₂ (Figure 7.2 (D)), CO₂ (Figure 7.2 (E)), CH₄ (Figure 7.2 (F)).

Figure 7.2 (A)

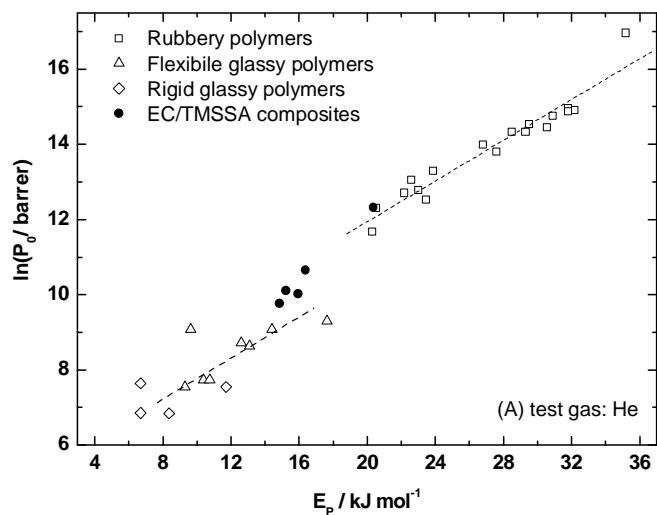


Figure 7.2 (B)

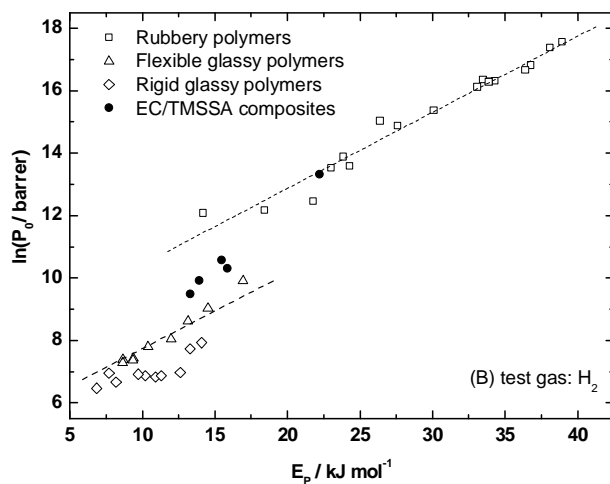


Figure 7.2 (C)

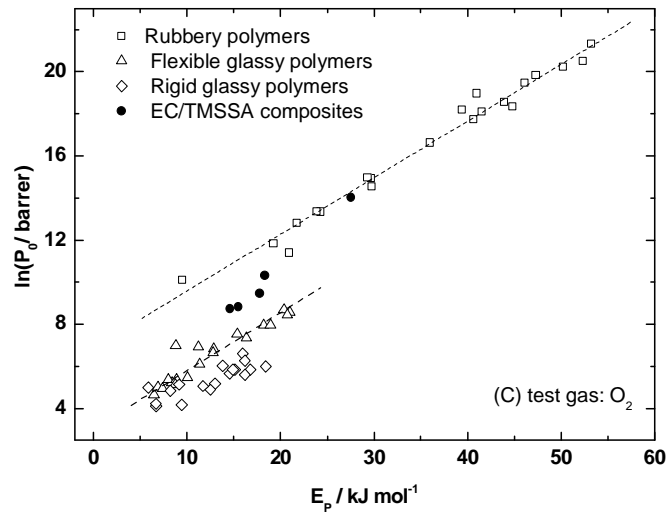


Figure 7.2 (D)

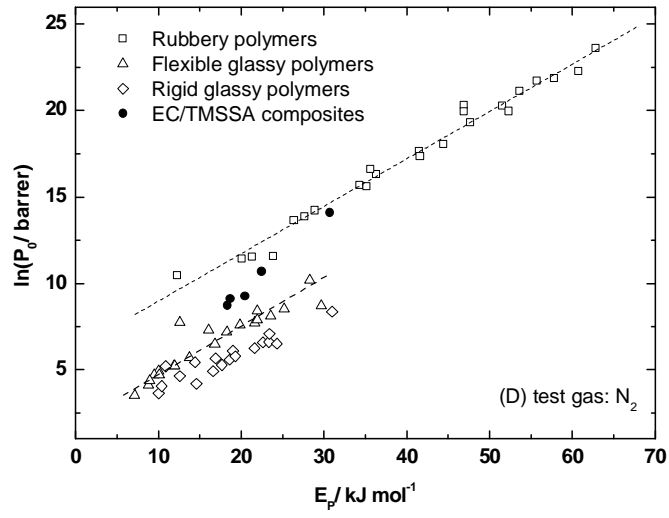


Figure 7.2 (E)

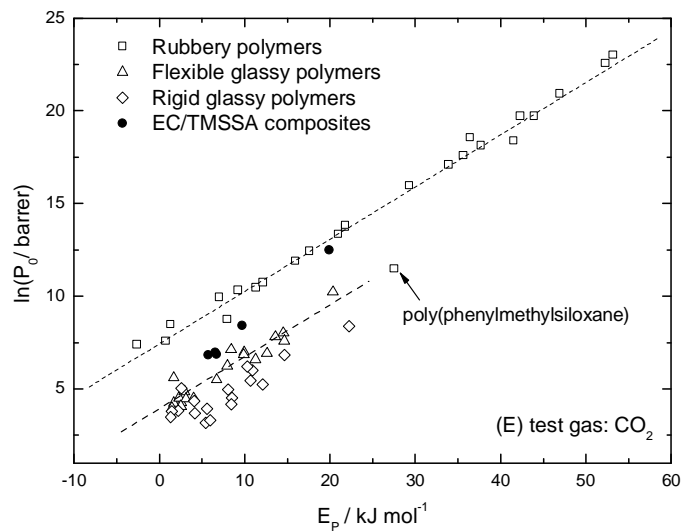
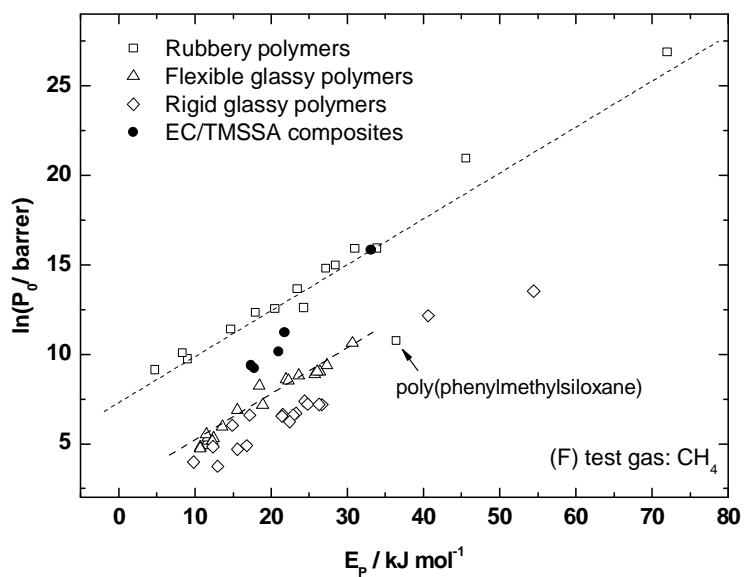


Figure 7.2 (F)



In Figure 7.2, the points of EC are close to the fitting lines of flexible glassy polymers. The possible reason is that EC has a relative low glass transition temperature as

compared to the reference glassy polymers. It is interesting to find that the points of EC/TMSSA composite membranes locate in the transition territory between the lines defined by rubbery polymers and glassy polymers. The points of EC/TMSSA1, EC/TMSSA2, EC/TMSSA3, and EC/TMSSA4 gradually approach to the line defined by rubbery polymers. In fact, the points of EC/TMSSA4 are even located in the lines referring to rubbery polymers. EC/TMSSA4 has the largest E_P value, it also has largest permeability among all the EC/TMSSA composite membranes due to the much higher $\ln P_0$ value. The special $\ln P_0$ vs. E_P relationship for EC/TMSSA composite membranes may suggest a different mechanism for permeating (or diffusion) in a filled system. This will be further discussed in $\ln D_0$ vs. E_D relationship. Since E_P is a sum of E_D and ΔH_S , and P_0 is a product of D_0 and S_0 , it is necessary to further study the $\ln D_0$ vs. E_D , and $\ln S_0$ vs. ΔH_S relationships. In Figure 7.3 (see data in Table 7.2), it studies $\ln D_0$ vs. E_D relationship for O₂, N₂, CO₂, and CH₄ in EC/TMSSA composite membranes. Basically, for each gas, these three points of EC/TMSSA2, EC/TMSSA3, and EC/TMSSA4 are in linear fitting lines. Similarly, the four fitting lines are primarily parallel and their intercept values should be ranked as O₂, N₂, CO₂, and CH₄, the same order as the diffusion coefficients of the four gases in EC/TMSSA composite membranes. The intercept of $\ln D_0$ vs. E_D is affected by the jump length term, and a small penetrant normally has a larger jump length.^{39, 54} It can also be seen from Figure 7.3 that, the points of EC/TMSSA1 show somewhat discrepancy. A more significant departure is found for pure EC. The behavior is demonstrated more clearly in a small chart (using methane as an example) in the right-bottom corner in Figure 7.3. Although methane is used for illustration in this small chart, the behavior of methane is quite similar as these of other three gases.

Figure 7.3 Correlation of natural logarithm of pre-exponential factor ($\ln D_0$) and activation energy of permeation (E_D) for four gases in EC/TMSSA composites. 1: EC/TMSSA1, 2: EC/TMSSA2, 3: EC/TMSSA3, 4: EC/TMSSA4.

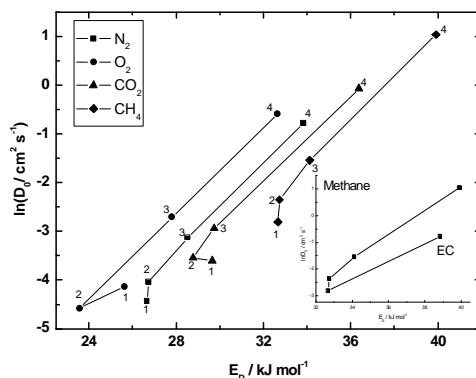


Figure 7.4 (see data in Table 7.2) further compares the $\ln D_0$ vs. E_D relationship for O_2 , N_2 , CO_2 , and CH_4 separately in EC/TMSSA composite membrane, together with other reference polymers mentioned above. Since the $\ln D_0$ vs. E_D relationship in pure component polymers has been discussed thoroughly in the relevant work,³⁹ here it just stresses that, one can see that the points of these composite membranes are located in the middle of the lines defined by rubbery and flexible glassy polymers. And once again, the points of EC/TMSSA4 are located in the lines referring to rubbery polymers. As it can be learned from Table 7.2, EC/TMSSA4 shows higher E_D values as compared to pure EC, and EC/TMSSA4 has also higher diffusivity. The $\ln D_0$ term represents the effects of entropy of diffusion and jump length. In EC/TMSSA4, due to the high loading of TMSSA fillers, the excess free volume partly or completely vanished. But, the diffusion process requires creating “microcavities” to accommodate the diffusing species (bearing in mind that in pure EC, the excess free volume provides the sites for hosting the diffusing species), which certainly requires larger entropy change. On the other hand, the addition of low molecular weight filler TMSSA increases EC chain mobility, which favors jump length.^{39, 54}

Figure 7.4 Correlation of natural logarithm of pre-exponential factor ($\ln D_0$) and activation energy of diffusion (E_D) for N_2 (Figure 7.4 (A)), O_2 (Figure 7.4 (B)), CO_2 (Figure 7.4 (C)), and CH_4 (Figure 7.4 (C)) in EC/TMSSA composite membranes.

Figure 7.4 (A)

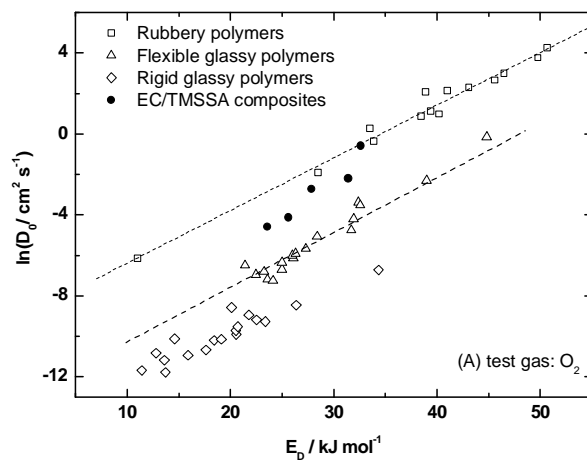


Figure 7.4 (B)

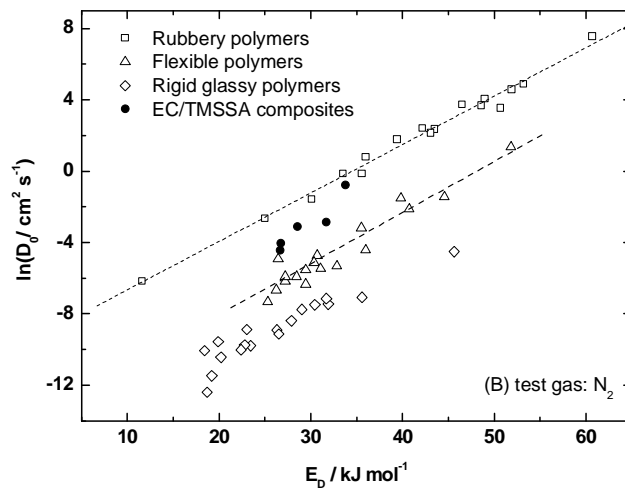


Figure 7.4 (C)

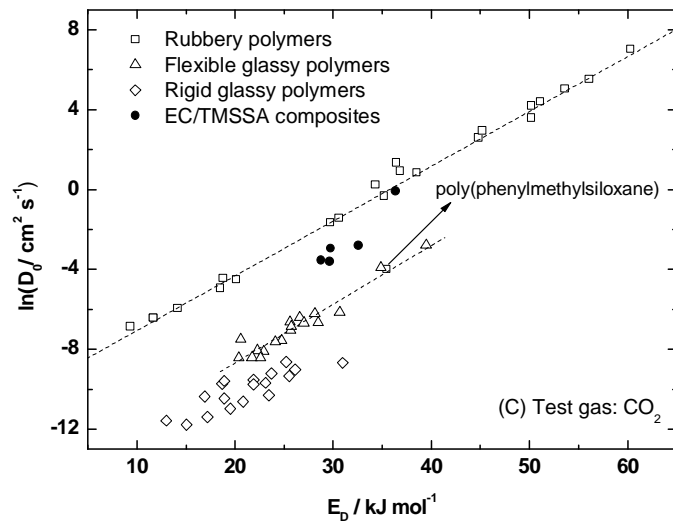
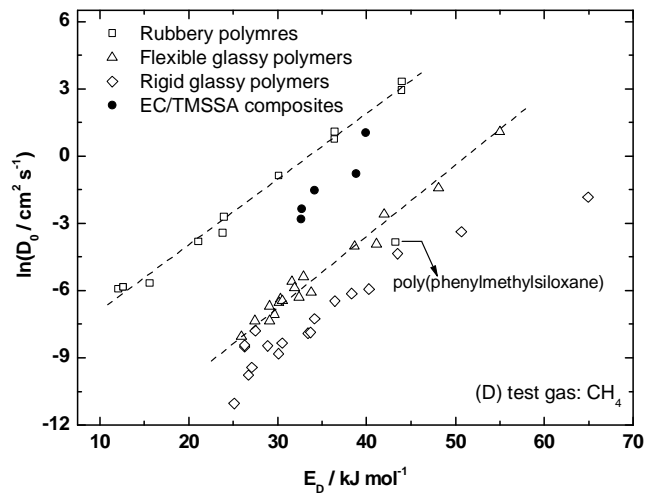


Figure 7.4 (D)



What is more, the observed special $\ln D_0$ vs. E_D behavior in EC/TMSSA composite membrane may suggest different diffusion mechanism in a polymer matrix containing low molecular weight filler, as compared to typical rubbery or glassy polymers. As stated by Freeman,³⁷ “the mechanism of small molecule diffusion in polymers is taken to be similar among a variety of polymers” when a linear relationship between $\ln D_0$ and E_D is obeyed. Following this argument, it seems different mechanisms may exist for rubbery polymers, flexible glassy polymers, and EC/TMSSA composite membranes. In a rubbery polymer, segments can rotate freely around the polymer backbone. In a glassy polymer, the segment motion is prohibited. However, things are different in EC/TMSSA composite membranes. Firstly, TMSSA may act as a plasticizer and enhance motion of EC chain, which facilitates segments motion. Secondly, the addition of TMSSA filler introduces short-time motional mode, which may facilitate the local motion.¹⁶ It seems that the different motional modes in EC/TMSSA composites lead to different diffusion mechanism as compared to typical rubbery or glassy polymers. This also supports the statement of Baker.⁵⁵ The author pointed out that, “the concept that the local environment around the permeating molecule determines the permeate’s diffusion coefficient is a key to understand diffusion in polymer membranes”.⁵⁵

Finally, the $\ln S_0$ and ΔH_S compensation will be discussed. For solvation process, the thermodynamics compensation is usually used to describe a variety of solutes in one single solvent.¹⁷⁻¹⁹ Hence, the data of $\ln S_0$ and ΔH_S of O₂, N₂, CO₂, and CH₄ in each polymer in Figure 7.5 (A) (see data in Table 7.3) is plotted. It suggests that there is a kind of compensation between $\ln S_0$ and ΔH_S , especially in the case of pure EC membrane. The linear relationship is not so good for TMSSA filled membranes, especially for EC/TMSSA4 membrane. A possible reason is that the ΔH_S values are relatively small (less negative) in EC/TMSSA4, particularly for N₂ and O₂. So, the data are less accurate because of experimental uncertainties. On the other hand, it can be seen that the line of pure EC is in the lowest part, and the line of EC/TMSSA4 is in the upper. The lines of EC/TMSSA1, EC/TMSSA2, and EC/TMSSA3 are in the middle. This indicates the compensation relation between $\ln S_0$ and ΔH_S is affected by polymer properties like excess free volume. In Figure 7.5 (B), $\ln S_0$ vs. ΔH_S relationship is also fitted by relating the data of each gas in five EC/TMSSA composites. Quite good linear relationship between $\ln S_0$ and ΔH_S are observed, and almost four parallel fitting lines can be seen, where the line of CO₂ has the largest

intercept value, then followed by those of CH₄, O₂, and N₂, which is in order of gas condensability.

Figure 7.5 Correlation of natural logarithm of pre-exponential factor ($\ln S_0$) and heat of solution (ΔH_s) for solution of N₂, O₂, CO₂, and CH₄ in EC/TMSSA composite membranes for relating (Fig. 7.5 (A)) data of different gases in a single polymer, (Fig. 7.5 (B)) data of each gas in EC/TMSSA composites.

Figure 7.5 (A)

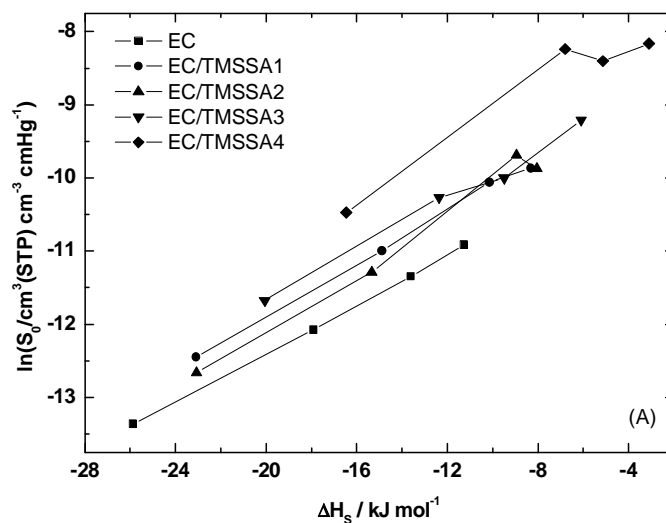


Figure 7.5 (B)

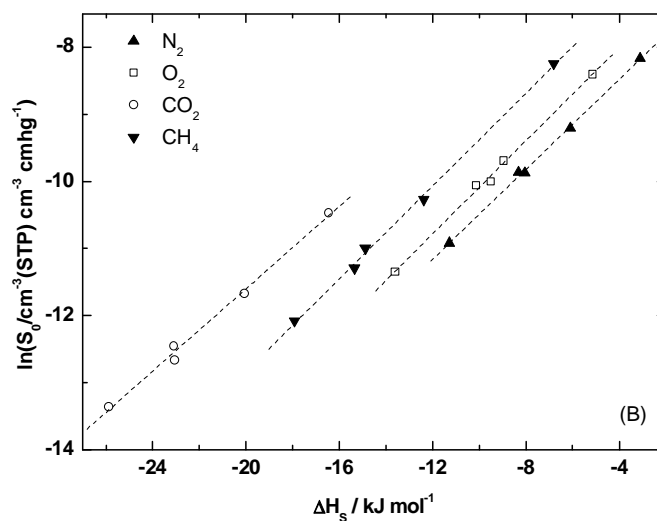


Figure 7.6 (see data in Table 7.3) further illustrates $\ln S_0$ vs. ΔH_S relationship for the four gases in EC/TMSSA composite membranes and other referred rubbery and glassy polymers. It can be found that the points for EC/TMSSA composite membranes exhibit somewhat different behavior as compared to rubbery and glassy polymers. However, there are not so clear differences between the four groups of polymers, as compared to what observed in the study of $\ln D_0$ vs. E_D , and $\ln P_0$ vs. E_P relationships. This could be due to the fact that the gas solubility is affected more by the nature of gas itself rather than polymer properties.²⁶ However, it seems to be interesting that, it could be found that the rigid glassy polymers are normally characterized by less negative ΔH_S values as relative to the flexible glassy polymers. This could be explained as the following. According to Gee,⁵⁶ the sorption process may be considered to consist of two separate thermodynamic stages: (1) condensation of the gas, an endothermic process, and; (2) mixing of the condensed gas with the polymer, an exothermic process. Hence, the ΔH_S can be expressed as the algebraic sum of an enthalpy of condensation, ΔH_{cond} , and an enthalpy change of mixing, ΔH_{mix} . The observed less negative ΔH_S value in rigid glassy polymers should be due to relative higher positive contribution of ΔH_{mix} which is affected by polymer flexibility.

Figure 7.6 Correlation of natural logarithm of pre-exponential factor ($\ln S_0$) and activation energy of diffusion (ΔH_S) in rubbery, flexible and rigid glassy polymers (data from refs 35, 42-54), as well EC/TMSSA composite membranes for different gases O₂ (Figure 7.6 (A)), N₂ (Figure 7.6 (B)), CO₂ (Figure 7.6 (C)), CH₄ (Figure 7.6 (D)).

Figure 7.6 (A)

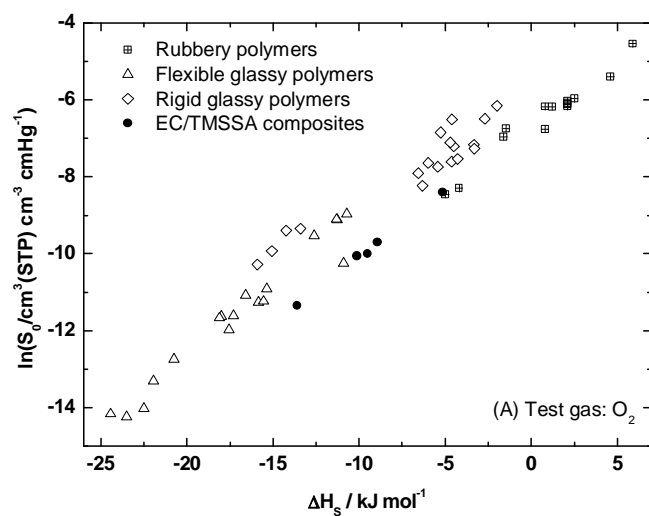


Figure 7.6 (B)

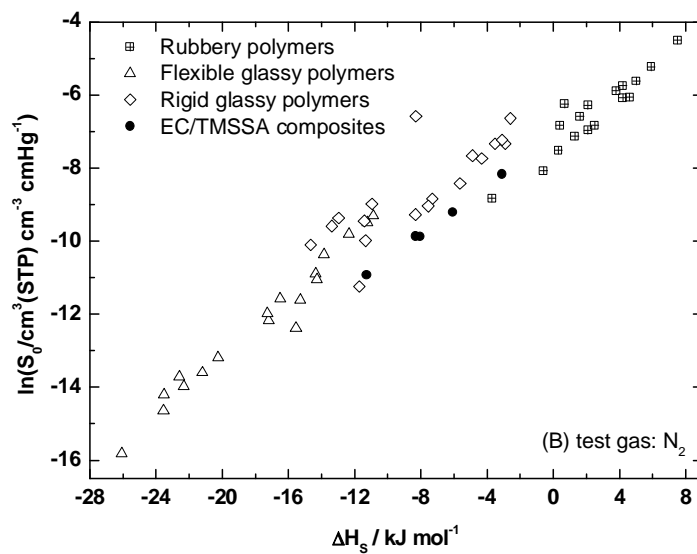


Figure 7.6 (C)

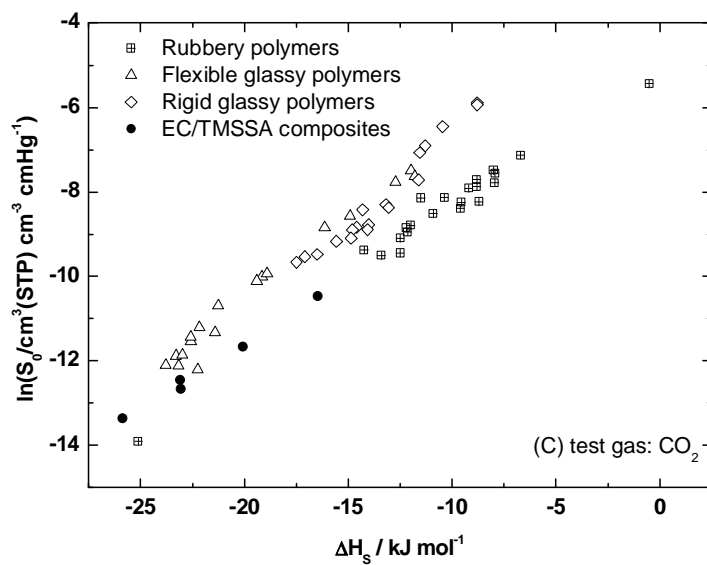
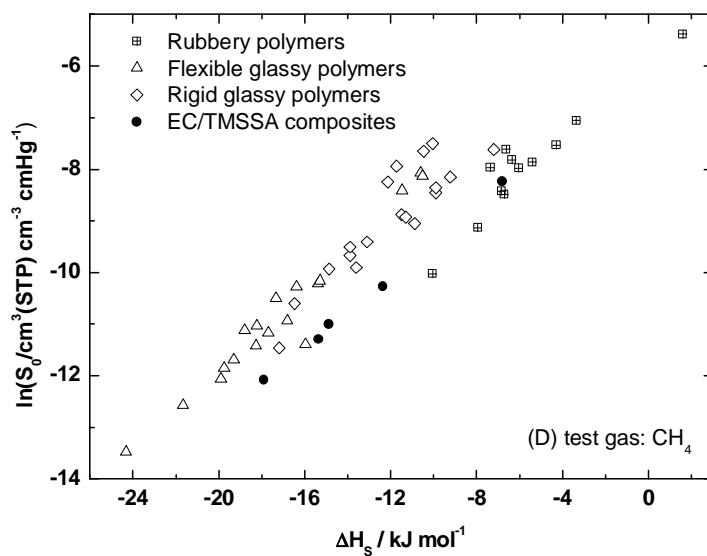


Figure 7.6 (D)



7.4 Conclusion

In the present work, the temperature dependence of gas transport in EC/TMSSA composite membranes is studied, and the compensation relations are compared, i.e., $\ln P_0 = \alpha_p + \beta_p E_p$, $\ln D_0 = \alpha_D + \beta_D E_D$, and $\ln S_0 = \alpha_s + \beta_s \Delta H_s$ in the composite membrane and other representative rubbery and glassy polymers. It is concluded that:

- (1) In EC/TMSSA composite membranes, ΔH_s gradually increases (becomes less negative) with TMSSA loading due to the loss in excess free volume.
- (2) E_D values of the composite membranes first decreases with the addition of TMSSA and then turns to increase with further addition of TMSSA. This could be explained by the competition effect between the facilitated chain motion and the loss in excess free volume.
- (3) E_p shows a similar trend like E_D for the reason that E_p is affected more by E_D than ΔH_s .
- (4) The E_p and $\ln P_0$, and E_D and $\ln D_0$ values for pure EC membrane obtained in the present work are systemically higher; and ΔH_s and $\ln S_0$ data are much lower (more negative) than those reported by Li et al.³⁹. However, the different sets of data give similar permeability, diffusivity, and solubility at room temperature. This suggests that experimental errors may cause the compensation between the activation energies (or heat of solution) and corresponding pre-exponent factors.
- (5) Regarding to $\ln D_0$ vs. E_D , and $\ln P_0$ vs. E_p relationship, the points of EC/TMSSA composite membranes fall in the gap between the lines corresponding to rubbery polymers and flexible glassy polymers. This could be ascribed to the different motions for diffusing (or permeating) in these two types of polymeric mediums.
- (6) A good linear relationship between $\ln S_0$ and ΔH_s can be maintained when it was applied to a single gas in rubbery or glassy polymers. The effect of polymer structure on the relationship of $\ln S_0$ vs. ΔH_s is insignificant.

7.5 References

1. Brubaker, D. W.; Kammermeyer, K. *Ind. Eng. Chem.* **1953**, *45*, **1145**.
2. Roberts, R. W.; Kammermeyer, K. *J. Appl. Polym. Sci.* **1963**, *7*, **2183**.
3. Maeda, Y.; Paul, D. R. *J. Polym. Sci., Part B: Polym. Phys.* **1987**, *25*, **957**.

4. Maeda, Y.; Paul, D. R. *J. Polym. Sci., Part B: Polym. Phys.* **1987**, *25*, **981**.
5. Maeda, Y.; Paul, D. R. *J. Polym. Sci., Part B: Polym. Phys.* **1987**, *25*, **1005**.
6. Maeda, Y.; Paul, D. R. *J. Membr. Sci.* **1987**, *30*, **1**.
7. Beck, M. I.; Tomka, I. *J. Polym. Sci., Part B: Polym. Phys.* **1997**, *35*, **639**.
8. Ruiz-Trevino, F. A.; Paul, D. R. *J. Appl. Polym. Sci.* **1997**, *66*, **1925**.
9. Ruiz-Trevino, F. A.; Paul, D. R. *J. Appl. Polym. Sci.* **1998**, *68*, **403**.
10. Larocca, N. M.; Pessan, L. A. *J. Membr. Sci.* **2003**, *218*, **69**.
11. Robeson, L. M. *Polym. Eng. Sci.* **1969**, *9*, **277**.
12. Vrentas, J. H.; Duda, J. L.; Ling, H.-C. *Macromolecules* **1988**, *21*, **1470**.
13. Ruiz-Trevino, F. A.; Paul, D. R. *J. Polym. Sci. Part B : Polym. Phys.* **1998**, *36*, **1037**.
14. Qiu, J.; Peinemann, K.-V. *German Patent application* **2006**
15. Hiltner, A.; Liu, R. Y. F.; Hu, Y. S.; Baer, E. *J. Polym. Sci. Part B : Polym. Phys.* **2005**, *43*, **1047**.
16. Xiang, T.-X. *J. Chem. Phys.* **1998**, *109*, **7876**.
17. Wilhelm, E.; Battino, R.; Wilcock, R. J. *Chem. Rev.* **1977**, *77*, **219**.
18. Abraham, M. H. *J. Am. Chem. Soc.* **1982**, *104*, **2085**.
19. Abraham, M. H. *J. Am. Chem. Soc.* **1979**, *101*, **5477**.
20. Katz, Y. *J. Chem. Soc. Faraday Trans.* **1985**, *81*, **579**.
21. Fletcher, A. J.; Thomas, K. M. *Langmuir* **2000**, *16*, **6253**.
22. Yampolskii, Y. P.; Kaliuzhnyi, N. E.; Durgarjan, S. G. *Macromolecules* **1986**, *19*, **846**.
23. Yampolskii, Y. P.; Soloviev, S. A.; Gringolts, M. L. *Polymer* **2004**, *45*, **6945**.
24. Van der Vegt, N. F. A. *J. Membr. Sci.* **2002**, *205*, **125**.
25. Bondar, V. I.; Freeman, B. D.; Yampolskii, Y. P. *Macromolecules* **1999**, *32*, **6131**.
26. Van Krevelen, D. W. *Properties of Polymers*, 3rd ed.; Elsevier, 1990.
27. Yampolskii, Y.; Shishatskii, S.; Alentiev, A.; Loza, K. *J. Membr. Sci.* **1998**, *148*, **59**.
28. Petropoulos, J. H. *Mechanisms and theories for sorption and diffusion of gases in polymers. Polymeric Gas Separation Membranes*; Paul, D. R., Yampolskii, Yu. P., Eds.; CRC Press: Boca Raton, FL, 1994; pp17-81.
29. Atkins, P. W. *Physical Chemistry*, 5th ed.; Oxford University Press: 1994; p 285 and p 879.
30. Liu, L.; Guo, Q.-X. *Chem. Rev.* **2001**, *101*, **673**.

31. Li, X.-G.; Kresse, I.; Xu, Z.-K.; Springer, J. *Polymer* **2001**, *42*, **6801**.
32. Meares, P. *J. Am. Chem. Soc.* **1954**, *76*, **3415**.
33. Pauly, S. *Permeability and diffusion data. Polymer Handbook*, 4th ed.; Brandrup, J., Immergut, E. H., Grulke, E. A., Eds.; John Wiley & Son, Inc.: 1999; VI/543-VI/569.
34. Poling, B. E.; Prausnitz, J. M.; O'Connell, J. J. P. *The properties of gases and liquids*, 5th edition.; Mc-Graw Hill: 2000.
35. Houde, A. Y.; Stern, S. A. *J. Membr. Sci.* **1997**, *127*, **171**.
36. Brandt, W. W. *J. Phys. Chem.* **1959**, *63*, **1080**.
37. Freeman, B. D. *Macromolecules* **1999**, *32*, **375**.
38. He, Y.; Yang, J.; Li, H.; Huang, P. *Polymer* **1998**, *39*, **3393**.
39. Zheng, J.-M.; Qiu, J.; Madeira, L. M.; Mendes, A. *J. Phys. Chem. B* **2007**, *111*, **2828**.
40. Stern, S. A.; Shah, V. M.; Hardy, B. J. *J. Polym. Sci. Part B: Polym. Phys.* **1987**, *25*, **1263**.
41. Nakagawa, T.; Nishimura, T.; Higuchi, A. *J. Membr. Sci.* **2002**, *206*, **149**.
42. Mogri, Z.; Paul, D. R. *Polymer* **2001**, *42*, **7781**.
43. Costello, L. M.; Koros, W. J. *J. Polym. Sci. Part B : Polym. Phys.* **1994**, *32*, **701**.
44. McCaig, M. S.; Seo, E. D.; Paul, D. R. *Polymer* **1999**, *40*, **3367**.
45. Xu, Z.-K.; Dannenberg, C.; Springer, J.; Banerjee, S.; Maier, G. *J. Membr. Sci.* **2002**, *205*, **23**.
46. Xu, Z.-K.; Dannenberg, C.; Springer, J.; Banerjee, S.; Maier, G. *Chem. Mater.* **2002**, *14*, **3271**.
47. Banerjee, S.; Maier, G.; Dannenberg, C.; Spinger, J. *J. Membr. Sci.* **2004**, *229*, **63**.
48. Xu, Z.-K.; Böhning, M.; Springer, J.; Glatz, F. P.; Mülhaupt, R. *J. Polym. Sci. Part B: Polym. Phys.* **1997**, *35* **1855**. Xu, Z.-K.; Böhning, M.; Springer, J.; Steinhauser, N.; Mülhaupt, R. *Polymer* **1997**, *38*, **581**.
49. Wang, Z.; Chen, T.; Xu, J. *Macromolecules* **2001**, *34*, **9015**.
50. Wang, Z.; Chen, T.; Xu, J. *Macromolecules* **2001**, *33*, **5672**.
51. Zimmerman, C. M.; Koros, W. J. *J. Polym. Sci. Part B: Polym. Phys.* **1999**, *37*, **1251**.
52. Van Amerongen, G. J. *J. Appl. Phys.* **1946**, *17*, **972**.
53. Lundstrom, J. E.; Bearman, R. J. *J. Polym. Sci.: Polym. Phys. Ed.* **1974**, *12*, **97**.

54. Charati, S. G.; Stern, S. A. *Macromolecules* **1998**, *31*, **5529**.
55. Baker, R. W. *Membrane Technology and Application*, 2nd ed.; John Wiley & Sons, Ltd, 2004.
56. Gee, G. *Quart. Revs.* **1947**, *1*, **265**.

8. Summary

This thesis has contributed to develop a series of novel composite membranes with new organic fillers silylated-saccharides, whose structure contains the bulky structure of the alkyl-silyl group that connects to various molecular weight saccharides via the flexible Si-O bond. The original of silylated-saccharides structure is intrigued by the combination of high free volume glassy polymer poly(trimethylsilyl-propyne) (PTMSP) and high flexible rubber polymer polydimethylsiloxane (PDMS).

When the rigid, high free volume polymer PTMSP is filled with silylated-saccharides, gas permeability, diffusivity, and solubility decrease consistently with the increasing filler content. This transport behavior is closely related to the tunable free volume by various extents of pore blockage. Specifically, the manipulation of FFV in PTMSP by the control addition of small fillers TMSG and TMSD1 provides a simpler way of tailoring the permeability/selectivity behavior via tuning of free volume in PTMSP compared to most of the synthesized polyacetylene polymers.^{1,2}

In contrast, in low free volume, glassy polymer ethylcellulose (EC), systematically increased gas permeability and diffusivity and decreased solubility with increasing silylated-saccharides filler content are observed. These transport properties mainly relate to the increased polymer chain flexibility and the loss in excess free volume. In particular, as organic filler, TMSG incorporation in EC not only shows better performance in O₂/N₂ separation compared to unfilled EC, but also demonstrates outstanding O₂/N₂ performance relative to EC filled with other alkyl-silylated glucose. The novel EC/TMSS composites can be applied for the oxygen enrichment due to readily formation of a super thin and defect-free selective layer with high permeability.^{3,4}

The compensation relation of $\ln P_0 = \alpha_p + \beta_p E_p$ was observed in PTMSP/TMSG and EC/TMSG systems. This relationship offers an approach to understand the transport mechanism.⁵ In the EC/TMSSA system, the compensation relations of $\ln D_0 = \alpha_d + \beta_d E_d$ and $\ln S_0 = \alpha_s + \beta_s \Delta H_s$ are also frequently observed. With increasing loading of TMSSA in EC, the systematically increased ΔH_s indicates a consistent loss in excess free volume, which is in good agreement with gradually

decreased activation energy of diffusion (E_D) resulting from decreased intra-molecular energy due to the facilitated chain motion. A comprehensive literature comparison of $\ln D_0$ vs. E_D , and $\ln P_0$ vs. E_P relationships is conducted. It is found out that the EC/TMSSA composite membranes fill the gap between rubbery polymers and flexible glassy polymers via controlled loading of TMSSA in EC.

8. Zusammenfassung

Diese Arbeit hat zu der Entwicklung einer Reihe von neuartigen Kompositmembranen mit neuen organischen Füllern beigetragen. Als Füller dienen silylierte Saccharide. Diese enthalten sperrige Alkylsilylgruppen, die über eine flexible Si-O Bindung gekoppelt sind an Saccharide mit unterschiedlichen Molekularmassen. Die Anwendung dieser Struktureinheit führt zu einer Kombination der Eigenschaften von Poly(trimethylsilyl-propyne) (PTMSP), einem glasartigen Polymer mit hohem freiem Volumen und dem hoch-flexiblen Kautschukpolymer Polydimethylsiloxan (PDMS).

Wenn das starre PTMSP Polymer mit hohem freiem Volumen nach und nach mit silylierten Sacchariden gefüllt wird, nehmen Gaspermeabilität, Diffusivität und Löslichkeit stetig ab. Die Erklärung für dieses Verhalten liegt in der Abnahme des freien Volumens durch Blockieren von Poren. Dieses kann man durch Zugabe von kleineren Füllern wie TMSG und TMSD1 in diesem spezifischen Fall einfacher bewirken, als für die meisten synthetisierten Polyacetylen-Polymere.

Im Gegensatz dazu nehmen im glasartigen Polymer Ethylcellulose (EC) mit niedrigem freiem Volumen die Gaspermeabilität und Diffusivität mit zunehmenden Füllergehalt systematisch zu. Die Löslichkeit nimmt kontinuierlich ab. Diese Transporteigenschaften hängen hauptsächlich mit der zunehmenden Beweglichkeit der Polymerketten und der Abnahme in freiem Volumen zusammen. Besonders der Einbau von TMSG als Füller in EC hat einen positiven Einfluss auf die Eigenschaften der Membran: das resultierende Membransystem zeigt im Vergleich zu unmodifiziertem EC und EC modifiziert mit anderen alkylsilylierten Glucosederivaten eine erhöhte Trennwirkung für das O_2/N_2 System. Diese neuartigen EC/TMSG Komposite können deswegen für die Sauerstoffanreicherung eingesetzt werden.

Die Kompensationsbeziehung $\ln P_0 = \alpha_p + \beta_p E_p$ wurde beobachtet im PTMSP/TMSG und EC/TMSG System. Diese Beziehung bietet einen Ansatz zum Verständnis des Transportmechanismus. Im EC/TMSSA System wurden auch die Kompensationsbeziehungen $\ln D_0 = \alpha_D + \beta_D E_D$ und $\ln S_0 = \alpha_S + \beta_S \Delta H_S$ festgestellt. Mit einer zunehmenden Beladung von EC mit TMSSA deutet die systematische Zunahme von ΔH_S auf eine stetige Abnahme des freien Volumens. Dies ist im Einklang mit der stetigen Abnahme der Aktivierungsenergie der Diffusion (E_D), verursacht durch die Abnahme an intramolekularer Energie durch die verbesserte Kettenbeweglichkeit. Eine umfassende Literaturstudie von „ $\ln D_0$ vs. E_D “ und „ $\ln D_0$ vs. E_p “ Beziehungen wurde durchgeführt. Es wurde festgestellt, dass die EC/TMSSA Kompositmembranen durch kontrolliertes Auffüllen von EC mit TMSSA die Lücke zwischen gummiartigen Polymeren und flexiblen glasartigen Polymeren schliessen.

8.1 References

1. Qiu, J.; Zheng, J.-M.; Peinemann, K.-V. *Macromolecules* **2006**, *39*, **4093**.
2. Qiu, J.; Zheng, J.-M.; Peinemann, K.-V. *Macromolecules* **2007**, *40*, **3213**.
3. Qiu, J.; Peinemann, K.-V. ; Wind, J.; Pingel, H. WO 2008/034581 A1, March, 27, 2008, (GKSS Forschungszentrum Geestacht GmbH).
4. Qiu, J.; Peinemann, K.-V. *Desalination*, **2006**, *199*, **113**
5. Zheng, J.-M.; Qiu, J.; Madeira, L. M.; Mendes, A. *J. Phys. Chem. B* **2007**, *111*, **2828**.

9. Appendix

9.1 Outline of Tables

Chapter 1

Table 1.1 Commercial applications and major suppliers of membrane gas separation units.

Table 1.2 Summary of the oxygen permeability and oxygen/nitrogen selectivity in TMS-substituted polymers and their precursor polymers.

Chapter 2

Table 2.1 Physical properties of trimethylsilylsaccharides (TMSS) fillers.

Table 2.2 Physical properties of ethylcellulose and poly(1-trimethylsilyl-1-propyne).

Chapter 3

Table 3.1 Gas permeability of the PTMSP/TMSG composite membranes at 30 °C

Table 3.2 Estimated volume of spherical TMSG and PTMSP FFV, respectively. The diameter of the TMSG molecule is about 10 Å, the PTMSP FFV radii expand from 1-9 Å from Hofmann et al.

Table 3.3 Selectivities of various gases over nitrogen in PTMSP with various amounts of TMSG at 30 °C

Table 3.4 Gas diffusion coefficients in a series of PTMSP/TMSG composite membranes at 30 °C in terms of the effective molecular diameter for six gases.

Table 3.5 Linear fitting parameters of k_1 , k_2 and regression R in the plots of the natural logarithm of gas diffusivity as a function of square of its effective diameter ¹⁶ in a series of PTMSP/TMSG composite membranes.

Table 3.6 Effective force constants for six gases ¹⁶ and their solubility coefficients in a series of PTMSP/TMSG composite membranes at 30 °C.

Table 3.7 Linear fitting parameters of k_3 , k_4 and regression R in the plots of the natural logarithm of gas solubility at 30 °C as a function of square of its effective force constant ¹⁶ in a series of PTMSP/TMSG composite membranes.

Table 3.8 Activation energy of permeation E_p and front factor P_0 for six light gases in a series of PTMSP/TMSG composite membranes.

Table 3.9 “Compensation effect” linear regression parameters in PTMSP/TMSG membranes.

Chapter 4

Table 4.1 Gas permeability coefficients of the EC/TMSG composite membranes at 30 °C.

Table 4.2 Gas diffusivity coefficients in a series of EC/TMSG composite membranes at 30 °C.

Table 4.3 Linear fitting parameters of K_1 , K_2 and regression R in the plots of the natural logarithm of gas diffusivity as a function of square of its effective diameter in a series of EC/TMSG composite membranes.

Table 4.4 Gas solubility coefficients in a series of EC/TMSG composite membranes at 30 °C.

Table 4.5 Activation energy of permeation E_p and the natural logarithm of front factor P_0 for six gases in a series of EC/TMSG composite membranes. (E_p in unit: kJ/mol, $\ln P_0$: dimensionless).

Chapter 5

Table 5.1 Gas permeabilities of the PTMSP/TMSD1, and PTMSP/TMSD500 composite membranes at 30 °C.

Table 5.2 Gas diffusivities of the PTMSP/TMSD1, and PTMSP/TMSD500 composite membranes at 30 °C, which are derived based on eq. 2.2 in chapter 2.

Table 5.3 Gas solubilities of the PTMSP/TMSD1, and PTMSP/TMSD500 composite membranes at 30 °C, which are derived based on eq. 1.1 in chapter 1.

Table 5.4 Gas permeabilities of the EC/TMSG, EC/TMSD1, and EC/TMSD500 composite membranes at 30 °C.

Table 5.5 Gas Diffusivities of the EC/TMSG, EC/TMSD1, and EC/TMSD500 composite membranes at 30 °C.

Table 5.6 Gas solubilities of the EC/TMSG, EC/TMSD1, and EC/TMSD500 composite membranes at 30 °C.

Chapter 6

Table 6.1 Gas permeability coefficients in EC and EC composite membranes incorporated with various silylated glucose fillers, DIPH and PAG.

Table 6.2 Gas diffusion and sorption coefficients in EC and EC composite membranes incorporated with various silylated glucose fillers, DIPH, and PAG.

Chapter 7

Table 7.1 Activation energy of permeation (E_p) and natural logarithm of pre-exponent factor ($\ln P_0$) for six light gases in EC/TMSSA composite membranes.

Table 7.2 Activation energy of diffusion (E_D) and natural logarithm of pre-exponent factor ($\ln D_0$) for four gases in EC/TMSSA composite membranes.

Table 7.3 Heat of solution (ΔH_S) and natural logarithm of pre-exponent factor ($\ln S_0$) for four gases in EC/TMSSA composite membranes.

9.2 Outline of figures

Chapter 1

Figure 1.1 Milestones in the development of membrane gas separations.

Figure 1.2 Schematic picture of gas molecule transporting through membrane.

Figure 1.3 schematically presents the relationship between polymer specific volume and temperature in rubber and glass state. ¹⁵ V_0 is the volume occupied by polymer chains, V_f refers to polymer specific volume, V_g is the polymer specific volume including unrelaxed free volume.

Figure 1.4 The chemical structure of poly(1-(trimethylsilyl)-1-propyne).

Figure 1.5 The chemical structure of polydimethylsiloxane.

Chapter 2

Figure 2.1 Synthesis of trimethylsilyl-glucose [TMSG]

Figure 2.2 Synthesis of trimethylsilyl-saccharides (TMSS)

Figure 2.3 The illustration of time-lag equipment constructed in GKSS Research Center, Geesthacht

Chapter 3

Figure 3.1: Normalized gas permeability coefficients for six gases (He(\square), H₂(\circ), CO₂(Δ), O₂(\blacktriangle), N₂(\bullet), and CH₄(\blacksquare)) and Maxwell model prediction(\blacklozenge) as a function of loading amount of TMSG in PTMSP.

Figure 3.2 Nitrogen permeability ($P(N_2)$) in four disubstituted acetylene polymers (\square) (PTMSP, PMP, PTMSDPA, PPP) ¹⁵ and in PTMSP/TMSG composites (\circ) as a function of reciprocal fractional free volume ($1/FFV$) of the polymer ¹⁵ and the loaded amounts of TMSG in vol.%, respectively. (1 barrer = 10^{-10} cm³ (STP) cm/(cm² s cmHg)).

Figure 3.3 Normalized selectivities for five gases (He (\square), H₂ (\circ), CO₂ (Δ), O₂ (\blacktriangledown), CH₄ (\diamond)) over nitrogen in the PTMSP/TMSG composites as a function of loading amount of TMSG.

Figure 3.4 Relationship between oxygen permeability and its selectivity over nitrogen for substituted polyacetylenes (\blacktriangle)¹⁹ and PTMSP/TMSG composite membranes in this study (\circ). The upper bound line comes from Robeson.¹⁷

Figure 3.5 Plots of the natural logarithm of gas diffusivity as a function of square of its effective diameter in a series of PTMSP/TMSG composite membranes (TMSG loading in PTMSP: 0.0% (\square), 4.9% (\circ), 9.2% (Δ), 17.7% (∇), 27.7% (\diamond), 45.8% (\blacksquare), 56.8% (\bullet)).

Figure 3.6 The nitrogen solubility coefficient (\circ) in PTMSP/TMSG composites as a function of TMSG loading amount at 30 °C as comparison of the additive model (\square).

Figure 3.7 Plots of the natural logarithm of gas solubilities at 30 °C as a function of their effective force constants in a series of PTMSP/TMSG composite membranes (TMSG loading in PTMSP: 0.0% (\square), 4.9% (\circ), 9.2% (Δ), 17.7% (∇), 27.7% (\diamond), 45.8% (\blacksquare), 56.8% (\bullet)).

Figure 3.8 Correlation of activation energy of permeation E_p and the front factor $\ln P_0$ in PTMSP/TMSG composites for six gases [(He(\square), H₂(\circ), CO₂(Δ), O₂(\blacktriangle), N₂(\bullet), CH₄(\blacksquare)) at various amount of TMSG in PTMSP . The Arabic numbers represent the loading volume content of TMSG in PTMSP (1.(0.0%), 2.(6.6%), 3(14.4%), 4.(17.7%), 5.(21.2%), 6.(28.5%), 7.(37.8%)).

Chapter 4

Figure 4.1 Density of EC/TMSG composites at R.T. as a function of TMSG loaded amount. The estimated density (expressed as (\bullet)) and experimentally measured density (expressed as (\blacklozenge)).

Figure 4.2 Glass transition temperatures of EC/TMSG composites as a function of TMSG loaded content.

Figure 4.3 Normalized gas permeability coefficients for six gases (He, H₂, CO₂, O₂, N₂, and CH₄) and Maxwell model prediction as a function of loading amount of TMSG in EC.

Figure 4.4 Relationship between helium permeability and its selectivity over methane for EC/TMSG composites and matrimid as well as PDMS. (Matrimid and PDMS data from reference¹⁶)

Figure 4.5 Relationship between $P(O_2)$ and $P(O_2)/P(N_2)$ as well as $P(CO_2)$ and $P(CO_2)/P(H_2)$ for EC/TMSG composites. Sample code is referred to Table 4.1.

Figure 4.6 The calculated oxygen production cost for 35-50% oxygen as a function of membrane performance referring to the combination of permeability and permselectivity in some of today's best commercial membranes and EC/TMSG composites.

Figure 4.7 Normalized gas diffusivity coefficients for four gases (CO_2 , O_2 , N_2 , and CH_4) as function of TMSG loading in EC.

Figure 4.8 The plots of the natural logarithm of gas (O_2 , N_2 , CH_4) diffusivity as a function of square of its effective diameter in a series of EC/TMSG composite membranes.

Figure 4.9 The relationship between k_1 and k_2 for EC/TMSG composites

Figure 4.10 The nitrogen solubility coefficient in EC/TMSG composites as a function of TMSG loading amount at 30 °C in comparison with those of the additive model.

Chapter 5

Figure 5.1 SEM photographs of the fracture cross-section of two series of composite materials (EC/TMSS (32 %) and PTMSP/TMSS (27 %)).

Figure 5.2 Normalized nitrogen permeability coefficients for PTMSP/TMSG (\square), PTMSP/TMSD1 (\circ), and PTMSP/TMSD500 (\diamond) as a function of loading amount of respective TMSS filler in PTMSP.

Figure 5.3 Normalized nitrogen permeability (P_m/P_0) (\square) in PTMSP/TMSD500 as function of TMSD500 loading content in PTMSP, in comparison of that of Maxwell model prediction¹¹ and Nielsen model¹³ prediction with consideration of geometric factor (L/W) of dispersion phase of TMSD500 in the continuous PTMSP phase. The geometric factor L/W is 1 (sphere) for the Maxwell model, and > 1 (nonsphere) for Nielsen model. The geometric factors are obtained from direct measurement the dispersion phase of TMSD500 in SEM. The $L/W = 5.1, 7.5, \text{ and } 10.2$ is the smallest value, average value, and largest value, respectively, from the experiment.

Figure 5.4 Normalized nitrogen diffusivity coefficients for PTMSP/TMSG (\square), PTMSP/TMSD1 (\circ), and PTMSP/TMSD500 (\diamond) as a function of loading amount of respective TMSS filler in PTMSP.

Figure 5.5 Relationship between oxygen diffusivity and its selectivity over nitrogen for PTMSP/TMSG (\blacksquare), PTMSP/TMSD1 (\blacklozenge), and PTMSP/TMSD500 (\diamond) composite membranes in this study. For comparison, this relationship for substituted polyacetylenes¹⁴ with various side groups, i.e., polyacetylenes with bulky or phenyl substituents (\circ) and polyacetylenes with long n-alkyl substituents (\bullet) are included.

Figure 5.6 Normalized nitrogen solubility coefficients in PTMSP/TMSG (\square), PTMSP/TMSD1 (\circ), and PTMSP/TMSD500 (\diamond) composites as a function of TMSS loading amount at 30 °C, in comparison of the additive model, as shown in a dash line.

Figure 5.7 Normalized nitrogen permeability coefficients for EC/TMSG (\square), EC/TMSD1 (\circ), and EC/TMSD500 (\diamond) as a function of loading amount of respective TMSS filler in EC.

Figure 5.8 Normalized nitrogen diffusivity coefficients for EC/TMSG (□), EC/TMSD1 (○), and EC/TMSD500 (◇) as a function of loading amount of respective TMSS filler in EC.

Figure 5.9 Normalized nitrogen solubility coefficients in EC/TMSG (□), EC/TMSD1 (○), and EC/TMSD500 (◇) composites as a function of TMSS loading amount at 30 °C, in comparison of the additive model, as shown in a dash line.

Figure 5.10 Selectivity of He/CH₄ in EC/TMSG (□), EC/TMSD1 (○), EC/TMSD500 (◇), PTMSP/TMSG (■), PTMSP/TMSD1 (●), and PTMSP/TMSD500 (◆) composites as a function of loading amount of respective TMSS filler.

Figure 5.11 Relationship between oxygen permeability and its selectivity over nitrogen for EC/TMSG (□), EC/TMSD1 (○), EC/TMSD500 (◇), PTMSP/TMSG (■), PTMSP/TMSD1 (●), and PTMSP/TMSD500 (◆) composite membranes in this study. For comparison, this relationship for several commercial air separation membranes ²¹ (e.g., poly(dimethylsiloxane) [PDMS], poly(4-methyl-1-pentene) [TPX], poly(2,6-dimethylphenylene oxide) [PPO], and polysulfone [PS]). The upper bound line comes from Robeson. ²²

Chapter 6

Figure 6.1 Permeability coefficients for CH₄ as a function of filler content in EC composite membranes incorporated with various silylated glucose fillers and two commercial fillers DIPH and PAG.

Figure 6.2 Normalized gas permeability coefficients for He, H₂, O₂, N₂, CO₂, and CH₄ as a function of filler content in EC/TMSG composite membrane.

Figure 6.3 Relationship between oxygen permeability and O₂/N₂ selectivity for EC composite membranes incorporated with various silylated glucose fillers and two commercial filler DIPH and PAG.

Figure 6.4 Relationship between oxygen permeability and O₂/N₂ selectivity for EC/TMSG composite membranes with different TMSG content and for TMS substituted PSF ¹⁰ and HFPSF ¹⁰ at different degree of substitution.

Figure 6.5 Relationship between oxygen permeability and O₂/N₂ selectivity for EC composite membranes incorporated with various silylated glucose fillers and for EC ¹³, PSF ¹⁰ and HFPSF ¹⁰ substituted with various silyl groups.

Figure 6.6 Diffusion coefficients for CH₄ as a function of filler extent in EC composite membranes incorporated with various silylated glucose fillers and two commercial fillers DIPH and PAG.

Figure 6.7 Normalized gas diffusion coefficients for O₂, N₂, CO₂, and CH₄ as a function of filler content in EC/TEG composite membrane.

Figure 6.8 Sorption coefficients for CH₄ as a function of filler extent in EC composite membranes incorporated with various silylated glucose fillers and two commercial filler DIPH and PAG.

Figure 6.9 Normalized gas sorption coefficients for O₂, N₂, CO₂, and CH₄ as a function of filler content in EC/TESE composite membrane.

Figure 6.10 Effect of various silyl group substitutions in EC membrane¹³ on the gas diffusion coefficients for O₂, N₂, CO₂, and CH₄.

Figure 6.11 Effect of various silyl group substitutions in EC membrane¹³ on the gas sorption coefficients for O₂, N₂, CO₂, and CH₄.

Chapter 7

Figure 7.1 Correlation of natural logarithm of pre-exponential factor ($\ln P_0$) and activation energy of permeation (E_p) for six gases in EC/TMSSA composite membranes. The points of either hollow or solid with same shape represent one type of gas.

Figure 7.2 Correlation of natural logarithm of pre-exponential factor ($\ln P_0$) and activation energy of permeation (E_p) in rubbery, flexible and rigid glassy polymers (data from refs 35, 42-54), as well EC/TMSSA composite membranes for different gases He (Figure 7.2 (A)), H₂ (Figure 7.2 (B)), O₂ (Figure 7.2 (C)), N₂ (Figure 7.2 (D)), CO₂ (Figure 7.2 (E)), CH₄ (Figure 7.2 (F)).

Figure 7.3 Correlation of natural logarithm of pre-exponential factor ($\ln D_0$) and activation energy of permeation (E_D) for four gases in EC/TMSSA composites. 1: EC/TMSSA1, 2: EC/TMSSA2, 3: EC/TMSSA3, 4: EC/TMSSA4.

Figure 7.4 Correlation of natural logarithm of pre-exponential factor ($\ln D_0$) and activation energy of diffusion (E_D) for N₂ (Figure 7.4 (A)), O₂ (Figure 7.4 (B)), CO₂ (Figure 7.4 (C)), and CH₄ (Figure 7.4 (C)) in EC/TMSSA composite membranes.

Figure 7.5 Correlation of natural logarithm of pre-exponential factor ($\ln S_0$) and heat of solution (ΔH_S) for solution of N₂, O₂, CO₂, and CH₄ in EC/TMSSA composite membranes for relating (Fig. 7.5 (A)) data of different gases in a single polymer, (Fig. 7.5 (B)) data of each gas in EC/TMSSA composites.

Figure 7.6 Correlation of natural logarithm of pre-exponential factor ($\ln S_0$) and activation energy of diffusion (ΔH_S) in rubbery, flexible and rigid glassy polymers (data from refs 35, 42-54), as well EC/TMSSA composite membranes for different gases O₂ (Figure 7.6 (A)), N₂ (Figure 7.6 (B)), CO₂ (Figure 7.6 (C)), CH₄ (Figure 7.6 (D)).

9.3 Dispose of Chemicals

All the chemicals used in this study are listed in table 9.3.1. They were disposed carefully according to their hazard codes in the appropriate containers.

Table 9.3.1 Hazardous chemicals used in this study and their safety data. *

Chemical substance	Hazard codes	Risk phrases	Safety phrases
Hexamethyldisilazane	F, C	11-20/21/22-34	16-26-36/37/39-45
Chlorotriethylsilane	C	10-14-22-35	16-26-36/37/39-43-45
Chlorotri- <i>iso</i> -propylsilane	C	34	26-27-36/37/39
1, 3-dimethyl-1, 1, 3, 3-tetraphenyldisilazane	Xi	36/37/38	26
Triethylamine	F,C	11-20/21/22-35	3-16-26-29-36/37/39-45
N,N-dimethylacetamide	T	61-20/21	53-45
Cyclohexane	F, Xn, N	11-38-50/53-65-67	9-16-25-33-60-61-62
Diethylphthalate	T	60-61	53-45
Dimethyl sulfoxide	Xi	36-37-38	26-37-39
Hexane	F, Xn, N	11-38-48/20-51/53- 62-65-67	9-16-29-33-36/37-61-62
Acetone	F	11	9-16-23-33
Methanol	F,T	11-23/24/25-39/23/24/25	7-16-36/37-45
Toluene	F, Xn	47-11-20	53-16-25-29-33
THF	F, Xi	11-19-36/37	16-29-33
Chloroform	Xn	22-38-40-48/20/22	36/37
Ethylcellulose	Xi	36/37/38	26-36

* The Hazard codes, risk phrase, and safety phrase data are collected from Sigma-Aldrich.

9.4 Statement

I declare that I have independently finished this thesis, and the presented thesis was completed by myself without any external helps except the cited references and open resources.

This origin of this work has not been presented to any inspecting authority in the same or a similar form before.

Jun Qiu

Weert, on 03.04.2009

9.4 Erklärung

Der Verfasser erklärt, die vorliegende Arbeit selbständig und ohne fremde Hilfe verfasst zu haben. Andere als die angegebenen Hilfsmittel und Quellen wurden nicht benutzt und die benutzten wörtlich oder inhaltlich entnommen Stellen sind als solche kenntlich gemacht.

Diese Arbeit hat in gleicher oder ähnlicher Form noch keiner Prüfungsbehörde vorgelegen.

Jun Qiu

Weert, den 03.04.2009

--End--